



## **POLITECNICO DI TORINO**

**Master's Degree Course in Automotive Engineering**

---

### **MASTER'S DEGREE THESIS**

**A method for the FRF estimation of an automotive transmission using  
experimental data from on-road vehicle tests**

**Advisor:**

Prof. Alessandro Vigliani

**Co-advisors:**

Prof. Enrico Galvagno

Prof. Mauro Velardocchia

**Candidate:**

Lorenzo Maggio

---

**ACADEMIC YEAR 2017/2018**

*Dedicated to Loris.*

## SUMMARY

1 - Introduction.....	1
2 - Signal processing for rotating machines measurements.....	2
2.1 - Fast Fourier Transform algorithm.....	2
2.2 - Order analysis .....	4
2.3 - Spectrogram .....	8
2.4 - Transfer function.....	12
3 - Frequency response function .....	16
3.1 - Model with 1 degree of freedom.....	16
3.2 - FRF's estimation algorithm .....	17
3.3 - Model with 3 degrees of freedom .....	24
3.4 - Validation of the FRF estimation algorithm basing on the 3 d.o.f. model results .....	34
4 - Experimental setup and measurements.....	42
4.1 - Vehicle characteristics .....	42
4.2 - Dual clutch gearbox .....	42
4.3 - Layout of the sensors installed during the tests .....	44
4.3.1 - Pick-ups .....	44
4.3.2 - Accelerometers.....	45
4.3.3 - Position transducers.....	46
4.3.4 - Instrumented half shaft with strain gauges for torque measurement.....	47
4.3.5 - Microphone .....	47
4.3.6 - Signals acquired from the vehicle's CAN network.....	48
4.4 - Tests performed during data acquisition.....	49
5 - Analysis of the experimental data.....	51
5.1 - Analysis of the engine's irregularities .....	51
5.2 - Analysis of the accelerometers .....	55
5.2.1 - Accelerometers of the engine's mount.....	56
5.2.2 - Accelerometers of the differential's mount.....	62
5.2.3 - Accelerometer of the gearbox's mount .....	67
5.3 - Estimation of the FRFs using the experimental algorithm .....	72
5.4 - A different application of the FRF algorithm .....	88
6 - Conclusions.....	90
Appendix A - Complete MATLAB codes .....	91
A.1 - FRF estimation algorithm .....	91
A.2 - Acceleration's computation function .....	95

A.3 - Analysis of the 3 d.o.f. model .....	97
Appendix B - Figures and tables indexes.....	102
B.1 - Figures index .....	102
B.2 - Tables index .....	103
Special thanks .....	104
Bibliographic notes .....	105

# 1 - INTRODUCTION

This thesis work is focused on the analysis of the torsional vibrations phenomena in a Dual Clutch Transmission (DCT) gearbox, starting from some experimental data measured during on-road vehicle tests.

The vehicle employed for the measurements is a segment C car displacing a 1.4 L gasoline engine coupled with a 6 gears DCT gearbox, on which an acquisition system has been installed to sample data signals coming both from the vehicle's CAN network and from some specially placed sensors.

The main target of this work, after the explanation of the main algorithm and procedure used for the data analysis and the description of the experimental setup present on the vehicle during the tests, is the development of a specific algorithm able to estimate the Frequency Response Functions (FRF) of the main mechanical components of the vehicle's powertrain starting from the experimental data.

The development of the algorithm includes also its validation, performed with a comparison of its results with the results of two simplified mechanical models of the vehicle's powertrain; after this activity, the algorithm is used to directly estimate the main FRFs from the data of the different tests.

## 2 - SIGNAL PROCESSING FOR ROTATING MACHINES MEASUREMENTS

The aim of the present work is to perform the validation of different mathematical model for the analysis of the torsional vibration due to DCT gearboxes. For this reason, during this work a lot of signals, both acquired during the on-vehicle tests or given as output from the models, have to be analysed. For this purpose, is necessary to introduce and describe the different tools and algorithms used to carry on the analysis.

### 2.1 - FAST FOURIER TRANSFORM ALGORITHM

During the tests performed on the vehicle, different pick-ups have been placed in order to measure the speed of some important gears (engine's flywheel, clutches, transmission gears, etc.); to better describe the algorithms used to analyse this type of signal, is useful to consider as example the speed signal of the flywheel acquired during a test performed with the vehicle stationary at idle with the gearbox in neutral position.

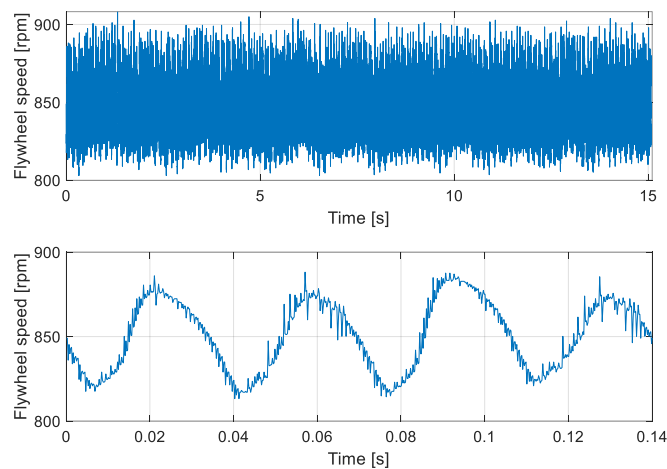


**Figure 2.1:** Speed signal of the engine flywheel during the idle test

Looking at the signal in **Figure 2.1**, as expected the speed is not constant during the test, due to variation of the engine's torque during the 2 revolutions of the crankshaft necessary to complete one engine's cycle typical of internal combustion engines, so the signal is characterized by a frequency content distributed between different harmonics at different frequencies.

Since these different harmonics can be correlated to different phenomena that occurs at different times during a complete engine's cycle, is useful to separate the contribution of the different harmonics that give rise to the total torsional oscillation that characterize the signal. For this purpose, it is possible to use the Fast Fourier Transform (FFT) algorithm: using this tool, the original signal defined in the

time domain can be analysed in the frequency domain; in this way is easier to distinguish the different frequency contents present in the measured signal.

In this work the environment in which the signals are processed and analysed is MATLAB, so is necessary to describe how the different tools are implemented in the MATLAB codes. The first step to perform the FFT analysis of the signal is the removal of the mean value from the original signal, since it is a constant value and in the frequency domain corresponds to a contribution at 0 frequency; after the mean value is removed, is possible to apply the FFT command already present in the MATLAB functions library.

```
x_fft=fft(s_det,N); % FFT of the signal
mod_fft=2*abs(x_fft(1:(length(x_fft)/2)+1))/(length(x_fft)); % FFT amplitude
phi_fft=angle(x_fft); % FFT phase
f=Fs/2*linspace(0,1,length(x_fft)/2+1); % Frequency axis
```

The inputs required by the FFT function are the signal to be analysed and the dimension of the window on which the algorithm is applied: the  $N$  parameter indicates the dimensions expressed in number of points of this window and is a very important input, since can affect the results of the function. Usually, three different criteria are used to set  $N$  and consequently the dimension of the window:

- Window equal to time duration of one period of the fundamental harmonic;
- Window equal to the total time-history available of the signal;
- Window equal to the total time-history available of the signal but truncated at the end of the last complete period of the fundamental harmonic.

The better solution is the third one, since in the first case only a small portion of the signal is used by the FFT function, so the noise present in the signal can't be sufficiently filtered by the function; another problem consists in the fact that the resolution in terms of frequency of the FFT's results is equal to the reciprocal of the time duration of the window, which in this case is too short. Considering the second case, the results are effectively less affected by the presence of the noise and the resolution is effectively improved, but the main problem of this solution is the leakage phenomenon, i.e. the dispersion of the amplitude contribution of one harmonic over different frequencies not belonging to this harmonic. The leakage effect can be reduced applying particular windows such as the Hanning or the Hamming windows: these windows are not rectangular, so the contributions of the time portions of the signal that are nearer to the ends of the window are attenuated, reducing the leakage

effect in the results. However, the usage of these windows requires the application of a corrective coefficient for the amplitude calculation coming from the FFT; the value of this corrective coefficient depends on the type of window used.

After the computation of the FFT of the signal, in the frequency domain two main information can be extrapolated: the amplitudes of the various contributions and their phases. At this point, the last step is to define the frequency axis necessary to plot in the MATLAB environment the obtained results; in **Figure 2.2** are depicted the results relative to the flywheel signal used as example.

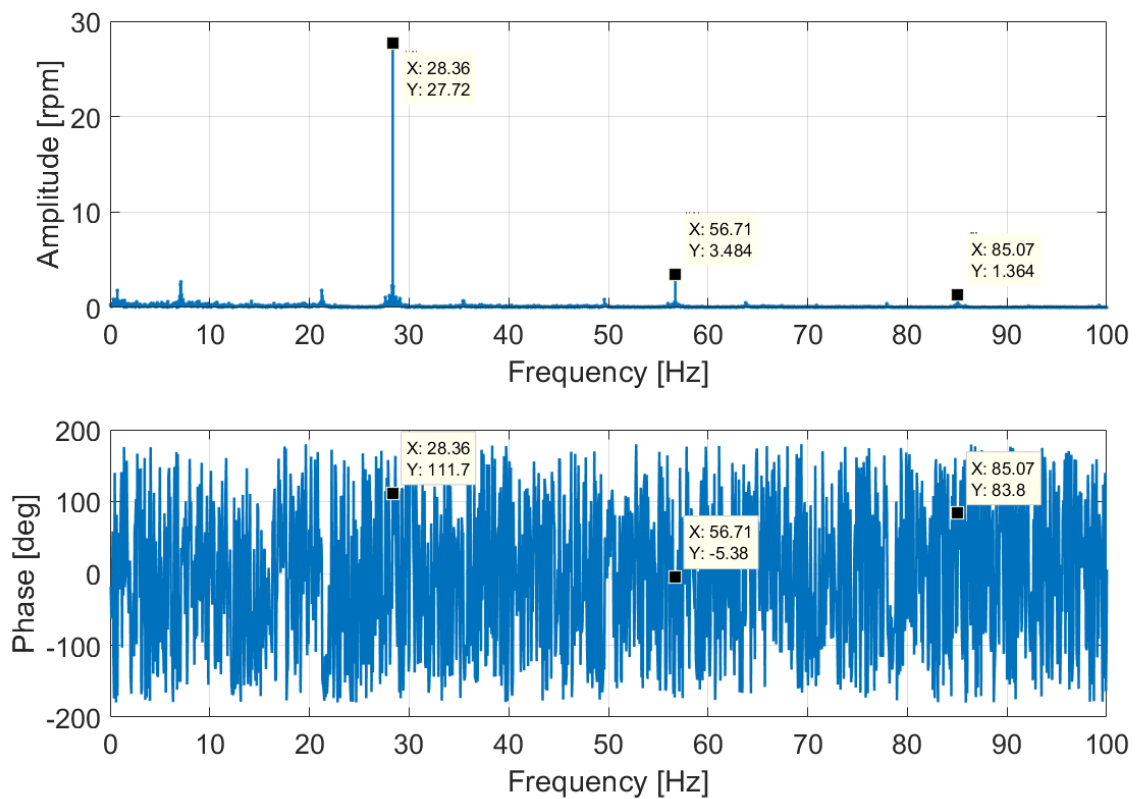


**Figure 2.2:** Amplitude and phase of the flywheel signal in the frequency domain

## 2.2 - ORDER ANALYSIS

One of the main limitations of the analysis of these types of signal using the FFT in the frequency domain is the fact that the results are significant only if the harmonics which compose the external forces (in this case torque, i.e. engine's irregularities) have a frequency almost constant; since in this work all the signal are referred to rotating machines, this means to have an almost constant rotating speed.

For this reason, is better to analyse the signals related to a varying rotational speed in the order domain. The main problem is that usually all the signals are acquired respect to the time, while if an

order analysis should be carried on, is necessary to know the values of the signals respect the angular position of one particular rotating mechanism. Entering in detail, if as example the speed signal of the lower secondary shaft of the gearbox is considered, two possible scenarios can be present:

- If is known the signal of the velocity of the shaft respect the angular position of the shaft itself, the analysis is carried on respect the shaft's orders;
- If is known the signal of the velocity of the shaft respect the angular position of the engine's crankshaft, the analysis is performed respect the engine's orders.

Since as previously said usually the signals are available in the time domain, is necessary to re-sample the original signal in the angular position domain (synchronous re-sampling); performing this step, is possible to decide the gear of which its angular position is used as the new domain of the signal.

Since the car's engine is the main source of rotation irregularities that affects all the rotating parts of the powertrain, usually is convenient to re-sample the signals respect the angular position of the crankshaft, i.e. the angular position of the engine's flywheel. Is also necessary to consider that also the angular position of the flywheel respect the time is not known, however this problem can be solved as described as follows. The MATLAB implementation of the commands used to perform the synchronous re-sampling is here reported.

```
theta=cumtrapz(t,s*6);           % integration of the velocity signal
delta_theta=[0:360/Z_fly:theta(end)]'; % theta axis definition
delta_t=interp1(theta,t,delta_theta,'linear'); % time vector with constant
                                           angular pitch
s_theta=interp1(t,s_det,delta_t,'linear'); % signal as function of theta
```

The first step required to perform the synchronous re-sampling is the integration of the speed signal of the flywheel respect the time, to obtain the angular position of the flywheel itself respect the time. In this way, looking at the final angular position value of this new signal, is possible to define a fair spaced angular position vector going from zero to this final value. The number of points of this vector depends on the maximum order of the engine that can be analysed, and this depends on the number of teeth interfacing the pick-up used to acquire the original speed signal. Due to the way in which this vector has been defined, is clear that is characterized by a constant angular pitch; it means that now is necessary to obtain a new time vector characterized by points which are not fair spaced in the time domain, but that are corresponding to instant of times in which the angular position's variation is constant.

This step is very important, so in order to better understand it is useful to consider a fictitious angular position's signal as function of the time with a parabolic trend: in **Figure 2.3** is shown on the left side how a constant time pitch corresponds to a non-constant angular pitch, while on the right side is shown that a constant angular pitch leads to non-constant time intervals.

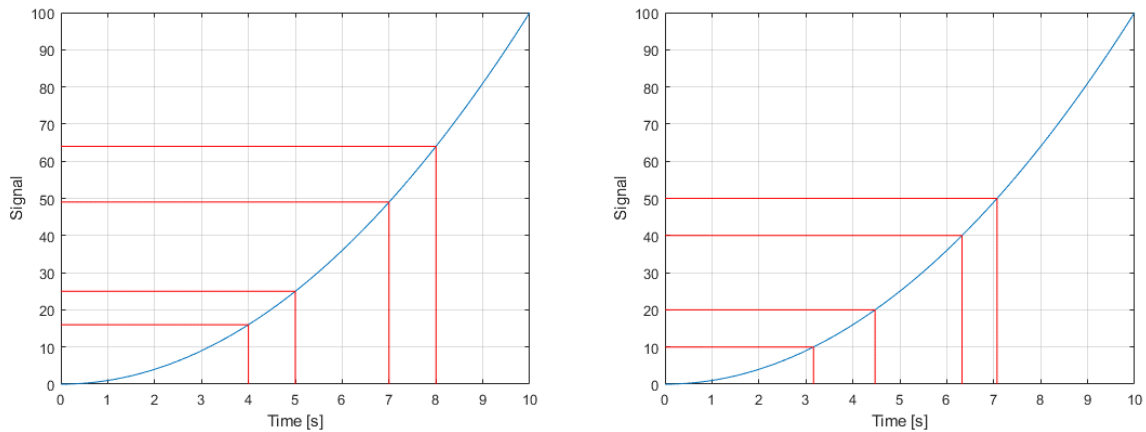


**Figure 2.3:** Graphical representation of the synchronous re-sampling

The new time vector is obtained interpolating the created angular position vector between the angular position of the flywheel as function of time and the original time vector; at this point finally with a second interpolation, is possible to obtain the original signal re-sampled respect to the angular position.

After having obtained the desired signal, is necessary to apply the same FFT function used previously: this time, instead of obtaining the same information (i.e. the amplitudes and the phases of the different contributions) in the frequency domain, these results are available in the orders domain. The final step consists in the definition of the new abscissa of the plot of the results, which is the vector of the orders; all these steps are implemented in the code with the following commands.

```
L=Z_fly/delta_ord;           % maximum order considered
N=L;                         % corresponding number of revolutions expressed
                             % in points
s_fft=fft((s_theta(1:L)),N); % application of the FFT function
mod_s=2*abs(s_fft(1:N/2+1))/L; % amplitude calculation
phi_s=angle(s_fft)/pi;      % phase calculation
ord=[0:1:N/2]*delta_ord;    % orders vector
```

Looking at the code is possible to notice that after a certain orders resolution has been defined, this value influence both the definition of the vectors of the order and the window (in this case is an angular position's window instead of a time window) used by the FFT function. Increasing the

number of revolutions considered, also the order resolution increases (the delta-order decreases), since they are reciprocal in the same way that in the case of the FFT in the frequency domain.

Since the number of revolutions of the crankshaft is a parameter that affects the obtained results, in the plots is useful to indicate the number of revolutions considered.

To make a comparison between the results obtained using the FFT in the frequency domain shown in **Figure 2.2**, applying the order analysis to the same signal depicted in **Figure 2.1**, the results obtained are shown in **Figure 2.4**.

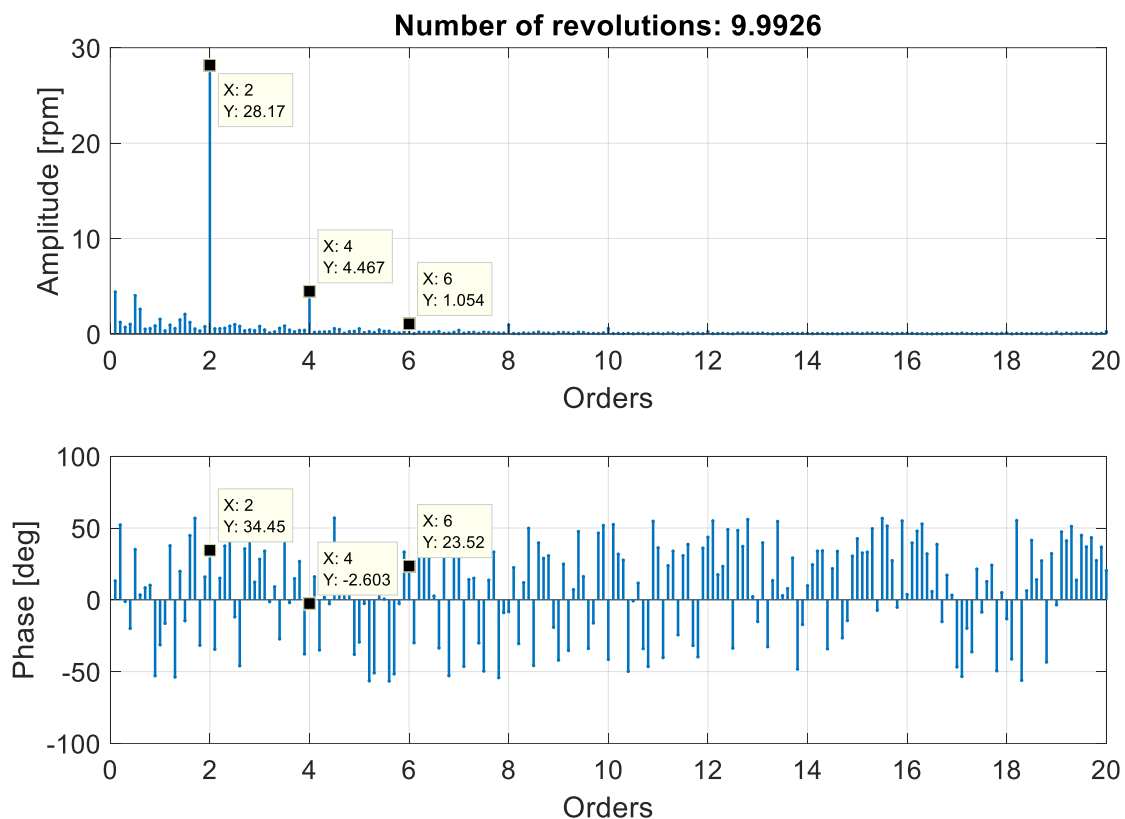


**Figure 2.4:** Amplitude and phase of the flywheel signal in the orders domain

Comparing the two results, is possible to observe that the main contribution in terms of amplitude is given to the second order, corresponding in the frequency domain to 28.36 Hz, since in this case is considered a test during which the engine is rotating at constant speed, and consequently the second order contribution is kept at constant frequency.

This type of analysis can be applied not only to speed signals, but also to other different signals such as those coming from accelerometers or others: in these cases, the signals are re-sampled respect the engine's angular position and analysed respect the engine's orders.

## 2.3 - SPECTROGRAM

Another useful tool used for the analysis of the signal is the spectrogram, thanks to which is possible to graphically follow the amplitude of the different harmonic contributions that compose the signal during all the time periods in which it has been acquired. The spectrogram algorithm is implemented in the MATLAB environment simply using the homonymous function, but is important to pay attention to the different parameters of the function that can dramatically affect the results.

```
t_wind=0.9; % time duration of the window in seconds
wind=t_wind*Fs; % number of points of the FFT windows
ol_perc=90/100; % percentage of overlap
ol=ol_perc*window; % overlap in number of points
k=wind/(sum(hanning(wind))); % calculation of the corrective factor for the
window
[S,F,T]=spectrogram(signal,wind,ol,[],Fs);
%% plot
surf(T,F,20*log10(k/wind*2*(abs(S))), 'EdgeColor', 'none')
```

The three most important inputs of this function are the signal, the dimension of the windows over which the FFT is computed and the overlap between the different windows: these last two parameters are required since practically the spectrogram function performs a certain number of FFTs over a portion of the signal delimited by the size of the window; then the window is shifted over another portion of the signal depending on the value of the overlap parameter. It is also important to notice that the dimension of the window is affecting the resolution of the results in terms of frequency: in particular, the frequency resolution is equal to the reciprocal of the time duration of the window. Another important aspect is that as default the MATLAB spectrogram function uses an Hanning's window: this means that when the results relative to the amplitude have to be plotted, it is necessary to consider the corrective factor  $k$  and the number of points of the window  $wind$  in order to obtain the correct results.

To better understand the importance of these parameters, it is better to consider as example the flywheel speed signal depicted in **Figure 2.5**, acquired during a Run Up test performed with the gearbox in neutral position.

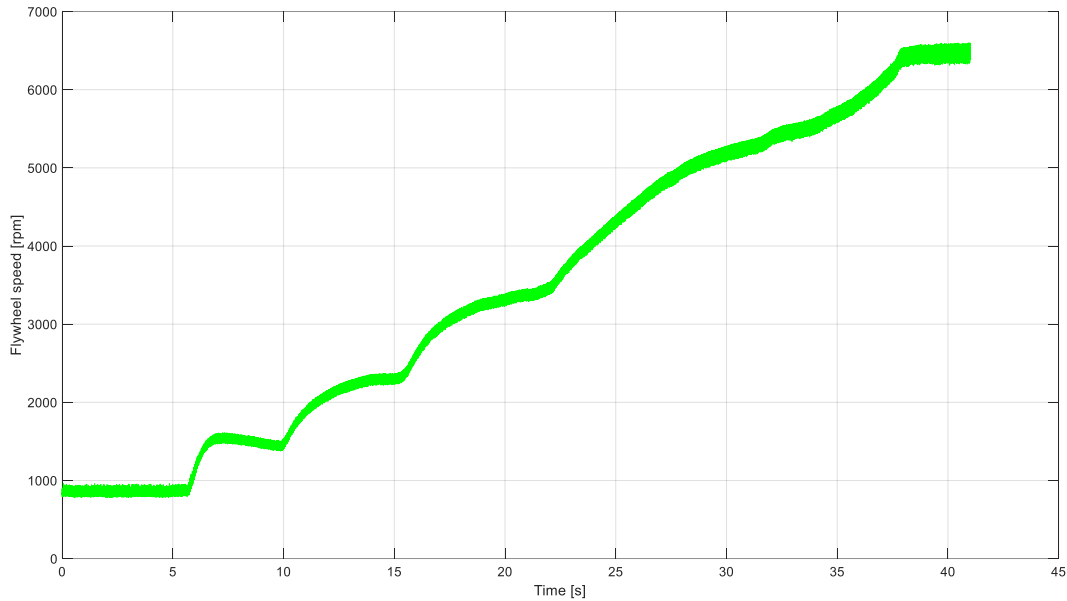


**Figure 2.5:** Flywheel speed signal acquired during the Run Up test

Using this signal after the removal of its mean value, four different spectrograms are now applied: the parameters of the different cases are resumed in **Table 2.1**.

Signal characteristics	Sampling freq. ( $F_s$ ): 20 kHz	Range: 778-6'580 rpm
Spectrogram #	Windows size [s]	Window's overlaps [%]
1	$2.5 \cdot F_s$ (2.5 s)	95%
2	$0.2 \cdot F_s$ (0.2 s)	95%
3	$2.5 \cdot F_s$ (2.5 s)	10%
4	$0.2 \cdot F_s$ (0.2 s)	10%

**Table 2.1:** Parameters of the two different spectrograms

The four different resulting spectrograms are shown in **Figure 2.6**; as expected, is possible to notice a very significant difference in terms of resolution both in time and in frequency: for this reason, is very important to carefully set the parameters of the function in order to optimize the results.

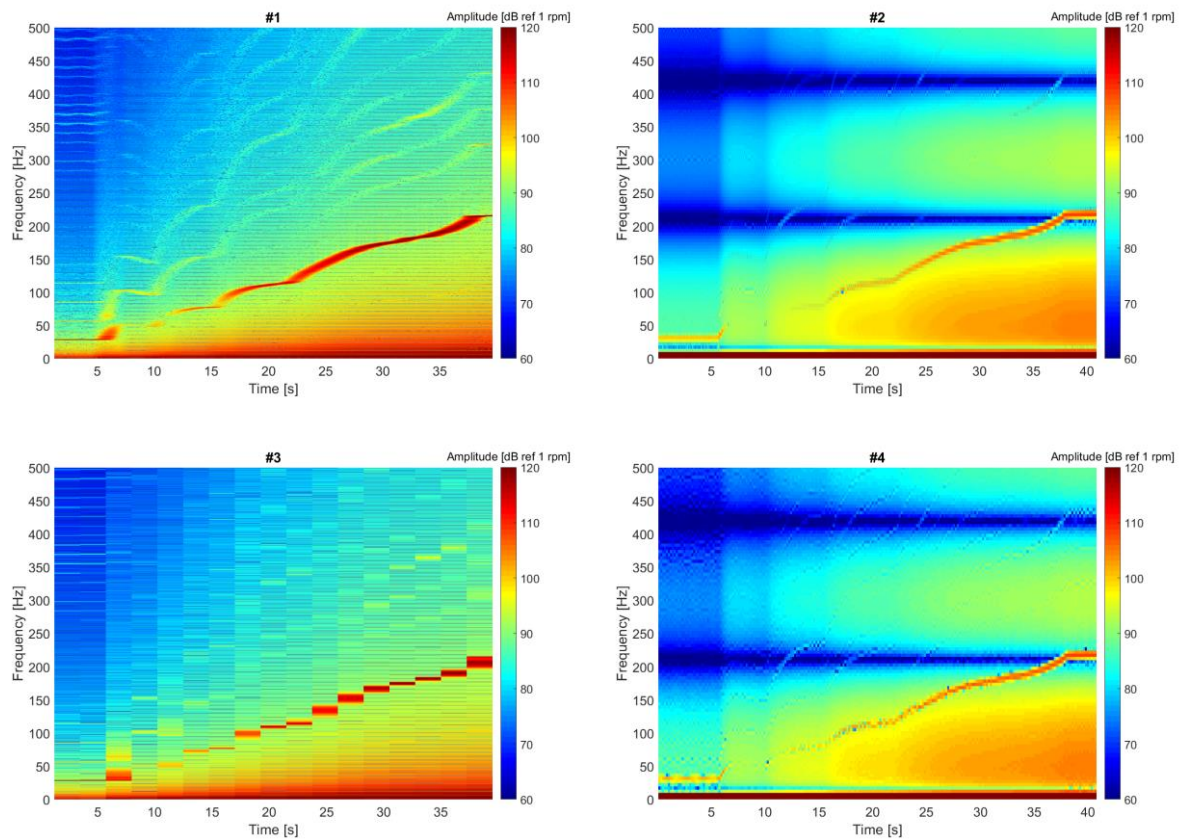


Figure 2.6: Spectrograms of the Run Up speed signal - 4 cases

As seen in the previous example, the spectrogram is a tool used to qualitatively and quantitatively describe the trend of the amplitude of the different harmonics of the signal in a 3D plot as function both of the time instant and of the frequency. Another possibility is to analyse the signal applying a spectrogram in the order domain: in this case the amplitudes of the different harmonics are described in terms of orders instead of frequency and revolutions instead of time.

The first step required to use the order spectrogram is the synchronous re-sampling of the signal in the same way described in the order analysis chapter; after the synchronous signal is computed, the spectrogram function can be applied with the following commands.

```

Fs_ord=2*max_ord; % maximum order analysed
ord_res=0.1; % forced orders resolution
t_win=1/ord_res; % time duration of the windows
WIND=round(t_win*Fs_ord); % windows dimension
ol=round(0.9*WIND); % overlap of the windows
[S,O,G]=spectrogram(s_theta>window(@rectwin,WIND),ol,[],Fs_ord);

```

Looking at the MATLAB code, is clear that the parameters required by the function are different respect the spectrogram in the frequency domain. The inputs required by the function are the following, listed in the same order that they are in the function's input:

- Synchronous re-sampled signal;
- Imposed rectangular windows for the FFTs performed by the function, corresponding to a time duration of the windows expressed in orders;
- Overlaps of the windows;
- Frequency vector expressed in orders;
- Parameter which value is equal to the double of the maximum order.

Using this type of spectrogram, is better to impose a rectangular window instead of using the default Hanning's window in order to not reduce the contribution of the portions of the signal which are near to the window's border; in **Figure 2.7** the two windows are graphically represented.

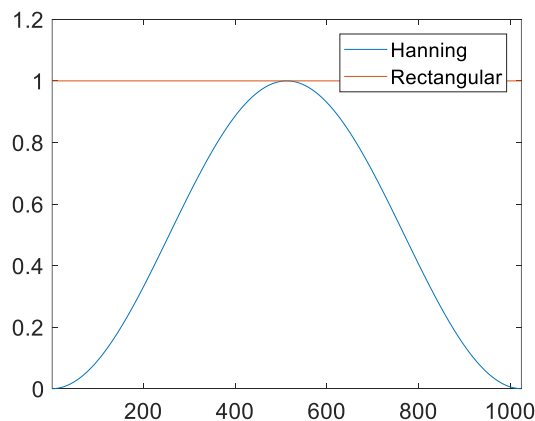


**Figure 2.7:** Hanning's window and rectangular window

Is important to notice that in the case of the orders spectrogram the three outputs are different than in the case of the spectrogram in frequency: while the  $S$  matrix contains the complex numbers, which are the results of the FFTs as in the case of the frequency spectrogram, the other two outputs are the vector  $O$ , which contains the orders at which the spectrogram has been computed depending on the decided orders resolution, and the vector  $G$ , which is the vector of the revolutions.

Using again as example the signal shown in **Figure 2.5**, applying the order spectrogram the result is the one plotted in **Figure 2.8**.

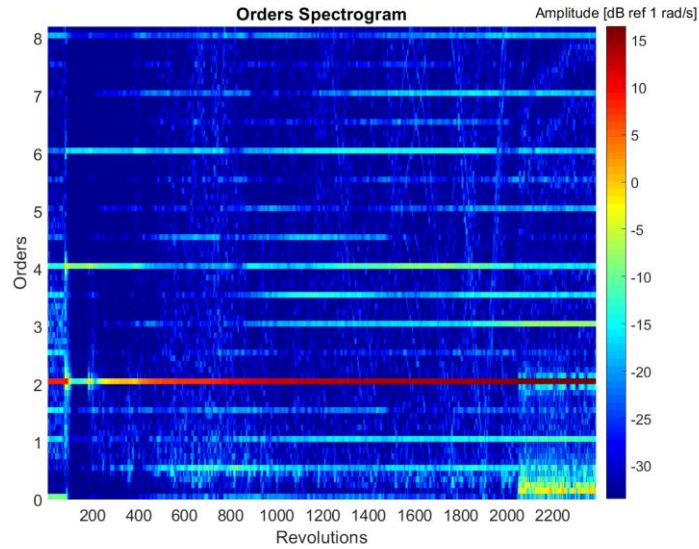


**Figure 2.8:** Orders spectrogram of the Run Up speed signal

Observing the resulting spectrogram, is possible to notice the horizontal lines corresponding to the different orders of the harmonics which compose the signal; the trend of the amplitude of each harmonic is followed by the coloured axis during the revolutions performed by the crankshaft. In this plot, the amplitude of each order is visible easier that in the case of the frequency spectrogram, so it means that is also easier to extract the numerical values corresponding to each order from the matrix given as output by the spectrogram function; the utility of this operation will be discussed in the next chapter.

## 2.4 - TRANSFER FUNCTION

The transfer function is used to put in relationship a given input and a given output by means of a physical quantity that is function of the frequency considered. The physical variables of the inputs and the outputs can be different, so as consequence different types of transfer functions exists.

In order to better understand the meaning of the different FRFs, is possible to consider the two signals depicted in **Figure 2.9**.

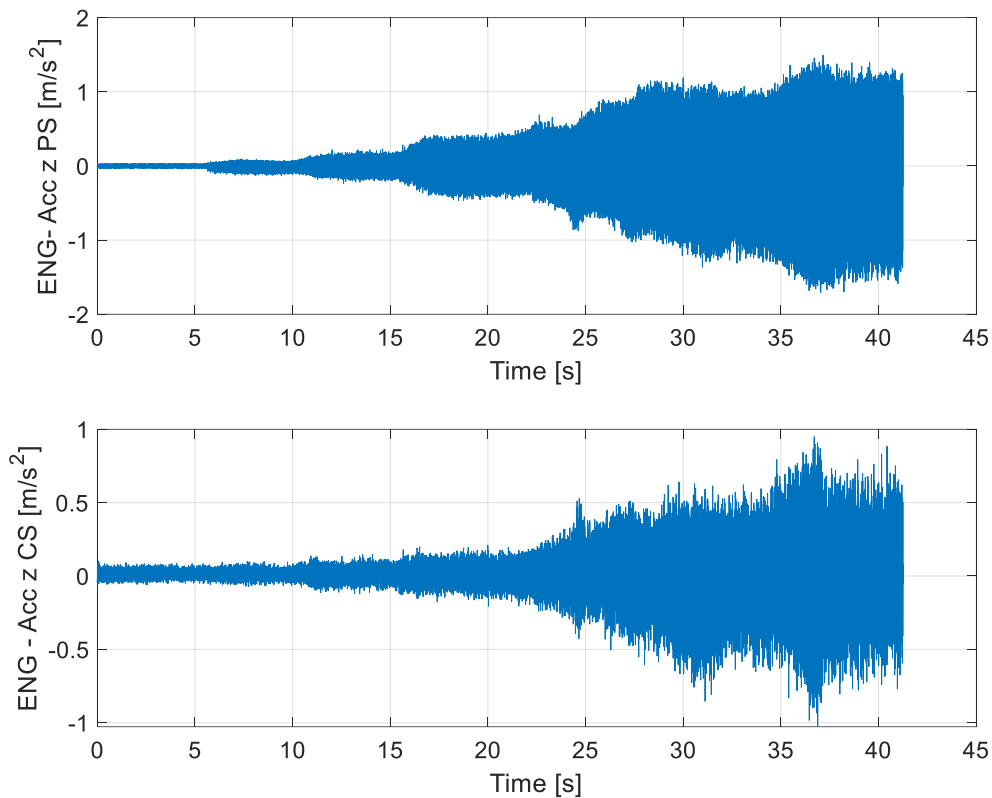


**Figure 2.9:** Signal of the 2 accelerometers of the engine’s mount during the Run Up test

The two signals are measured by two different accelerometers placed near the gearbox’s mount of the powertrain: in particular, they are the measure of the accelerations along the  $z$  direction, and one accelerometer is positioned on the powertrain side of the mount (PS - signal above), while the other one is placed on the chassis side (CS - signal below). It is clear that the mount gives a certain damping effect on the oscillation transmitted by the powertrain to the chassis, so this damping (filtering) effect can be represented by a transfer function in which the input is the signal measured in the powertrain side while the other measured signal is the output.

In the MATLAB environment, the computation of this transfer function can be performed using a command called *tfestimate*: this function is able to compute the transfer function as a complex number, from which is possible to extract both its magnitude and phase as function of the frequency at which the engine mount is excited. Another very useful function is *mscohere*, thanks to which is possible to know point by point the reliability of the estimation made using the *tfestimate* command. In the code, all the results are obtained with the implementation of the following commands:

```

t_win=0.2; % time duration of the window
tfwindow=t_win*Fs; % dimension of the FFT window
ol_perc=0.7; % percentage of overlap
NFFT=[]; % parameter used to set the number
of the FFT points
tfnooverlap=ol_perc*tfwindow; % overlap of the windows
[Tf,FF]=tfestimate(s_d,s_u,tfwindow,tfnooverlap,NFFT, Fs);
[Tfc,FFc]=mscohere(s_d,s_u,tfwindow,tfnooverlap,NFFT,Fs);
%% plots
subplot(3,1,1)
plot(FF,20*log10(abs(Tf)),'-o') % magnitude plot
set(gca,'xscale','log')
subplot(3,1,2)
plot(FF,angle(Tf).*180/pi,'-o') % phase plot
subplot(3,1,3)
plot(FFc,Tfc) % coherence plot

```

The inputs of the two functions used are exactly the same, and are similar to the parameters used as input for the MATLAB spectrogram function, since also these functions are based on a sequence of different FFTs applied of a window which translates over the time-histories of the signals.

In order these inputs are:

- Input signal;
- Output signal;
- Windows of the FFTs;
- Overlap of the FFT's windows;
- Vector of the frequency at which the transfer function is estimated;
- Sampling frequency of the signals (equal for both signals).

In order to give a better interpretation of the results, is useful to plot the spectrograms of the two signals before the application of the *tfestimate* function; the two resulting spectrograms are shown in **Figure 2.10**.

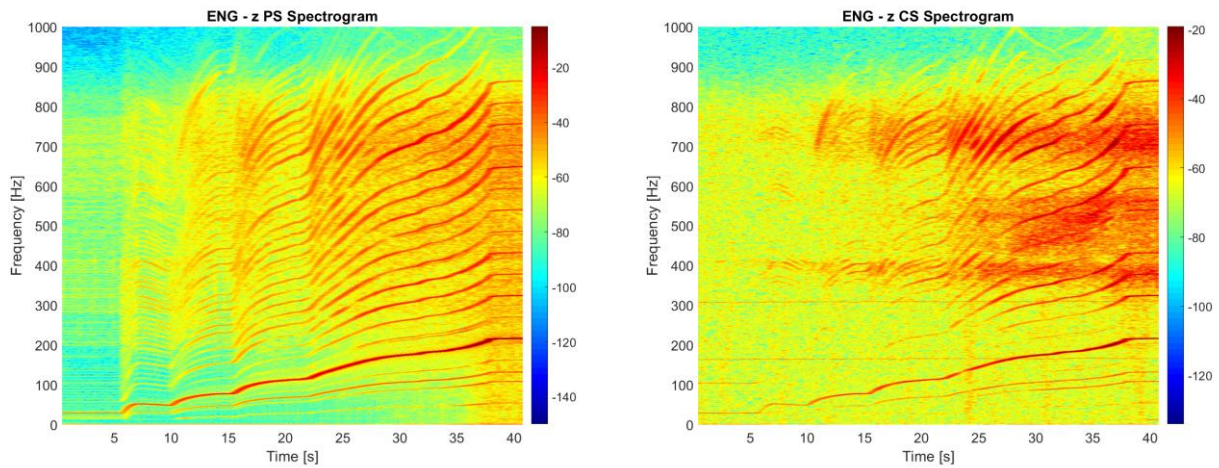


**Figure 2.10:** Spectrograms of the 2 signals used as input for *tfestimate*

The final results of the transfer function estimation are given by the three plots depicted in **Figure 2.11**, from which for each frequency is possible to know the magnitude, the phase and the reliability of these two values.

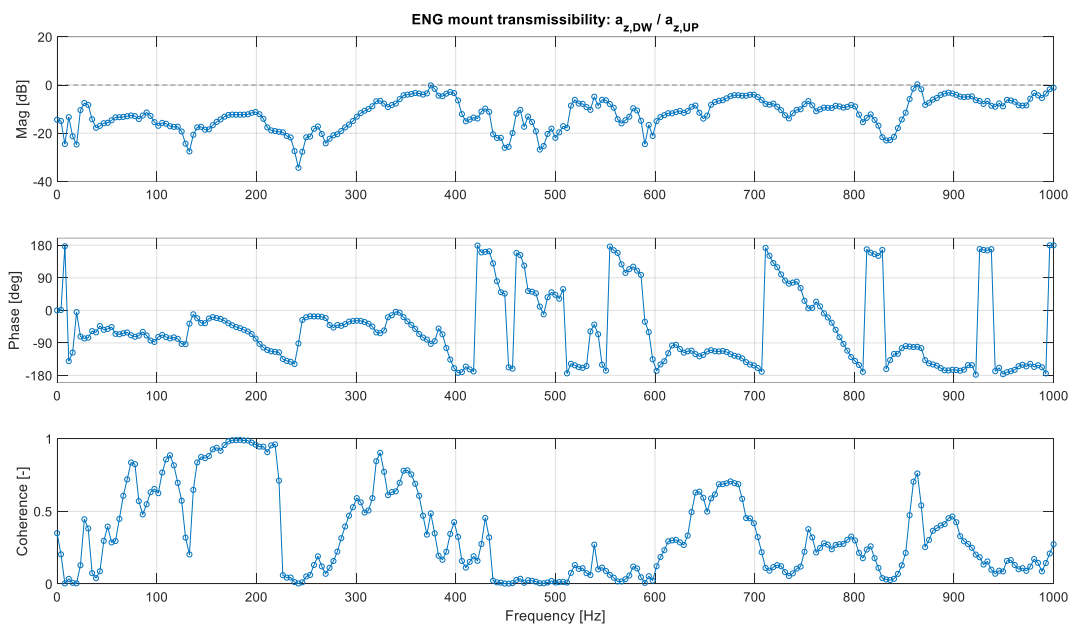


**Figure 2.11:** Result of the estimation of the transfer function (magnitude and phase) and its coherence

Observing the results relative to the estimation in terms of magnitude, the mount is characterized by good vibrations attenuation in the frequency range below 300 Hz; around 240 Hz is present an anti-resonance peak, in fact this value corresponds to the typical resonance frequency of the first bending mode of the powertrain. Instead, at low frequency the attenuation value is sufficiently high, but lower than expected.

### 3 - FREQUENCY RESPONSE FUNCTION

#### 3.1 - MODEL WITH 1 DEGREE OF FREEDOM

The Frequency Response Function (FRF) is used to put in relationship the output of a mechanical system and its input as function of the frequencies at which the input is applied. As usual, to better describe the meaning and the step necessary to use this tool, two examples are considered.

The first example consists in the mechanical system depicted in **Figure 3.1**.

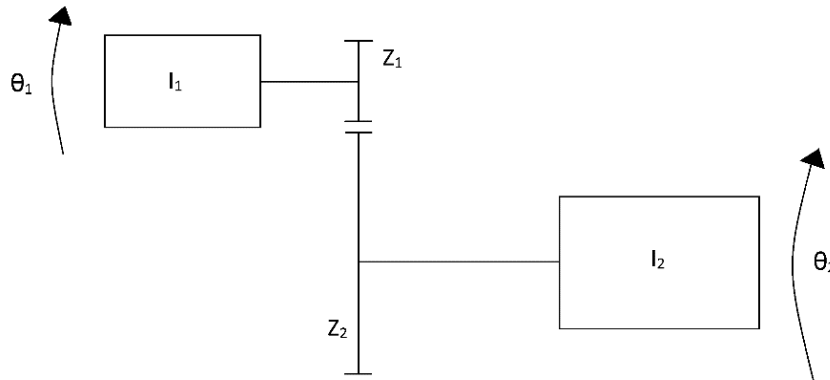


**Figure 3.1:** System with 1 torsional d.o.f.

The system consists in two rotating masses, described by their moments of inertia, connected by a speed reducer represented by its transmission ratio  $\tau = z_2/z_1$  higher than 1. Since the two rotating masses are rigidly connected by the reducer, the system shows only 1 degree of freedom (d.o.f.). Now, if it is assumed to apply a torque  $T_1$  to the inertia  $I_1$ , this will give rise to an angular acceleration  $\dot{\omega}_1$  of the first mass and an angular acceleration  $\dot{\omega}_2$  of the second mass. At this point, it is possible to calculate the relationship between the angular acceleration of the second mass and the torque applied to the first mass: this physical quantity is indicated as inertance  $\dot{\omega}_2/T_1$ . For this purpose, it is possible to represent the system with only one new rotating mass representing both the two masses of the original system, as depicted in **Figure 3.2**.

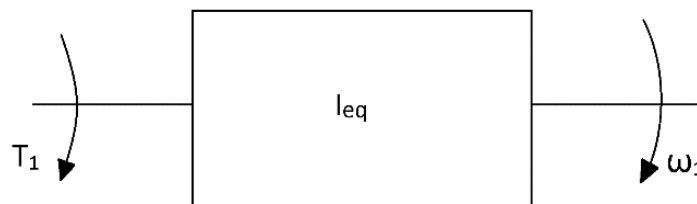


**Figure 3.2:** System with 1 d.o.f. with different representation

The total inertia  $I_{eq}$  of the new system can be computed as function of the two inertias of the original system and the transmission ratio  $\tau$ , according to the following equation:

$$I_{eq} = I_1 + \frac{I_2}{\tau^2}$$

Consequently, is possible to estimate the torque  $T_1$  applied to the equivalent inertia as function of the angular acceleration  $\dot{\omega}_1$ :

$$T_1 = \left( I_1 + \frac{I_2}{\tau^2} \right) \dot{\omega}_1 = I_{eq} \dot{\omega}_1$$

Through the transmission ratio, the relationship between the acceleration  $\dot{\omega}_2$  and the torque  $T_1$  can be simply calculated:

$$T_1 = I_{eq} \dot{\omega}_2 \tau$$

Finally, the inertance  $\dot{\omega}_2/T_1$  can be computed as the ratio between the two quantities:

$$In_{21} = \frac{\dot{\omega}_2}{T_1} = \frac{1}{I_{eq} \tau}$$

Looking at the last equation, is clear that the value of the computed inertance is constant respect the frequency, since this term doesn't appear in the equation. Since the computed inertance is a real number, the absolute value of the inertance is equal to  $|In_{21}|$  and the phase is equal to 0 for each value of frequency.

### 3.2 - FRF'S ESTIMATION ALGORITHM

Considering an automotive transmission is useful to compute the inertances of some of the rotating mechanism of the powertrain respect the torque provided by the internal combustion engine. In this case, the inertance is defined in the same way of the model described in the previous paragraph, i.e. as the ratio between the angular acceleration of the rotating element taken in consideration and the input torque of the engine.

The main problem of this calculation is that in the data set measured on the vehicle during the different tests the measurements of the accelerations of the gears and the torque of the engine are not available; consequently, is necessary to compute these signals starting from the velocity signal of the specific gear considered for the inertance calculation and from the engine's flywheel speed signal, from which the engine's torque can be computed. This computation can be described easier if, considering the 1 d.o.f. model previously analysed, following assumption are made:

- The inertia  $I_1$  represents the engine's crankshaft inertia;
- The inertia  $I_2$  represent the equivalent vehicle's inertia;
- The displacement  $\theta_1$  represents the angular position of the crankshaft;
- The displacement  $\theta_2$  represents the angular position of the differential.

Now is useful to build a realistic engine flywheel's speed signal, with known frequency content: for this purpose, in the Simulink environment the model depicted in **Figure 3.3** is built.

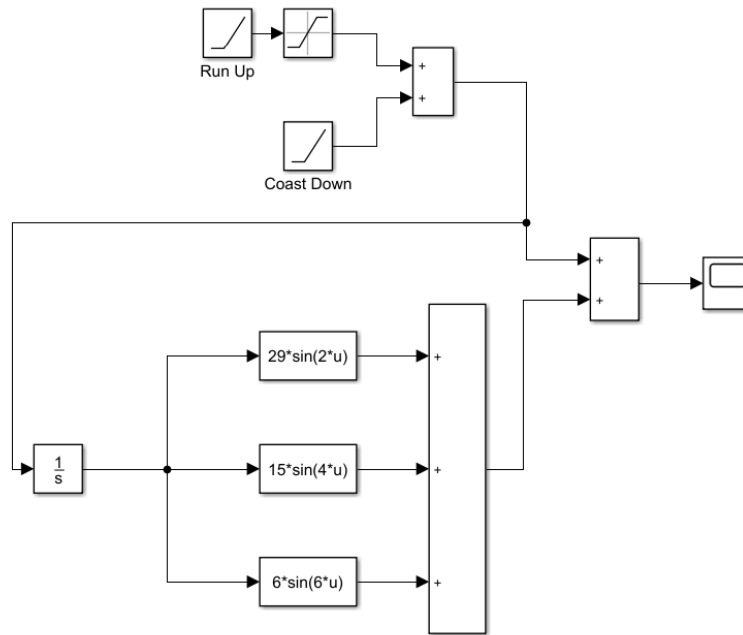


**Figure 3.3:** Simulink model used to build the fictitious flywheel signal

The model is aimed to generate a signal corresponding to a Sweep test characterized by a time duration of 50 s (Run Up of 25 s + Coast Down of 25 s) in which the flywheel speed varies between 800 and 5'000 rpm; integrating this speed signal, the fictitious angular position's signal is obtained. Then using the three function blocks, the harmonic contribution of the 2<sup>nd</sup>, 4<sup>th</sup> and 6<sup>th</sup> orders are added, as function of the angular position, with an amplitude equal respectively to 29, 15 and 6 rpm. The mathematical equation written in explicit form equivalent to the Simulink model is:

$$\omega(t) = \omega_0 + \frac{\partial\omega}{\partial t}t + A_2 \sin(2\theta + \varphi_2) + A_4 \sin(4\theta + \varphi_4) + A_6 \sin(6\theta + \varphi_6)$$

Where:

- $\omega_0$  is the starting speed of the signal (800 rpm);
- $\frac{\partial\omega}{\partial t}$  is the slope of the Run Up/Coast Down phases;

- $A_n$  is the amplitude corresponding to the order  $n$  (respectively 29, 15 and 6 rpm for the orders 2<sup>th</sup>, 4<sup>th</sup> and 6<sup>th</sup>);
- $\varphi_n$  is the phase of the order  $n$  (0 deg for all the orders).

Defining a transmission ratio between the flywheel and the differential's gear and multiplying the flywheel signal with this transmission ratio also a differential speed signal with known harmonic content is available. For this example, the fictitious ratio is assumed equal to 6:1, which is typical value for a third gear. At this point is possible to discuss the procedure to obtain the inertance  $\dot{\omega}_{DIFF}/T_{FLY}$  starting from these two signals, which are depicted in **Figure 3.4**.

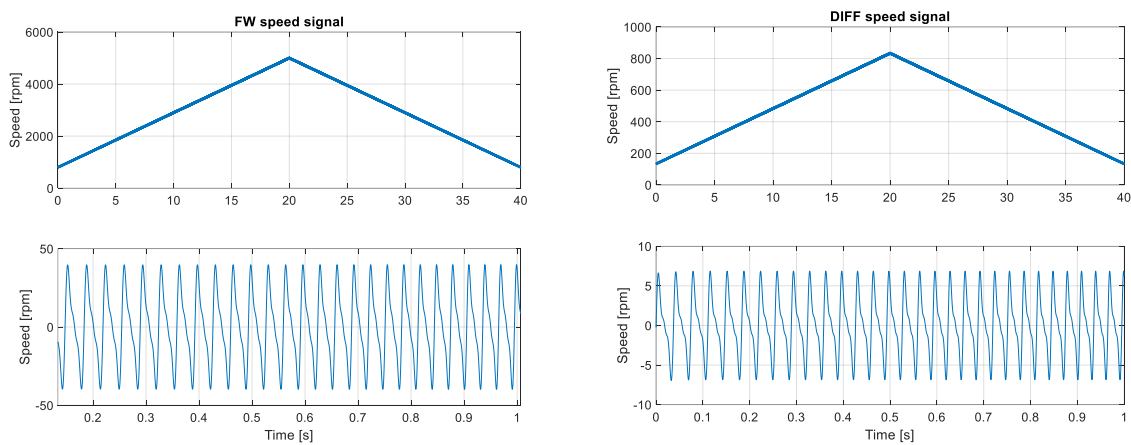


**Figure 3.4:** Fictitious speed signals of the flywheel and of the differential

As has been done for the order analysis, the first step is to perform a synchronous re-sampling of the two signals respect the angular position of the flywheel; after this, the orders spectrogram for both the signal is calculated. The two resulting spectrograms are shown in **Figure 3.5**. The code implementation of these two last passages is reported here.

```

theta=cumtrapz(t,s*6);           % integration of the velocity signal
delta_theta=[0:360/Z_fly:theta(end)]'; % theta axis definition
delta_t=interp1(theta,t,delta_theta,'linear'); % time vector with constant
                                         angular pitch
s_theta=interp1(t,s_det,delta_t,'linear'); % signal as function of theta
Fs_ord=2*max_ord;                % maximum order analysed
ord_res=0.1;                      % forced orders resolution
t_win=1/ord_res;                  % time duration of the windows
WIND=round(t_win*Fs_ord);         % windows dimension
ol=round(0.9*WIND);              % overlap of the windows
[S,O,G]=spectrogram(s_theta>window(@rectwin,WIND),ol,[],Fs_ord);

```

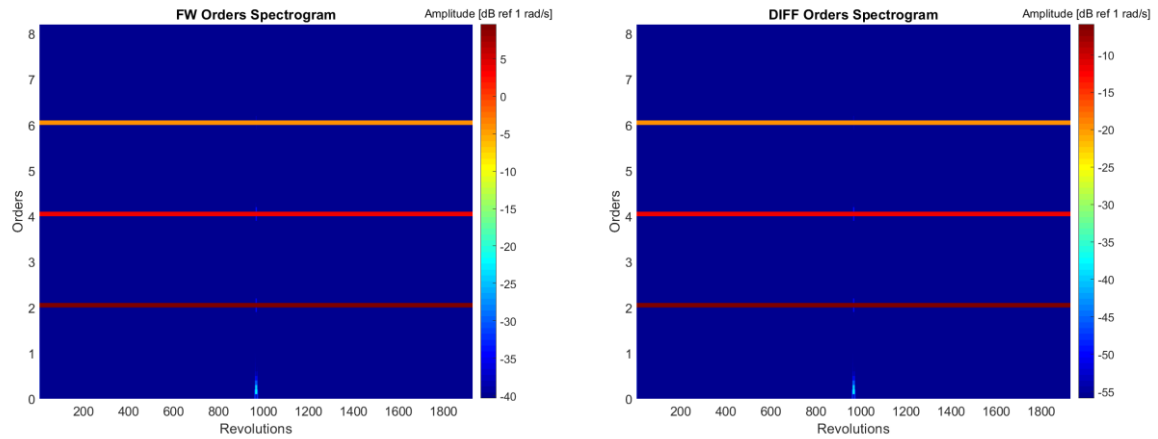


Figure 3.5: Orders spectrograms of the 2 signals

At this point is necessary to extract from the S matrix given by the spectrogram function the values of the lines corresponding to the orders which are interesting for the inertance calculation; since the harmonic content of the signal is known, is sufficient to extract the lines corresponding to the 2<sup>nd</sup>, 4<sup>th</sup> and 6<sup>th</sup> orders. This step is performed in MATLAB with the following commands.

```

for(cont=1:max_ord)                                % extraction of the rows
    ord_int(cont,:)=S(cont*2/ord_res+1,:);
    if(cont==6)
        break
    end
end
end

```

After the extraction of the rows, for each order in interest are now known the values of the amplitude of the velocity oscillations: the accelerations are computed according to the following equation.

$$\dot{\omega} = i \cdot 2 \cdot \pi \cdot f \cdot \omega$$

Where:

- $\dot{\omega}$  is the acceleration corresponding to one of the considered orders;
- $i$  is the imaginary unit;
- $f$  is the frequency;
- $\omega$  is the velocity oscillation of the orders of which the acceleration is calculated.

The frequency can be calculated interpolating the revolutions vector G given as output from the spectrogram between the vector of the angular position of the flywheel theta and the original speed

signal of the flywheel  $s$ . Dividing the obtained value in rpm by 60 the frequency  $f$  is known and the acceleration of each order can be computed.

```

speed=interp1(theta./360,s,G,'linear','extrap'); % computation of the speed
                                                    % s is the original speed signal
                                                    % of the flywheel
f_g=(speed/60); % calculation of the frequency
acc=j*2*pi.*f_g.*ord_int; % accelerations

```

Knowing the value of the accelerations corresponding to each considered order for both the flywheel's and the differential's signals, is necessary to estimate the torque of the engine, considered as approximation equal to the product between the equivalent inertia  $I_{eq}$  and the flywheel's acceleration; obviously, as will be discussed, this approximation will introduce an error negligible under certain conditions. Finally, computing point by point the ratio between the angular acceleration of the differential and the engine's torque, the corresponding inertance is obtained. Since is necessary to verify that the values obtained from the script are equal to what can be analytically calculated as shown in the previous paragraph, is useful to define some reasonable values for the equivalent inertia of the model and for the transmission ratio. In **Table 3.1** are reported these values together with the expected value for the inertance (absolute value and phase) computed according to the 1 d.o.f. model equations.

<b>Value of the inertia <math>I_1</math> (typical value of the inertia of a crankshaft)</b>	0.2	$[kg\ m^2]$
<b>Value of the inertia <math>I_2</math> (reported at the differential)</b>	100	$[kg\ m^2]$
<b>Overall transmission ratio between crankshaft and differential</b>	6	$[-]$
<b>Equivalent inertia <math>I_{eq}</math></b>	2.9778	$[kg\ m^2]$
<b>Expected modulus of the inertance</b>	-25.04	$[dB\ ref\ 1\ \frac{rad}{s^2}]$
<b>Expected phase of the inertance</b>	0	$[deg]$

**Table 3.1:** Values used for the inertance calculation of the 1 d.o.f. model

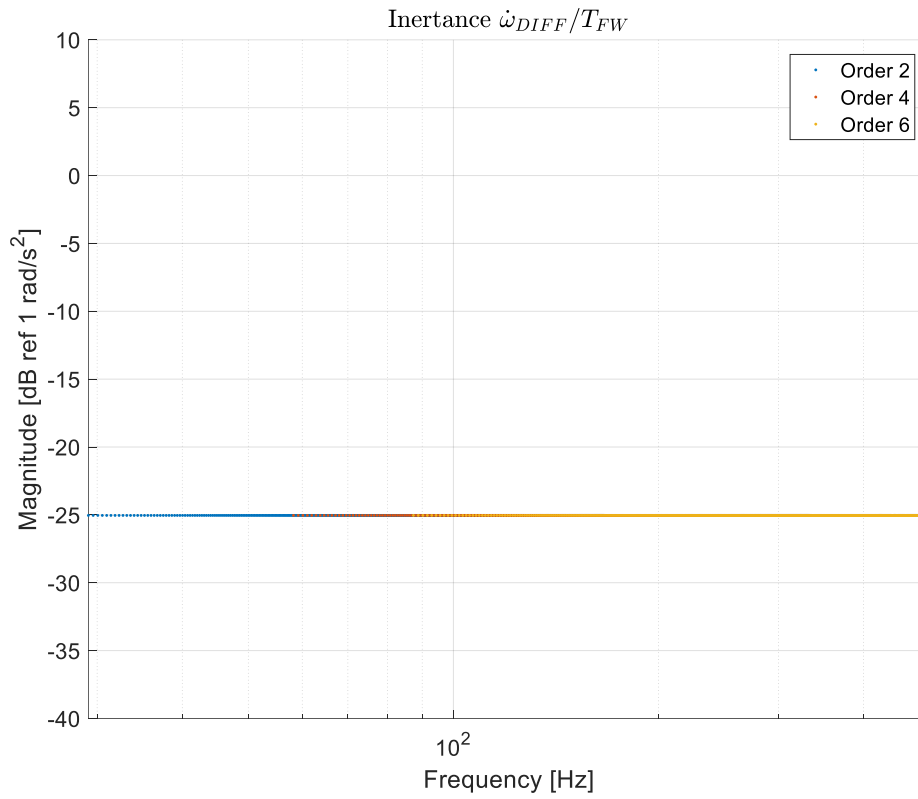


**Figure 3.6:** Inertance of the differential's acceleration respect the engine's torque - Run Up phase

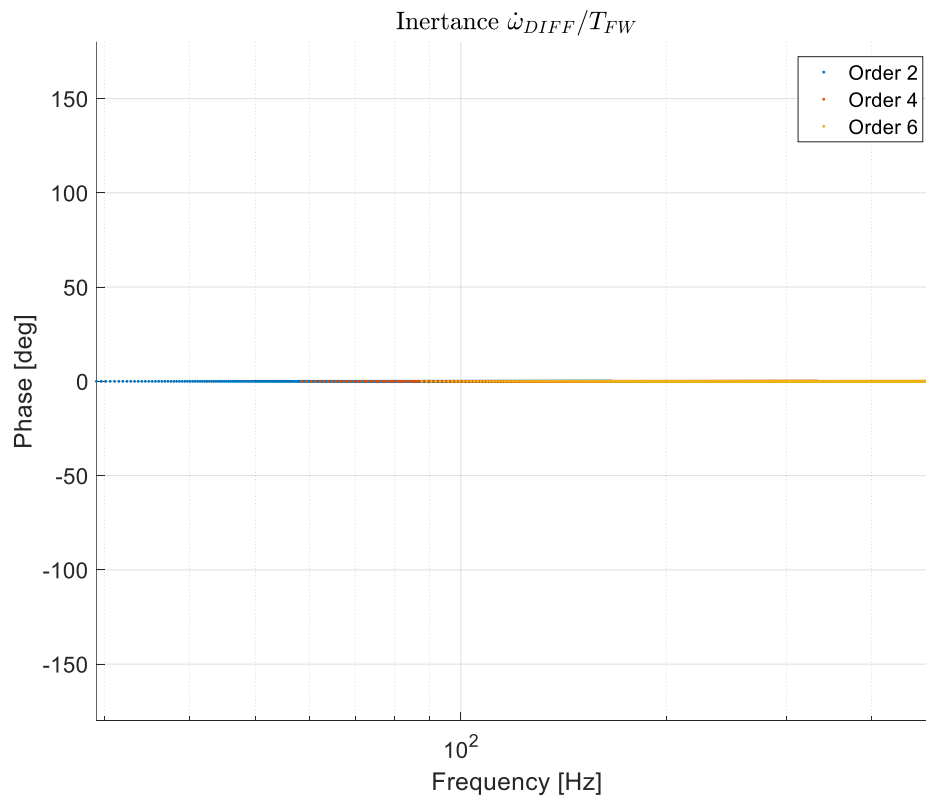


**Figure 3.7:** Inertance of the differential's acceleration respect the engine's torque - Phase

As is possible to see from **Figure 3.6** and **Figure 3.7**, the values obtained from the MATLAB implementation of the FRF experimental algorithm matches with the one coming from the analytic calculations: in fact, considering the modulus, the value matches with the one derived analytically from the 1 d.o.f. model.

$$In_{2,1} = 20 \log_{10} \left( \frac{1}{I_{eq} \tau} \right) = 20 \log_{10} \left( \frac{1}{2.9778 \cdot 6} \right) = -25 \text{ dB ref } 1 \frac{\text{rad}}{\text{s}^2}$$

From a practical point of view, it can occur that the value of the inertia  $I_2$  will not be available, as will happen during the analysis of the data coming from the vehicle experimentation: in these cases, is however possible to compute the torque using only the inertia  $I_1$  and not the value of the equivalent inertia. For this reason, a certain error due to the lower estimation of the torque will occur, consequently giving an overestimation of the inertance; this aspect should be considered when the results are discussed.

In **Figure 3.8** are schematically reported all the operations necessary to compute the inertance of a generic signal respect the engine torque, since as previously said the vehicle's engine is the main source of irregularities that determine the vibrations on the entire powertrain. This procedure, as will be discussed in the next paragraph, will require a further validation before the effective application to the data measured from the vehicle tests.

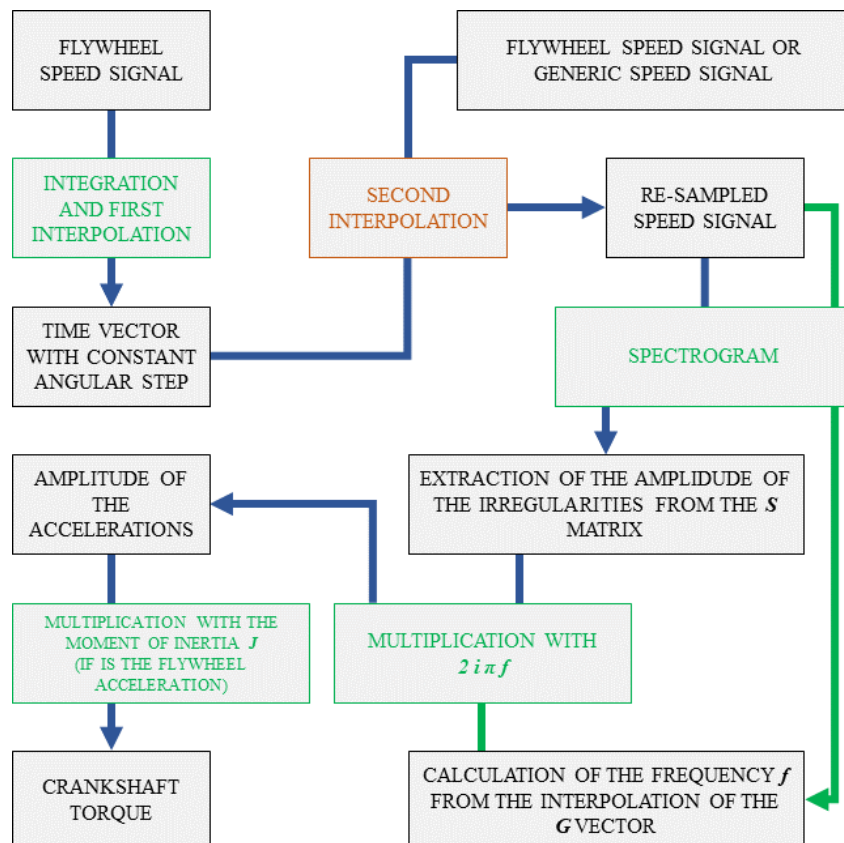


**Figure 3.8:** Block diagram of the operations required to compute the inertance

### 3.3 - MODEL WITH 3 DEGREES OF FREEDOM

As previously anticipated, the model with 1 d.o.f. is excessively simplified to represent the behaviour of part of the powertrain of a real vehicle. For this reason, a model with a larger number of degrees of freedom can be more suitable to validate the procedure described in the last paragraph. Increasing to three the number of the degrees of freedom, a possible solution for the new model for the algorithm validation could be the one shown in **Figure 3.9**.

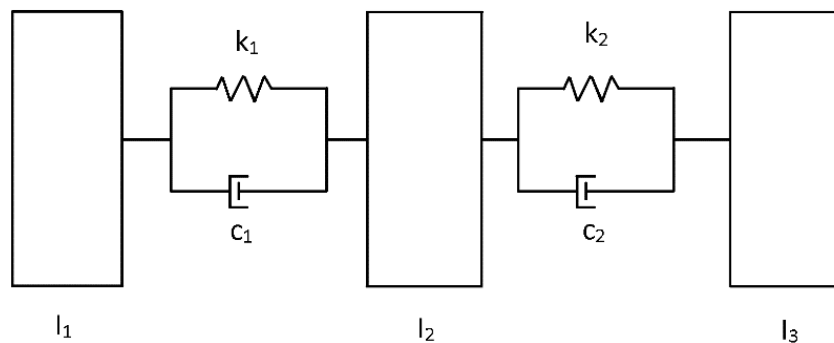


**Figure 3.9:** Model with 3 d.o.f.

Observing the picture, the model is composed by three masses represented by their moments of inertia  $I_1$ ,  $I_2$  and  $I_3$ , while the connection between the masses is represented by damping coefficients ( $c_1$  and  $c_2$ ) and stiffness coefficients ( $k_1$  and  $k_2$ ).

These parameters are used to represent the following vehicle's components:

- The inertia  $I_1$  represents the flywheel;
- The inertia  $I_2$  represents the powertrain's transmission;
- The inertia  $I_3$  represents the equivalent inertia of the vehicle;
- The stiffness coefficient  $k_1$  and the damping coefficient  $c_1$  represents the torsional damper of the flywheel;
- The stiffness coefficient  $k_2$  and the damping coefficient  $c_2$  represents the torsional behaviour of the drive axles and of the transmission.

The first step necessary to perform this validation is the writing of the equation of motion of each one of the three inertias of the model:

$$I_1 \ddot{\theta}_1 + c_1(\dot{\theta}_1 - \dot{\theta}_2) + k_1(\theta_1 - \theta_2) = T_1$$

$$I_2\ddot{\theta}_2 + c_1(\dot{\theta}_2 - \dot{\theta}_1) + c_2(\dot{\theta}_2 - \dot{\theta}_3) + k_1(\theta_2 - \theta_1) + k_2(\theta_2 - \theta_3) = T_2$$

$$I_3\ddot{\theta}_3 + c_2(\dot{\theta}_3 - \dot{\theta}_2) + k_2(\theta_3 - \theta_2) = T_3$$

The system of the three equations of motion in matrix form is the following:

$$\mathbf{I}\ddot{\theta} + \mathbf{C}\dot{\theta} + \mathbf{K}\theta = \mathbf{T} = \begin{Bmatrix} T_1 \\ T_2 \\ T_3 \end{Bmatrix}$$

Where  $\theta$ ,  $\dot{\theta}$  and  $\ddot{\theta}$  are respectively the generalised coordinates vector and his derivatives. Considering the steady state response to harmonic excitation, the forcing term  $T$  can be expressed using the complex notation:

$$T = T_0 e^{i\omega t}$$

The response of the system is harmonic with the same frequency of the forcing function and with a certain phase and amplitude oscillation:

$$\theta = \theta_0 e^{i\omega t}$$

$$\dot{\theta} = i\omega\theta_0 e^{i\omega t}$$

$$\ddot{\theta} = -\omega^2\theta_0 e^{i\omega t}$$

Substituting these expressions in the system of the equations of motion:

$$\mathbf{I}(-\omega^2\theta_0 e^{i\omega t}) + \mathbf{C}(i\omega\theta_0 e^{i\omega t}) + \mathbf{K}(\theta_0 e^{i\omega t}) = T_0 e^{i\omega t}$$

The exponential term can be simplified and the term  $\theta_0$  can be grouped:

$$(-\omega^2\mathbf{I} + i\omega\mathbf{C} + \mathbf{K})\theta_0 = T_0$$

Where:

$$(-\omega^2\mathbf{I} + i\omega\mathbf{C} + \mathbf{K}) = \mathbf{K}_{dyn}$$

Which is the dynamic stiffness matrix. At this point, is possible to directly link the complex vector  $\theta_0$  to the vector of the external torques  $T_0$  computing the inverse of the dynamic stiffness matrix:

$$\theta_0 = (\mathbf{K}_{dyn})^{-1}T_0 = \boldsymbol{\alpha}T_0$$

The matrix  $\boldsymbol{\alpha}$ , the inverse of the dynamic stiffness matrix, is also called receptance matrix, and is important to notice that all the elements of this matrix are functions of the frequency  $\omega$ . Deriving this matrix is possible to obtain the mobility matrix, and with a second derivative the inertance matrix is obtained.

These matrices put in relationship the external torques vector with the corresponding derivatives of the vector  $\theta_0$ :

$$\begin{aligned}\dot{\theta}_0 &= i\omega\alpha T_0 \\ \ddot{\theta}_0 &= -\omega^2\alpha T_0\end{aligned}$$

Where  $i\omega\alpha$  is the mobility matrix and  $-\omega^2\alpha$  is the inertance matrix. The last equation can now be written in explicit form:

$$\begin{Bmatrix} \ddot{\theta}_1 \\ \ddot{\theta}_2 \\ \ddot{\theta}_3 \end{Bmatrix} = -\omega^2 \begin{bmatrix} \alpha_{11} & \alpha_{12} & \alpha_{13} \\ \alpha_{21} & \alpha_{22} & \alpha_{23} \\ \alpha_{31} & \alpha_{32} & \alpha_{33} \end{bmatrix} \begin{Bmatrix} T_1 \\ T_2 \\ T_3 \end{Bmatrix}$$

At this point, since the aim of this model is to evaluate the inertance of a general rotating mechanism of the powertrain respect the torque applied to the engine, is necessary to consider only the last equation of the entire system written in matrix form.

The equation is the following one:

$$\ddot{\theta}_3 = -\omega^2(\alpha_{31}T_1 + \alpha_{32}T_2 + \alpha_{33}T_3)$$

The only external torque applied in the real vehicle is the engine's torque, so consequently the two torques  $T_1$  and  $T_2$  can be set equal to zero:

$$\ddot{\theta}_3 = -\omega^2\alpha_{31}(\omega)T_1$$

Dividing both the sides of the equation by the torque, the inertance  $In_{3,1}$  can be finally computed as:

$$In_{3,1} = -\omega^2\alpha_{31}$$

All the operations described until this point are implemented in the MATLAB code below: in this way, assigning some reasonable values to the inertias, the damping coefficients and the stiffness coefficients of the model, reported in **Table 3.2**, is possible to graphically observe the values of the modulus and the phase of the inertance  $In_{3,1}$ , shown in **Figure 3.10**.

```
%% 3 DOF model's parameters
I1=0.2;
I2=0.05;
I3=2.7278;
```

```

K1=800;
K2=25000;
c1=2;
c2=5;
%% matrices definition
M=diag([I1,I2,I3]);
K=[K1,-K1,0;-K1,K1+K2,-K2;0,-K2,K2];
C=[c1,-c1,0;-c1,c1+c2,-c2;0,-c2,c2];
%% for cycle for the computation of the receptance, mobility and inertance matrices
% frequency vector
f=logspace(-1,3,1000);
w_vet=2*pi*f;
for cont=1:length(w_vet)
    w=w_vet(cont);
    K_dyn=(K+i*w*C-M*w^2);           % dynamic stiffness matrix
    Rec=K_dyn^-1;                   % receptance matrix
    Mob=j*w*Rec;                     % mobility matrix
    Iner=-w^2*Rec;                   % inertance matrix
    % extraction of the FRFs in interest
    Iner_31(cont)=Iner(3,1);         % response w3_dot/T1
    Iner_13(cont)=Iner(1,3);         % response w1_dot/T3
    Iner_11(cont)=Iner(1,1);         % autoinertance w1_dot/T1
end

```

$I_1$	0.2	$[kg\ m^2]$	$C_1$	2	$[Nm\ \frac{s}{rad}]$	$K_1$	800	$[\frac{Nm}{rad}]$
$I_2$	0.05	$[kg\ m^2]$	$C_2$	5	$[Nm\ \frac{s}{rad}]$	$K_2$	40'000	$[\frac{Nm}{rad}]$
$I_3$	2.7278	$[kg\ m^2]$						

**Table 3.2:** Numerical values assigned to the 3 d.o.f. model's parameters

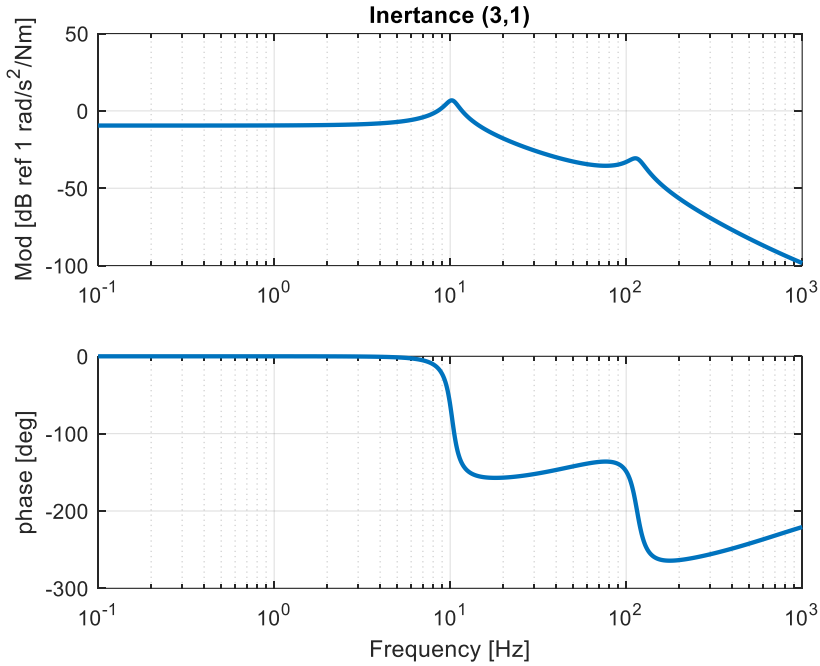


**Figure 3.10:** Inertance  $In_{3,1}$  - Amplitude and phase

In order to easily compare the results of this model to the results of the 1 d.o.f. model, the following criteria have been used to set the values of the parameters of the model, representing with a certain realism a vehicle's powertrain:

- The sum of the three inertia is equal to the equivalent inertia of the 1 d.o.f. model;
- The inertia of the first mass is equal for both the models;
- The inertia  $I_3$  has the value of the inertia reported to the crankshaft of a vehicle of 1'080 kg with a wheel radius of 0.3 m and a transmission ratio equal to 6, as in the 1 d.o.f. case;
- The value of the stiffness  $K_1$  is a typical value for a DMF;
- The stiffness  $K_2$  is equivalent to the stiffness of a drive shaft reported to the crankshaft.

In the same way that has been computed the inertance  $In_{3,1}$ , is possible to compute the inertance  $In_{1,1}$ , also called auto-inertance, which is defined as the ratio between the angular acceleration  $\ddot{\theta}_1$  (i.e. the angular acceleration of the crankshaft) and the applied torque  $T_1$ . The plot of the auto-inertance of the model is depicted in **Figure 3.11**.

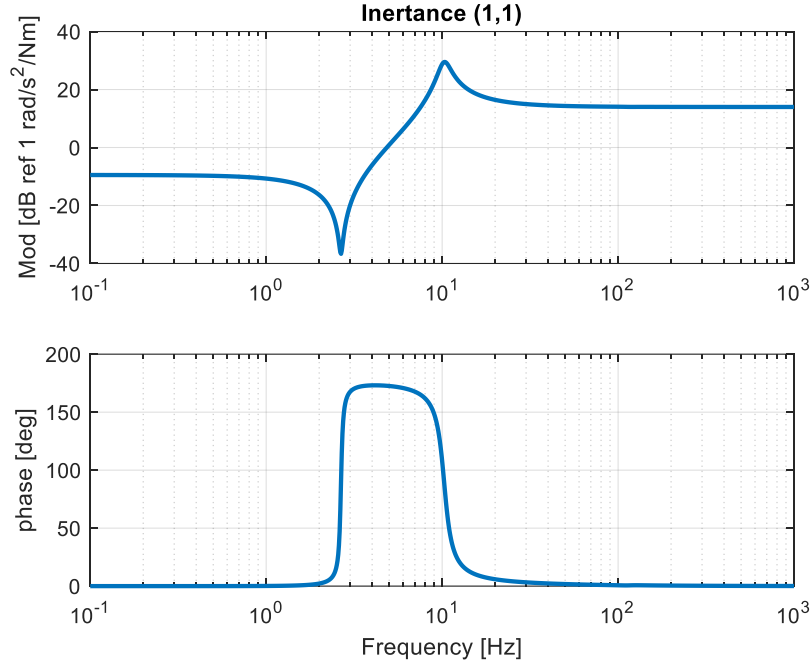


**Figure 3.11:** Inertance  $In_{1,1}$  - Amplitude and phase

Looking at the values of the modulus of the auto-inertance, is clear that in a certain range of frequency the inertance is characterized by an anti-resonance peak followed by a resonance peak. Outside of this range, the values of the inertance tends asymptotically to certain values; is of fundamental importance to notice that the asymptotic value for frequencies tending to 0 is different from the value of the inertance for frequencies tending to infinite. In particular, for high frequencies the inertance tends to a value equal to the reciprocal of the inertia  $I_1$ , while for low frequencies the inertance tends to a lower value, because all the masses of the system participate to the low frequency vibration and so the inertia to be considered in this case is given by the sum of the three inertias:

$$In_{1,1,lf} = 20 \log_{10} \left( \frac{1}{I_1 + I_2 + I_3} \right) = 20 \log_{10} \left( \frac{1}{2.9778} \right) = -9.478 \text{ dB ref } 1 \frac{\text{rad}}{\text{s}^2}$$

Value from MATLAB:

$$In_{1,1,lf} = -9.489 \text{ dB ref } 1 \frac{\text{rad}}{\text{s}^2}$$

The same verification is performed for the frequencies tending to infinite:

$$In_{1,1,hf} = 20 \log_{10} \left( \frac{1}{I_1} \right) = 20 \log_{10} \left( \frac{1}{0.2} \right) = 13.98 \text{ dB ref } 1 \frac{\text{rad}}{\text{s}^2}$$

For high frequencies, the value obtained from the model is:

$$In_{1,1,hf} = 13.98 \text{ dB ref } 1 \frac{\text{rad}}{\text{s}^2}$$

This trend is very important because since in the experimental data the signal of the engine's torque is not available, as already seen the torque value is approximated as the product between the instantaneous acceleration of the crankshaft and its inertia. For this reason, the torque estimation performed in this way can be considered sufficiently reliable only for sufficiently high frequencies. Consequently, is necessary to define a frequency value, corresponding to the point in which the maximum admissible error is made, from which the estimation can be considered reliable; for this reason, a tolerance band with the width of  $\pm 1$  dB is defined.

The tolerance band is shown in **Figure 3.12**: from this operation, the frequency value from which the estimation can be defined as reliable is set at 30 Hz.

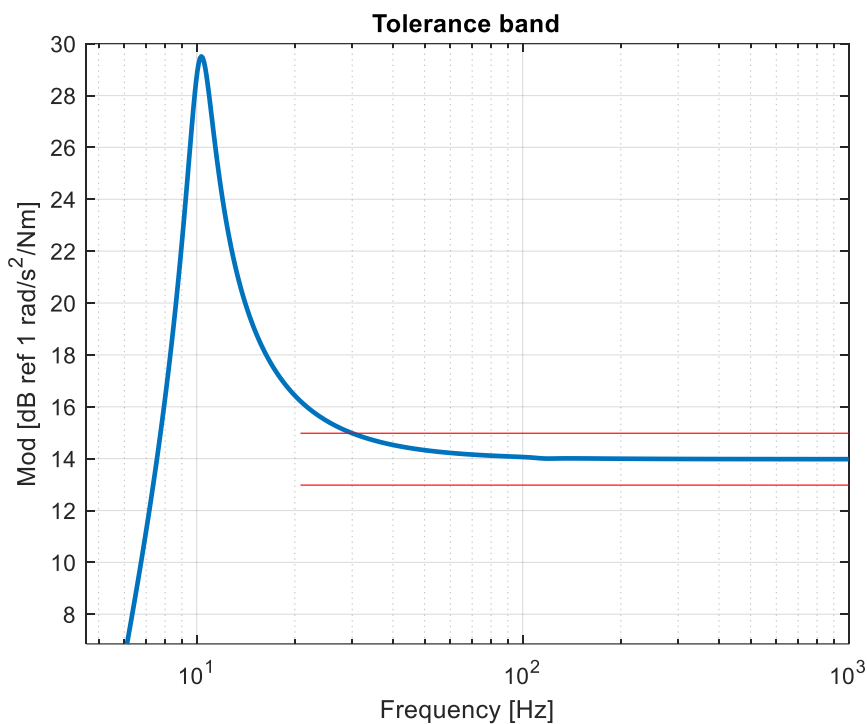


**Figure 3.12:** Application of the tolerance band for the definition of the reliable frequencies range

Since all the data are referred to a 4 stroke 4 cylinders engine, the frequency of 30 Hz corresponds to the value of the firing frequency a 900 rpm: this means that the estimation has an error lower than 1 dB for rotational speed higher than this value. At this point, the next step is to compute the response of the 3 d.o.f. model given by an arbitrary external torque  $u(t)$ . This response is computed through the convolution integral of the external torque and the response of the system to the impulse  $h(t)$ .

In general, the convolution integral is defined as:

$$x(t) = \int_0^t F(t - \tau)g(\tau)d\tau$$

Where:

- $F(t)$  correspond to the external torque;
- $g(\tau)$  is the impulse response of the system;
- $\tau$  is a dummy variable of integration.

In order to compute the impulse response of the system, which is an intrinsic characteristic of the system, is useful to remember that the FFT of the impulse response of a system corresponds to its frequency response function; consequently, since the inertance  $In_{3,1}$  is already known, is possible to reconstruct the impulse response of the system applying an Inverse Fast Fourier Transform (IFFT) to the FRF. From a practical point of view, since the entire operation of the impulse response computation will be performed in the MATLAB environment, two additional steps are necessary before the application of the IFFT algorithm.

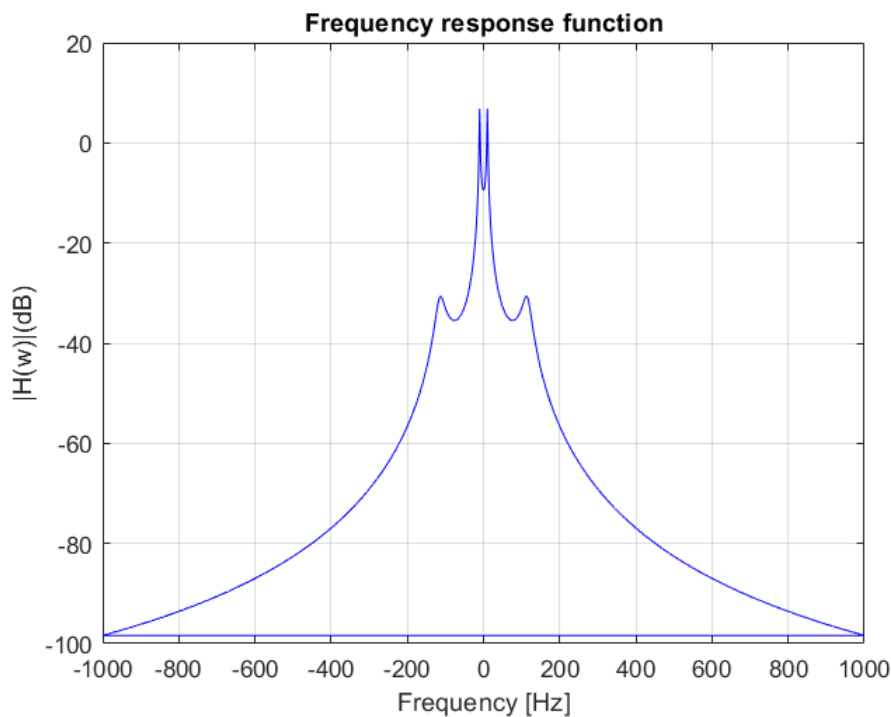


**Figure 3.13:** FRF of the model mirrored for negative frequencies

The first step consists in the symmetric mirroring of the inertance  $In_{3,1}$  respect the  $y$  (modulus) axis, in order to obtain the value of this inertance for frequencies ranging from  $-F_S/2$  to  $F_S/2$  where  $F_S$  is the sampling frequency for which the inertance has been defined in the script of the 3 d.o.f. model. Results for this first step are shown in **Figure 3.13**. The second step is aimed to adjust the sampling frequencies of the inertance and the one of the arbitrary external torque's signal for which the response must be computed: this operation is performed through an interpolation of the inertance's FRF respect the frequency points at which the input signal is defined.

After this, is possible to apply the IFFT algorithm obtaining the impulse response of the system, shown in **Figure 3.14**. The code implementation of these passages is the following.

```

%% engine's torque estimation:  $T = I \cdot \dot{w}$ 
w_eng=n_eng*pi/30;           % n_eng is the generated speed signal
w_dot=diff(w_eng)./diff(t_n_eng); % derivation for acceleration's calculation
T_eng=I1*w_dot;             % torque calculation
%% 3 DOF response due to the torque input
% input definition
u=T_eng;
t=t_n_eng ;
% inertance(3,1) : amplitude and phase
F=f;
AMP=abs([Iner_13]);
PHA=180/pi*phase([Iner_13]);

```

After the resampling of the two signals, the response to the given input is computed with the code below.

```

% FRF vector that meets IFFT requirements
H=AMP.*exp(1i*PHA*pi/180);
%% impulse response
h_imp_FEM_=ifft(H).*N/T; % N/T is a correction for the time window
                        % N is the number of points of the time vector
                        % T is the input's time duration
%% convolution, time-domain
w_3_dot_ = (conv(u,h_imp_FEM_))*dt; % dt is the reciprocal of the sampling frequency

```

The second input required for the convolution integral is the signal of the input external torque; for simplicity, this torque signal is built starting from the same velocity signal (fictitious flywheel speed signal) given as input for the 1 d.o.f. model described previously; deriving this signal and multiplying it for the inertia  $I_1$ , the value of the external torque  $T_1$  is available.

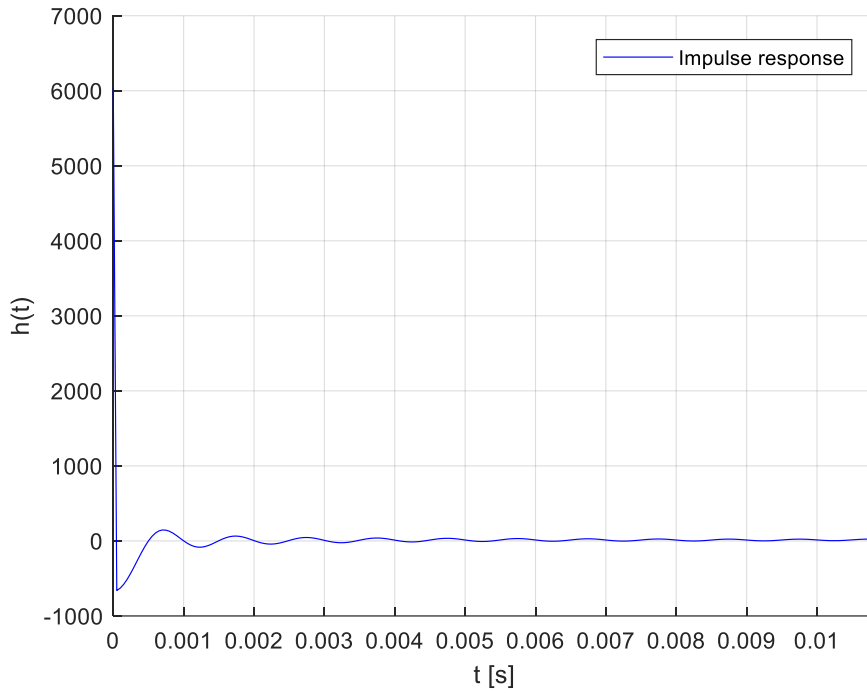


**Figure 3.14:** Impulse response of the 3 d.o.f. model's system

Finally, applying the convolution integral the response of the system to this particular input external torque is calculated: this value corresponds to the instantaneous acceleration  $\ddot{\theta}_3$  given by the defined external torque's signal. The trend of this acceleration is depicted in **Figure 3.15**.

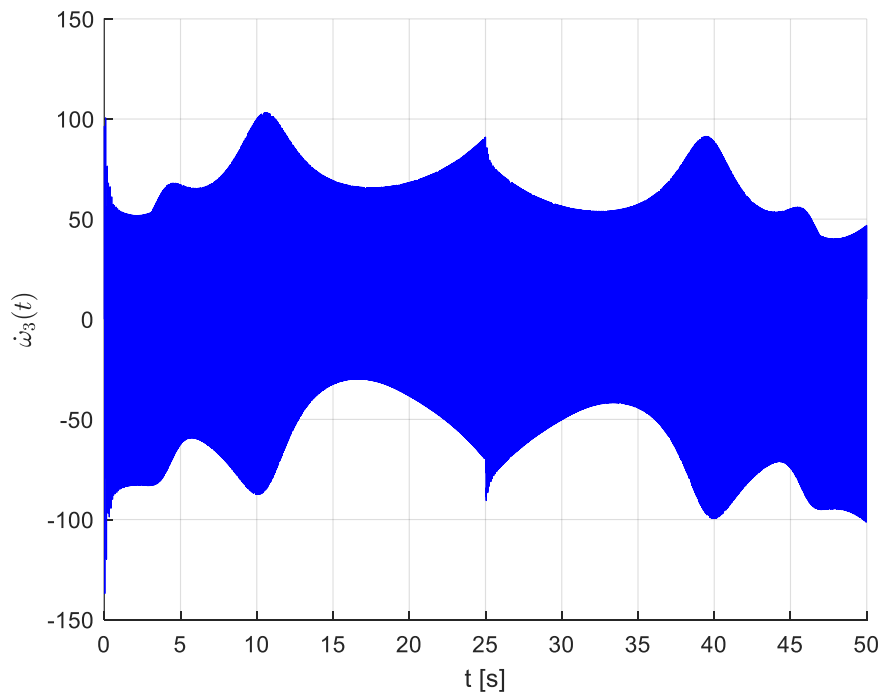


**Figure 3.15:** Response of the system to the defined input

Since the experimental FRF estimation algorithm is constructed to compute the inertance starting from two speed signals, in order to validate also this step of the code is useful to run the script giving as inputs the speed signal with known harmonic content used to compute the torque  $T_1$  and the speed signal  $\dot{\theta}_3$ : this signal can be computed by integrating the instantaneous acceleration's signal and adding the starting value of the signal. In this case, the added starting value is equal to the starting value of the input speed signal, in this case equal to 800 rpm. Now, is possible to run the experimental FRF algorithm and to compare these inertance results to the inertance analytically computed from the 3 d.o.f. model.

### 3.4 - VALIDATION OF THE FRF ESTIMATION ALGORITHM BASING ON THE 3 D.O.F. MODEL RESULTS

As already said, a second validation of the FRF algorithm using the results of the 3 d.o.f. model described in the previous paragraph is needed. In order to consider validated the operation performed by the code, the inertance computed using as input the two signals of speed of the first and the third mass of the 3 d.o.f. model should approximate with a relatively small error the inertance derived from the model shown in **Figure 3.9**. These two speed signals are depicted in **Figure 3.16**.

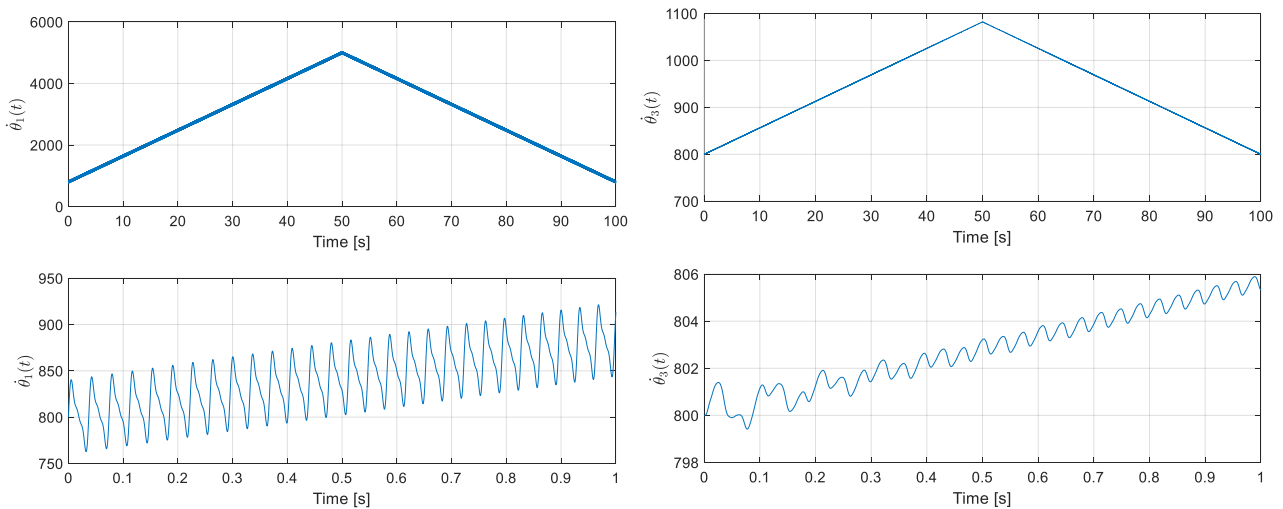


**Figure 3.16:** Speed signals of the model: speed of the first inertia (on the left) and of the third inertia (on the right)

After the usual resampling of the two signals respect the angular position of the first mass (i.e. the crankshaft), the two orders spectrograms are computed and depicted in **Figure 3.17**.

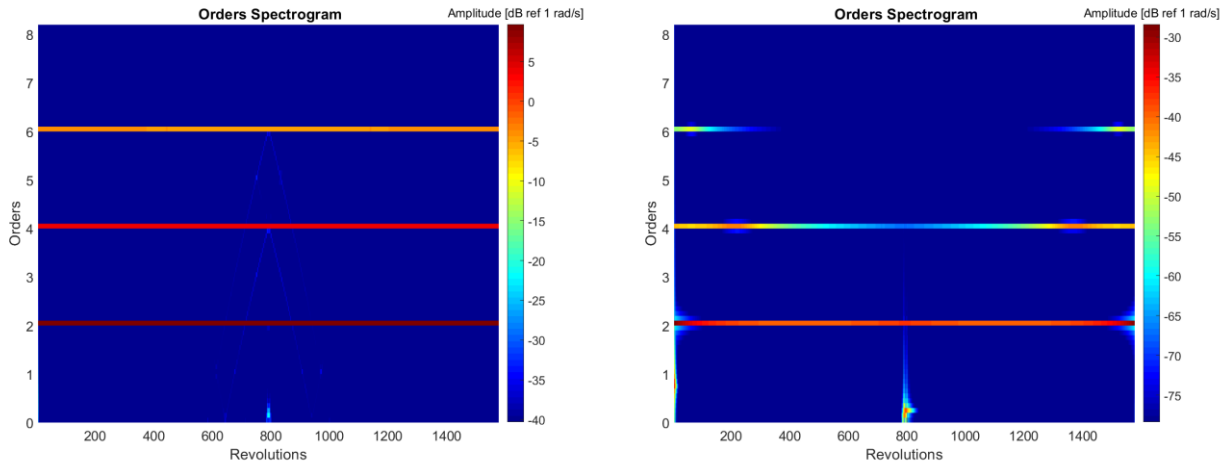


**Figure 3.17:** Orders spectrograms of the 2 signals

Using the same procedure of extraction of the rows from the  $S$  matrix corresponding to the orders in interest (2<sup>nd</sup>, 4<sup>th</sup> and 6<sup>th</sup> orders) and computing for each order the acceleration as function of the particular frequency, is possible to proceed with the inertance calculation. As already specified, is important to remember that since the torque applied to the first mass is approximated as the product  $T_1 = I_1 \ddot{\theta}_1$ , this approximation is valid only for sufficiently high frequencies. At this point, the inertance is computed both in terms of amplitude and phase, and the results are shown in **Figure 3.18** and **Figure 3.19** in comparison with the inertances derived from the 3 d.o.f. model.

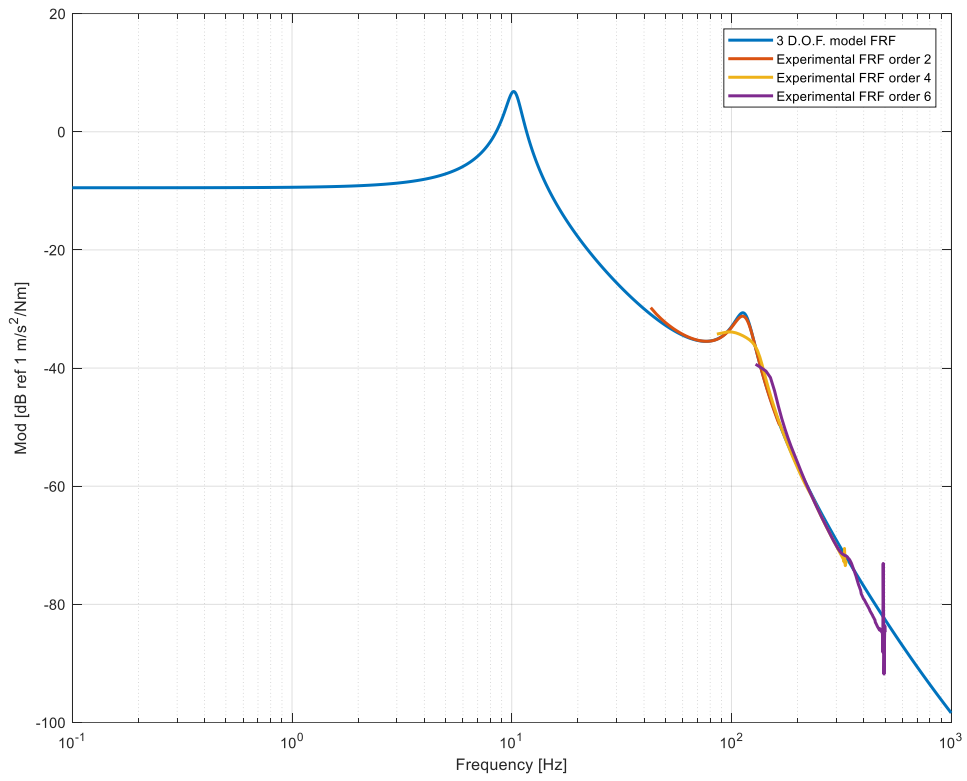


Figure 3.18: Comparison between the experimental inertance and the one of the model - Amplitude

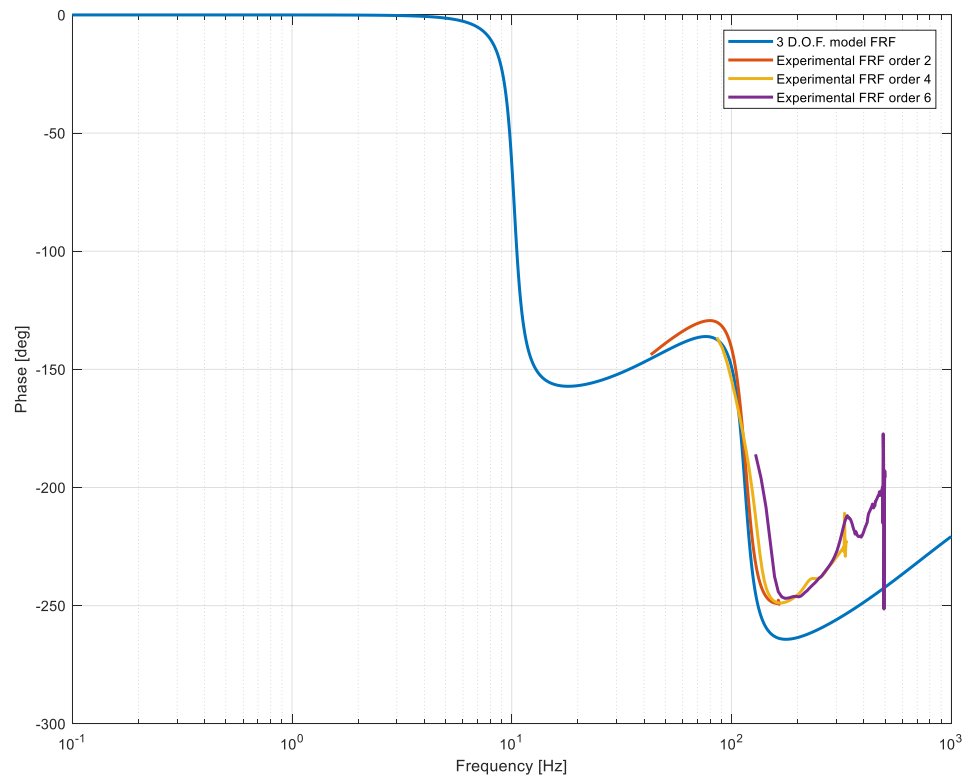


Figure 3.19: Comparison between the experimental inertance and the one of the model - Phase

As is possible to see from the plots, the experimental algorithm approximates the analytic results obtained from the 3 d.o.f. model with sufficient accuracy. With this second validation, it is possible to assert that the application of the MATLAB script to the experimental data coming from the measurements on the vehicle will give results with an acceptably low error level. However, at the extremes of the frequency range of the three orders, and more in particular for the 4<sup>th</sup> and the 6<sup>th</sup> ones, there are some points in which the value of the FRF has a significative difference from the results of the 3 d.o.f. model; for this reason, the range of frequency of each order is shortened with the following criteria:

- The 2<sup>nd</sup> order is plotted for the full range;
- The 4<sup>th</sup> order's range starts at the end frequency of the range of the 2<sup>nd</sup> order;
- The 6<sup>th</sup> order's range starts at the end frequency of the range of the 4<sup>th</sup> order.

Also at the end of the frequency range of the 6<sup>th</sup> order some values show a significative error: however, in practical application also the contribution of the orders higher that the 6<sup>th</sup> are considered, so in this range the considered values of inertance will correspond to a higher order, as example the 8<sup>th</sup>.

In this way, the resulting FRF plots are depicted in **Figure 3.20** and **Figure 3.21**.

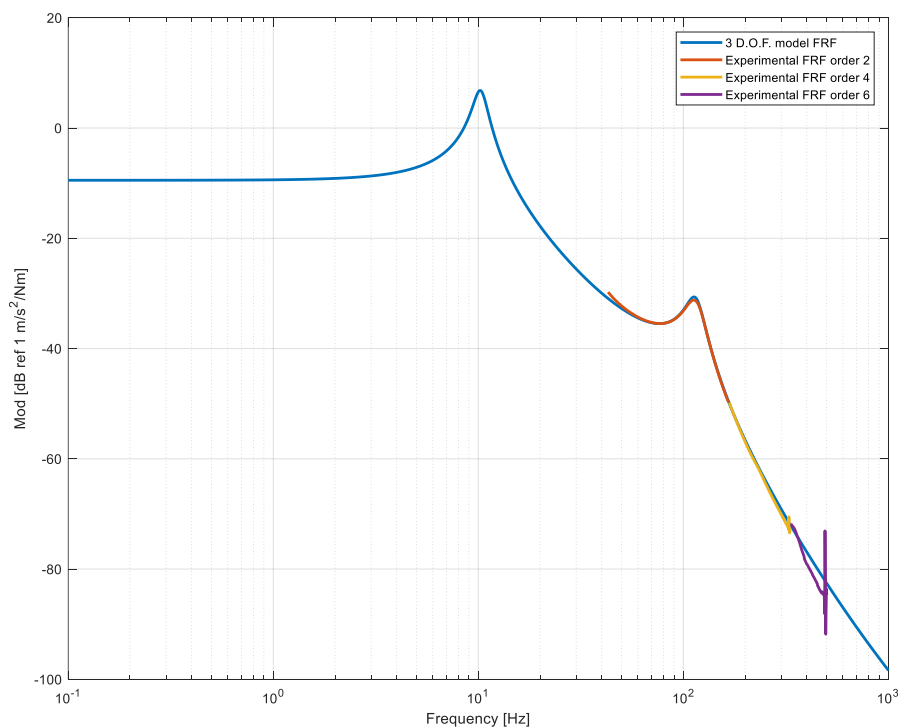


**Figure 3.20:** FRF's amplitudes comparison - Shortened frequency range

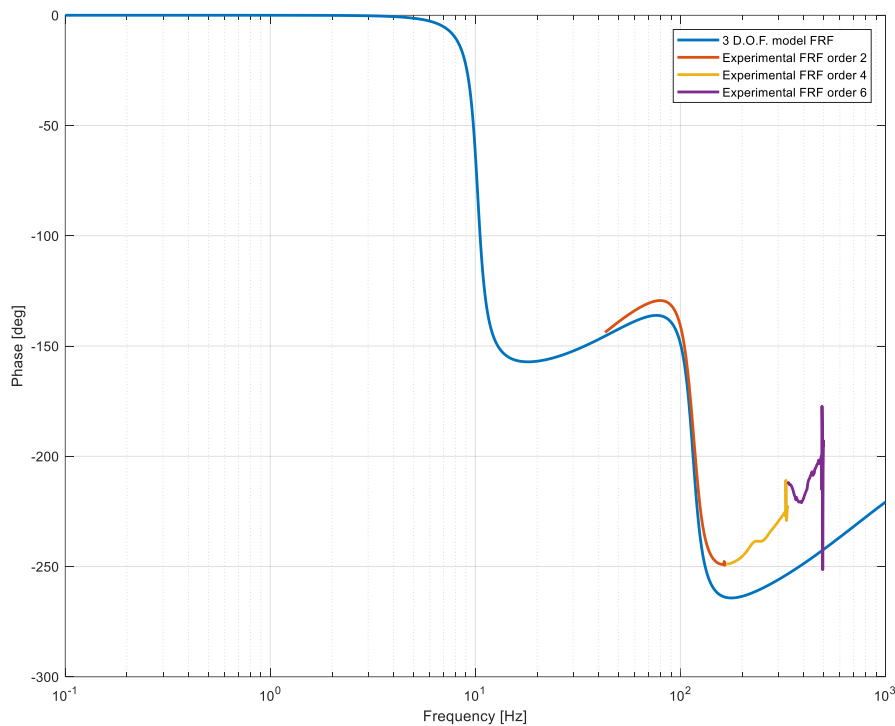


**Figure 3.21:** FRF's phases comparison - Shortened frequency range

Is noticeable that the FRF estimation is defined in a range of frequencies compatible with an engine's torque estimated for values higher than 40 Hz.

Considering now the MATLAB implementation of the 3 d.o.f. model and the application of the FRF estimation algorithm to its results, is possible to observe that several different parameters are defined in order to generate the two speed signals used as input by the FRF algorithm. Is very useful to change these parameters to control the behaviour of the output results: if also varying these parameters the output of the algorithm approximates the inertances of the model with a reduced error, the script will be verified and it will be used to analyse the experimental data coming from the on-vehicle measurements.

In the MATLAB script of the 3 d.o.f. model, there are two main parameters that can affect the results obtained from the FRF algorithm:

- The time duration of the Run Up (and Coast Down) phase, i.e. the slope of these phases, since a higher slope means a faster transition through the frequency range for each order;
- The amplitudes of the three harmonics components.

Considering the first results used for the validation of the algorithm (**Figure 3.20** and **Figure 3.21**), the corresponding values for the three parameters are reported in **Table 3.3**.

Sampling frequency	Phases time duration	Harmonic's amplitudes
2'000 Hz	25 s	29-15-6 rpm

**Table 3.3:** Parameters of the 3 d.o.f. model signals for the previous results

Now, if the two parameters are varied one by one, is possible to separately observe the effects on the results. Two different analyses are carried on with the parameters described in **Table 3.4**.

#	Sampling frequency [Hz]	Phases time duration [s]	Harmonic's amplitudes [rpm]
1	2'000	10	58-30-12
2	2'000	50	29-15-6

**Table 3.4:** Parameters of the 3 d.o.f. model's signals varied for the final validation

The results of the first case in terms of amplitude and phase are shown in **Figure 3.22** and **Figure 3.23**.

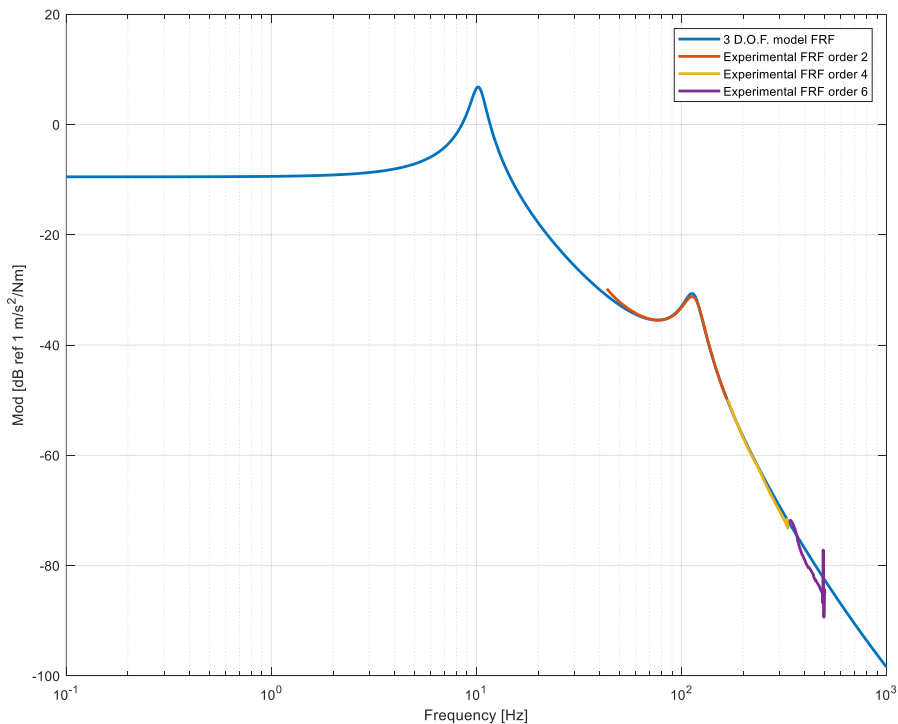


**Figure 3.22:** FRF's amplitudes comparison - Variation of orders amplitude

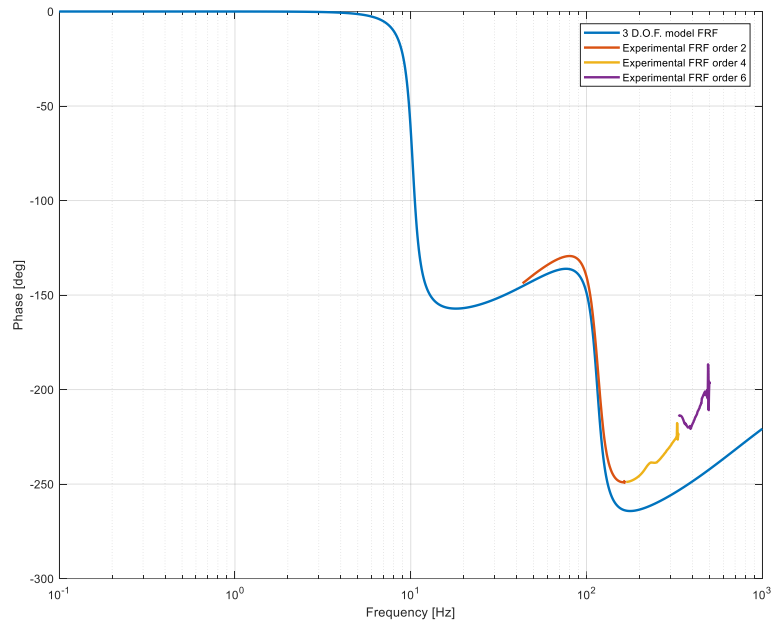


**Figure 3.23:** FRF's phases comparison - Variation of orders amplitude

As is possible to see from the graphical results, the variation of the amplitudes of the harmonic components of the generated input signal of the 3 d.o.f. model gives rise to a small error only in terms of phase: the amplitudes results remain practically unchanged.

Considering now the variation of the time duration of the Run Up and Coast Down phases (case #2), the resulting plots are the ones in **Figure 3.24** and **Figure 3.25**.

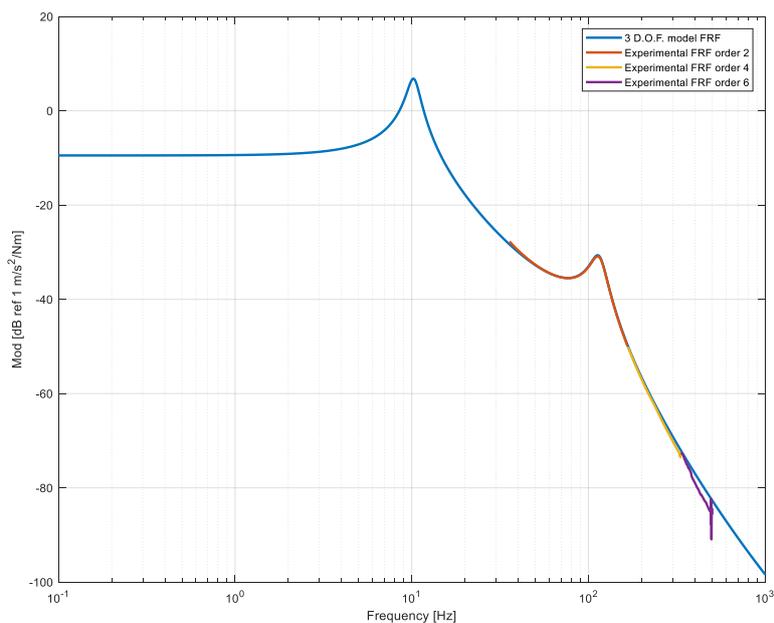


**Figure 3.24:** FRF's amplitude comparison - Variation of Sweep phases durations

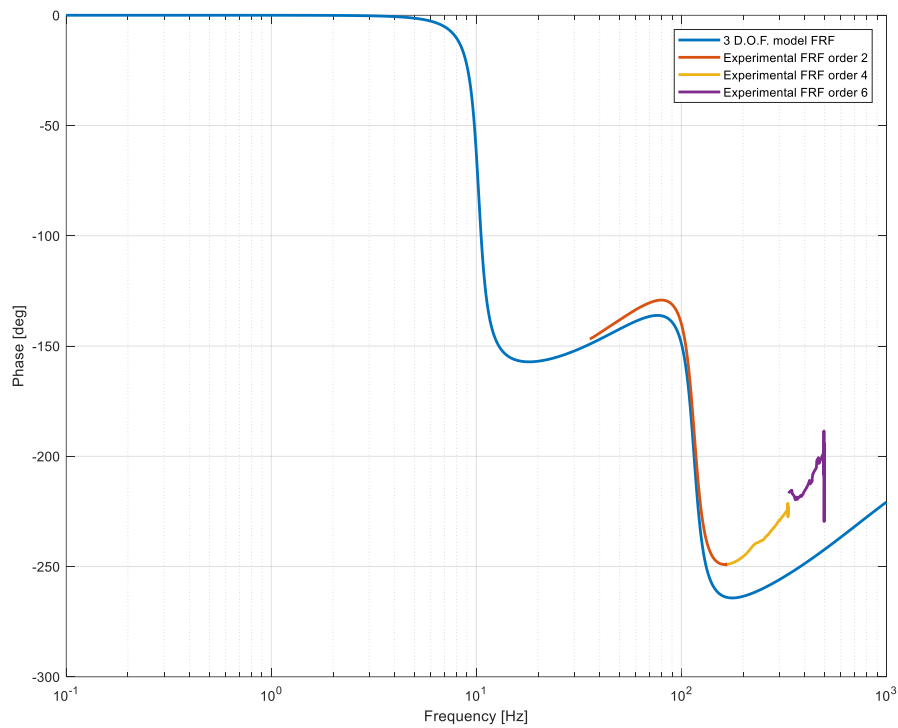


**Figure 3.25:** FRF's phases comparison - Variation of Sweep's phases duration

Also in this case, the main difference is visible in terms of phase, while considering the amplitudes the difference between this and the previous case are negligible.

At this point, the FRF estimation algorithm can be finally considered valid for the analysis of the experimental data. However, in some cases during this analysis, it could be necessary a tuning procedure on the parameters of the estimation algorithm, depending on the particular trend and characteristics of each signal used as input for the script.

## 4 - EXPERIMENTAL SETUP AND MEASUREMENTS

### 4.1 - VEHICLE CHARACTERISTICS

All the amount of data used during this work have been acquired on the same vehicle during several different tests. The vehicle employed is displacing a 1.4 L supercharged gasoline engine with front wheels drive; the engine is coupled with a Dual Clutch Transmission (DCT) gearbox, of which the vibrational behaviour is the main topic of this work. The main technical details of the vehicle are listed in **Table 4.1**.

<b>Vehicle's data - C segment passenger car</b>	
<b>Displacement</b>	1'368 cm <sup>3</sup>
<b>Max power</b>	125 kW at 5'500 rpm
<b>Max torque</b>	250 Nm
<b>0-100 km/h</b>	7.7 s
<b>CO<sub>2</sub> emissions</b>	121 g/km
<b>NEDC fuel consumption</b>	5.2 L / 100 km

**Table 4.1:** Technical data of the vehicle

### 4.2 - DUAL CLUTCH GEARBOX

The gearbox installed on the vehicle, as previously said the DCT with dry clutches (DDCT), characterized by 6 gears plus the reverse and a maximum transmissible torque of 350 Nm. The gearbox is composed by two coaxial primaries shafts: the shaft of the odd gears is the internal one, while the primary shaft of the even gears is external and hollow; the relative rotation between the two shaft is guaranteed by two bearings installed between them. The primary shaft of the odd gears is connected to one of the two secondary shafts, which is called Lower Secondary Shaft (LSS) and supports the 1<sup>st</sup>, 3<sup>rd</sup> and 5<sup>th</sup> gears; the other primary shaft is connected to the Upper Secondary Shaft, which carries the 2<sup>nd</sup>, 4<sup>th</sup>, 6<sup>th</sup> and reverse gears. Each primary shaft is connected to one clutch: the shaft of the odd gears is connected to a normally closed clutch called K1, while the other shaft is connected to the normally opened K2 clutch. Both the two secondary shafts are connected to the final drive, so from an operational point of view the DCT gearbox behaves as two different gearboxes working in synergy.

In **Figure 4.1** the layout of the gears and the bearings of the gearbox are schematically depicted.

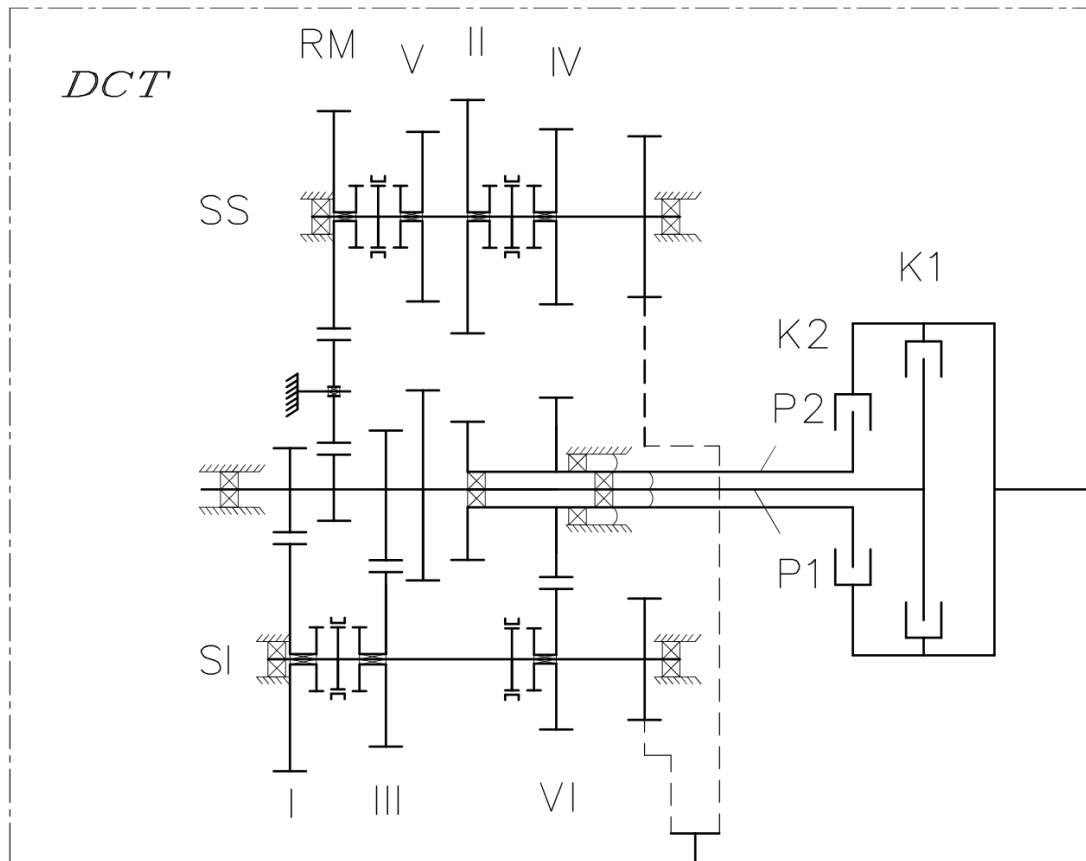


**Figure 4.1:** Schematic representation of gears and bearing in the gearbox

One particularity of the two clutches is that the K1 clutch is commanded by a hydraulic actuator controlled in terms of position, while the K2 clutch actuator is also hydraulic but controlled by the force exerted on the plate (i.e. hydraulic pressure). Also the selectors of the gears are actuated by means of a complex hydraulic system, fed by an accumulator containing oil at the pressure of 60 bar which is connected to a hydraulic circuit directly machined on the internal part of the gearbox's case; the system is controlled by electronically actuated valves which operates the engagement and disengagement of the gears. All the operations are controlled by an electronic module that contains the angular velocity sensors of the gears and the positions sensors of the different actuators.

In **Figure 4.2** is shown the CAD model of the assembly of the entire gearbox, in which is visible the Double Mass Flywheel (in grey), the oil accumulator (purple), the actuators system (light blue) and the case of the gearbox (yellow) in which the hydraulic circuit is machined. Is also possible to notice on the left figure the actuator of the K1 clutch.

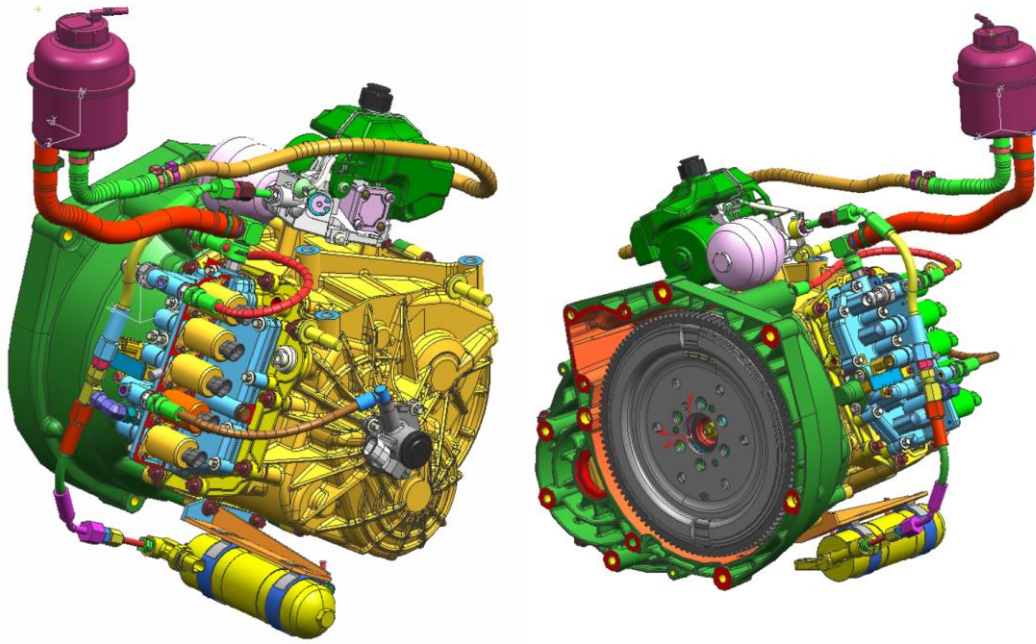


Figure 4.2: 3D CAD model of the gearbox

### 4.3 - LAYOUT OF THE SENSORS INSTALLED DURING THE TESTS

Since a lot of data are necessary to validate the models of the gearbox, different type of sensor have been installed on the vehicle during the tests. In this paragraph the different sensors are listed and for each sensor the positions in which the sensors of that type have been installed are indicated.

#### 4.3.1 - PICK-UPS

During the tests, several pick-ups are used to measure the angular velocity of some gears of which this information is not already available on the CAN network of the vehicle. In total seven pick-ups are installed on the vehicle; the main parameters of the pick-ups are the acquisition frequency, equal to 20 kHz for all of them, and the sensitivity, which depends on the number of teeth of the gear of which the velocity signal is sampled. The seven speed signals are acquired using an LMS acquisition system.

Is necessary to specify that the measure unit of the signals acquired is the  $rev(diff)$ : this unit is defined as the angle travelled during one sampling interval. To convert this unit in revolutions per minute (rpm), the following formula is used:

$$n[rpm] = n[rev(diff)] * 60 * Fs$$

Where  $F_s$  is the sampling frequency of the signal.

In **Table 4.2** the positions of the different sensors are listed, indicating also the sensitivity of each pick-up.

#	Position	Sensitivity	Acquired signal	Unit
1	2 <sup>nd</sup> mass of the DMF	$Z = 135$	n_FW	<i>rev(diff)</i>
2	1 <sup>st</sup> gear on the LSS	$Z = 13$	n_I	<i>rev(diff)</i>
3	2 <sup>nd</sup> gear on the USS	$Z = 25$	n_II	<i>rev(diff)</i>
4	3 <sup>rd</sup> gear on the LSS	$Z = 23$	n_III	<i>rev(diff)</i>
5	Pinion of the USS	$Z = 16$	n_SS	<i>rev(diff)</i>
6	Pinion of the LSS	$Z = 16$	n_SI	<i>rev(diff)</i>
7	Differential's crown	$Z = 71$	n_DIFF	<i>rev(diff)</i>

**Table 4.2:** Positions of the pick-ups installed on the vehicle's powertrain

#### 4.3.2 - ACCELEROMETERS

Since the measurements of the accelerations is a very important data necessary to characterize the vibrational behaviour of the gearbox, several MEMS accelerometers have been placed in the vehicle's powertrain. The working principle of these accelerometers is based on a seismic mass connected to two conductive plates: when the seismic mass oscillates, a variation on the capacitance of the two plates occurs and this variation is converted into an analog signal through an Application Specific Integrated Circuit (ASIC).

During the tests, seven accelerometers are employed, and is important to notice that each accelerometer gives as output three different signals, which are the accelerations along the three orthogonal components  $x$ ,  $y$  and  $z$ . The list of the accelerometers, the acquired signals, their acquisition frequency and their sensitivities, are specified in **Table 4.3**.

#	Position	Acquired signal	Sensitivity $\frac{mV}{g}$	Acquisition frequency [kHz]	Unit
1	Gearbox mount, powertrain side	GBX_mount_Acc_x_US	39.653	2	$g$
		GBX_mount_Acc_y_US	39.370	2	$g$
		GBX_mount_Acc_z_US	39.672	2	$g$

2	Gearbox mount, chassis side	GBX_mount_Acc_x_DS	39.909	2	<i>g</i>
		GBX_mount_Acc_y_DS	39.453	2	<i>g</i>
		GBX_mount_Acc_z_DS	39.927	2	<i>g</i>
3	Engine mount, powertrain side	ENG_mount_Acc_x_US	39.850	2	<i>g</i>
		ENG_mount_Acc_y_US	40.030	2	<i>g</i>
		ENG_mount_Acc_z_US	40.030	2	<i>g</i>
4	Engine mount, chassis side	ENG_mount_Acc_x_DS	39.632	2	<i>g</i>
		ENG_mount_Acc_y_DS	39.874	2	<i>g</i>
		ENG_mount_Acc_z_DS	39.785	2	<i>g</i>
5	Differential mount, powertrain side	DIFF_mount_Acc_x_US	19.850	2	<i>g</i>
		DIFF_mount_Acc_y_US	20.151	2	<i>g</i>
		DIFF_mount_Acc_z_US	19.890	2	<i>g</i>
6	Differential mount, chassis side	DIFF_mount_Acc_x_DS	39.793	2	<i>g</i>
		DIFF_mount_Acc_y_DS	39.844	2	<i>g</i>
		DIFF_mount_Acc_z_DS	39.764	2	<i>g</i>
7	Gearbox case	GBX_Acc_x	10.150	20	<i>g</i>
		GBX_Acc_x	10.390	20	<i>g</i>
		GBX_Acc_z	9.690	20	<i>g</i>

**Table 4.3:** List of the accelerometers used during the tests

Looking at the data in the table above, it is possible to notice that for each of the three mounts that connect the powertrain to the chassis of the vehicle a couple of accelerometers are placed, one on the powertrain side of the mount (US - upstream) and one on the chassis side (DS - downstream). Measuring the acceleration on both side of the mount allows to compute the damping effect due to the presence of the mechanical joint by analysing the two signals and comparing the results, as example using the *tffestimate* function in MATLAB as is shown in the previous chapter.

In addition to these three couples of accelerometers, a high frequency accelerometer is installed directly on the gearbox case, to evaluate the vibration induced by the gearbox.

All the signals coming from these seven sensors are acquired by an IMC acquisition system.

### 4.3.3 - POSITION TRANSDUCERS

To characterize the behaviour of the three mounts of the powertrain, also three position transducers (model MT2A) are installed, one for each mount. These sensors measure the linear displacement of

the mounts along the  $x$  direction: in particular, the differential's sensor measures the displacement as positive if its direction is the same of the travelling direction of the vehicle, while the other two transducers measure the displacement in the opposite direction. The signals are acquired by an IMC acquisition system and the main parameters of the sensors are listed in **Table 4.4**.

#	Position	Acquired signal	Sensitivity [ $mV/V/mm$ ]	Acquisition frequency [ $kHz$ ]	Unit
1	Engine mount	GBX_mount_pos_X	2.471	2	$mm$
2	Gearbox mount	ENG_mount_pos_X	2.472	2	$mm$
3	Differential mount	DIFF_mount_pos_X	2.474	2	$mm$

**Table 4.4:** List of the position transducers

#### 4.3.4 - INSTRUMENTED HALF SHAFT WITH STRAIN GAUGES FOR TORQUE MEASUREMENT

For each one of the two drive axles that connects the differential to the two front wheels, a strain gauge is placed in order to measure the amount of torque transmitted. Knowing the value of the torsional deformation of each axle and its elastic deformation characteristics (geometry, material) is possible to compute the torque transmitted. The two analog signals are acquired by an IMC acquisition system; they are specified in **Table 4.5**.

#	Position	Acquired signal	Sensitivity [ $\frac{Nm}{V}$ ]	Acquisition frequency [ $kHz$ ]	Unit
1	Front left wheel's drive shaft	FL_HS_torq	374.545	20	$Nm$
2	Front right wheel's drive shaft	FR_HS_torq	372.942	20	$Nm$

**Table 4.5:** Main parameters of the extensometers

#### 4.3.5 - MICROPHONE

A Pre-Polarized Free-Field microphone (model 377B02) is placed near to the driver's seat in order to acquire the noise level transmitted by the chassis from the powertrain to the cockpit. The sensor is designed using some corrective strategies to compensate the disturbance caused by the presence of

the microphone itself inside the sound field. The analog signal sampled by the sensor, which characteristics are specified in **Table 4.6**, is acquired by an IMC acquisition system.

#	Position	Acquired signal	Sensitivity $\left[\frac{mV}{Pa}\right]$	Acquisition frequency [kHz]	Unit
1	Driver's seat	Mic_pass	50	20	Pa

**Table 4.6:** Microphone characteristic

In **Figure 4.3** the position of all the sensors described are schematically depicted; some signals (indicated by the green rectangle) are acquired from the CAN data network (see next paragraph).

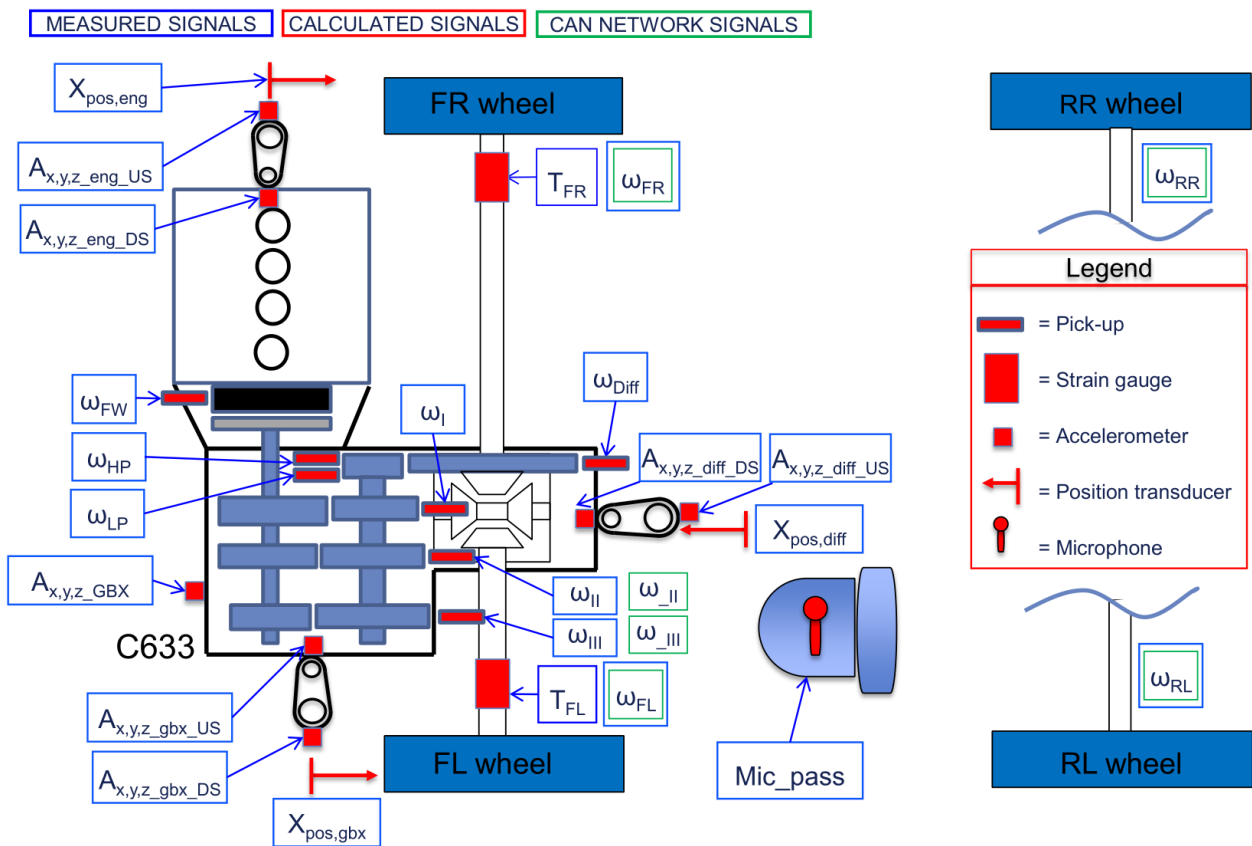


**Figure 4.3:** Schematisation of the layout of the sensors

#### 4.3.6 - SIGNALS ACQUIRED FROM THE VEHICLE'S CAN NETWORK

A lot of signals that can be useful for these analysis does not require the installation of a specific sensors for their measurements, since they are already acquired by sensors present in the stock vehicle and managed by the ECU for normal vehicle's operations. These signals are present in the CAN

network of the vehicle, so is sufficient to acquire them simply connecting the IMC acquisition system to the electronic circuits of this network.

Since also some of the amount of signals transmitted by the CAN network are useful for the aim of this work, in **Table 4.7** some of the most important signals used during the various analysis are listed as examples.

Signal	Description	Acquisition frequency [kHz]	Unit
ClutchEngaged	Indicates the status of the two clutches, and it's an in common signal for both clutches. Its value is 0 when a clutch is engaged and 1 when a clutch or both are slipping.	100	—
GasPedalPosition	Indicates the percentage of actuation of the gas pedal by the driver.	100	%
VehicleSpeedVSOSig	It is the mean speed of the vehicle.	100	km/h

**Table 4.7:** Main signals acquired by the CAN network of the vehicle

#### 4.4 - TESTS PERFORMED DURING DATA ACQUISITION

After having discussed the setup employed during the test, is necessary to describe what types of tests have been performed during the data acquisition. The sampling of all the signals, both the ones coming from the sensor installed and the other signals acquired by the CAN network, starts in the time instant in which one generic test starts. Now, all the different manoeuvres performed during the tests are listed and described:

- **Engine's cranking:** with the gearbox's selector in the neutral position and the brake pedal pushed, the engine is cranked.
- **Engine's shutdown:** the test is performed in the same way of the cranking, but in this case the engine is shut off.
- **Sweep test:** the test can be performed either in neutral position with stationary vehicle or in one of the six gears with moving vehicle. The aim of the test is to explore all the rotational speed reachable by the engine, to characterize the vibrational behaviour of different components of the

powertrain, so usually during a sweep test the engine's speed is varied, using the gas pedal command, from the idle conditions to the maximum speed, and back again to idle. It is useful to divide the Sweep test in the Run Up phase (from idle to maximum speed) and Coast Down phase (from maximum speed to idle).

- **Tip-In and Tip-Out:** the test is performed two times for each gear ratio. During this manoeuvre, the gas pedal command passes quickly from a value of 0% to a pre-fixed percentage (30% for one test and 100% for another test): this is the Tip-In test. The Tip-Out test consists in the quick release of the gas pedal.
- **Idle test:** in the same conditions of the engine's cranking test, during this the engine's speed is maintained constant for a certain period. The test is carried on at different speed's levels: 1'000, 2'000, 3'000, 4'000, 5'000 and 6'000 rpm.
- **Vehicle's braking from 100 to 0 km/h:** the vehicle, after having been taken to the speed of 100 km/h, is braked strongly pushing on the brake pedal. The braking is managed by the ABS system of the vehicle and the gears downshifts are managed by the TCU.
- **Slabs:** the vehicle passes at constant speed on concrete slabs which length is equal to 7 m and separated one from the other by a discontinuity (a small step). The test is performed both at 20 km/h and 40 km/h.
- **Short wave:** the vehicle crosses at constant speed a road segment characterized by waves distant 0.7 m one from the others; in this way, the wheels are stressed in counterphase. The test is performed both at 20 km/h and 40 km/h.
- **Long wave:** the vehicle crosses at constant speed a road segment characterized by waves distant 12 m one from the others; in this way, the wheels are stressed in counterphase. The test is performed both at 20 km/h and 40 km/h. Eventually, the road segment can be also provided with speed bumps.

Between all these tests, one the most relevant is the Sweep test: the main reason is that since during this test the engine's speed goes from idle to the maximum speed, with only one test is possible to analyse the vibrational behaviour of the different gears and mechanical components, allowing to condensate the results and to separately analyse the behaviour of the gearbox in the six different gears ratios available.

## 5 - ANALYSIS OF THE EXPERIMENTAL DATA

### 5.1 - ANALYSIS OF THE ENGINE'S IRREGULARITIES

One of the main aspects that influence the vibrational behaviour of the gearbox and the entire powertrain of the vehicle is the fact that the torque is supplied by an internal combustion engine; as is known, the torque supplied by an engine is not constant during the two revolutions performed by the crankshaft necessary to complete one thermodynamic cycle, due to the firing order of the four cylinders of the engine. To consider this aspect during the analysis of the experimental data, is useful to start by analyse the entities of these irregularities.

For this purpose, is necessary to consider the velocity signal of the flywheel, which is the most representative of the rotational speed of the engine, since the flywheel is rigidly connected to the crankshaft and, unlike the velocity signals of other gears downstream in the powertrain, is not affected by the presence of coupling between toothed gear, which gives rise to phenomena of gear rattle and whine.

Two different tests are considered during this first analysis: the first test is an idle test, in which the rotational speed of the engine is the idle one, while the second test is a Run Up test performed with stationary vehicle and the gearbox in neutral position. Of particular importance is the last test, because during this one the engine's speed is varied from idle to the maximum; in this way, simply analysing this signal, is possible to obtain the results over a wide range of frequencies.

The signal measured during the idle test is the one depicted in **Figure 5.1**.

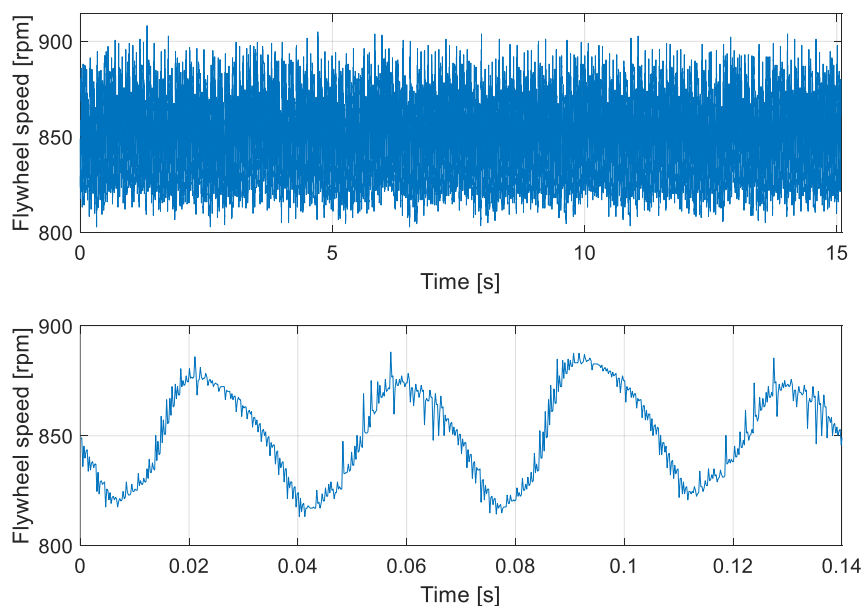


**Figure 5.1:** Velocity signal of the flywheel measured during the idle test

Looking at the picture, in the part below is shown a portion of the signal in which is clearly visible the fundamental harmonic of the signal; as already said in the chapter relative to the signals processing, is very useful to truncate the signal at the end of one period of this harmonic maintaining the longest possible time-history of the signal, to decrease both the noise effect and the leakage phenomena.

Applying the FFT function, is possible to graphically represent the amplitudes and the phases of the harmonics contents of the signal in the frequency domain; these results is depicted in **Figure 5.2**.

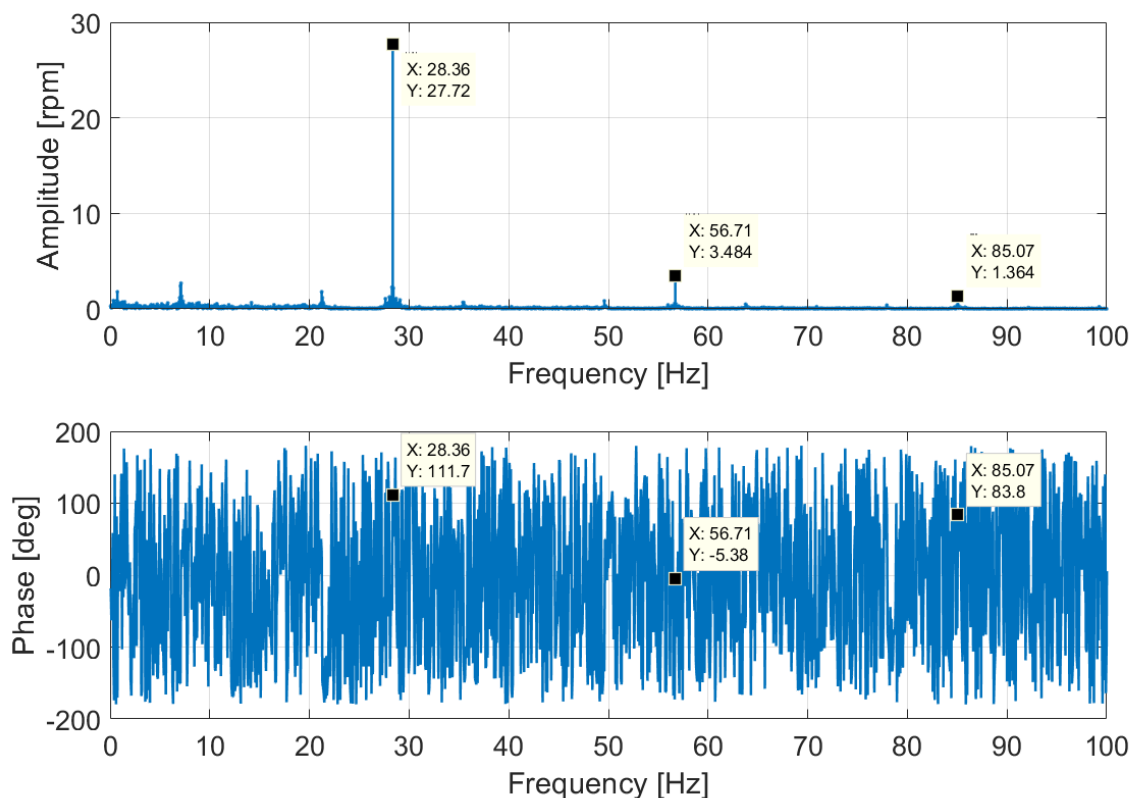


**Figure 5.2:** Amplitudes and phases of the idle velocity signal in the frequency domain

The main contribution in terms of irregularities is the one clearly visible at the frequency of 28.36 Hz: this frequency corresponds to the contribution of the second order, i.e. the firing orders of the four cylinders engine. There are also some relevant contributions corresponding to the 4<sup>th</sup> and the 6<sup>th</sup> orders, but their values of amplitude are one order of magnitude lower than the main contribution of the 2<sup>nd</sup> order.

Now, the same analysis is performed considering the Run Up test; as it has been already specified in the second chapter of this work, since during this test the mean rotational speed of the engine is varied, is more useful to perform the analysis in the order domain. The velocity signal of the flywheel during this test is the one in **Figure 5.3**.

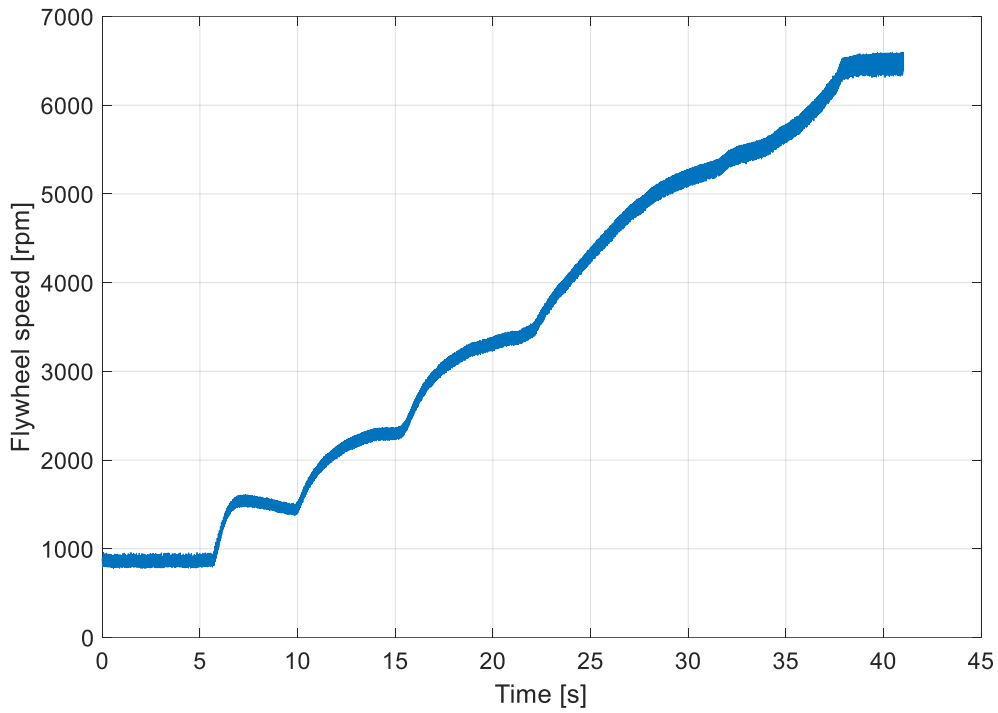


Figure 5.3: Velocity signal of the flywheel measured during the Run Up test

While in Figure 5.4 are shown the results relative to the order analysis of this signal.

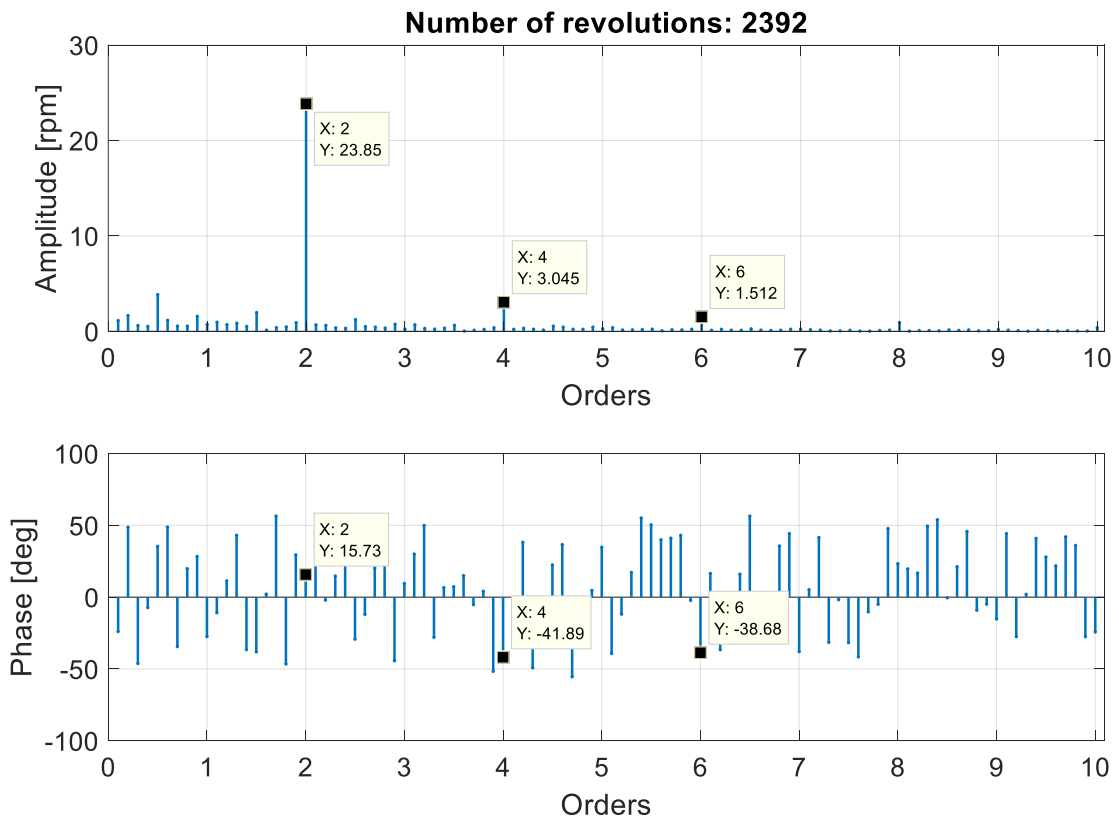
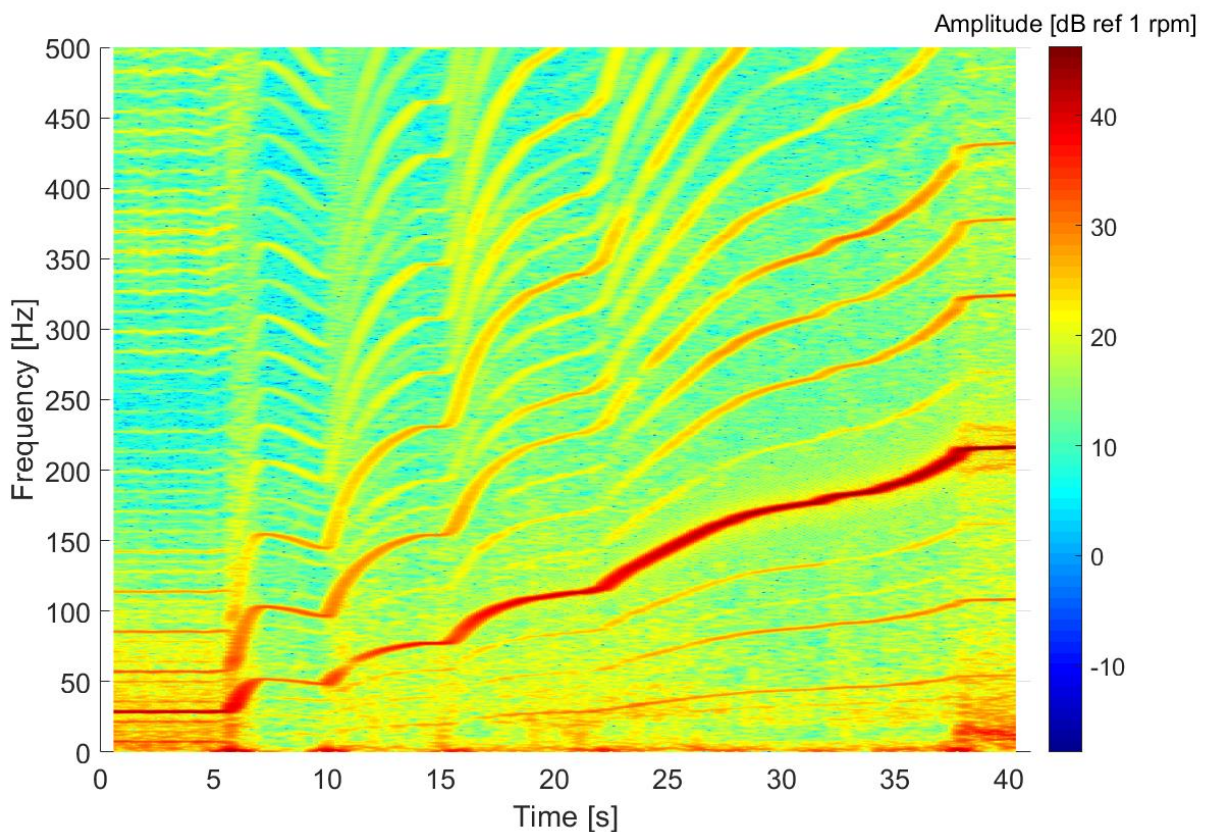


Figure 5.4: Amplitudes and phases of the Run Up signal in the order domain

Comparing these last results with the ones of the analysis of the idle test's signal, focusing on the amplitude, the values corresponding to the more relevant orders (the 2<sup>nd</sup>, the 4<sup>th</sup> and the 6<sup>th</sup>) are different from the previous case. This is due to the fact that the results of the order analysis are averaged along the considered time-history of the signals (in these cases, is considered all the available time-history truncated at the end of one period of the fundamental harmonic). Observing the velocity signal, as example, in the time intervals in which the speed is varied with a higher slope, the torsional oscillation contribution due to the firing of the cylinders (2<sup>nd</sup> order) is lower respect to the contribution at idle speed, so the final result is affected by this behaviour.

Is also possible to observe the values in term of amplitudes using the spectrogram: in this way, the variation of the contribution of each order as function of the time instant will be clearly visible; the spectrogram of the signal is shown in **Figure 5.5**.



**Figure 5.5:** Spectrogram of the signal of the Run Up test

The most visible contribution in the spectrogram is the one corresponding to the 2<sup>nd</sup> order. As it has been already seen from the raw signal, there is a time interval (roughly from 6 to 16 seconds) in which the contribution of the 2<sup>nd</sup> order is lower respect the others time instant of the test; this is the reason why in the amplitudes plot the total averaged value of the 2<sup>nd</sup> order is lowered than the corresponding value obtained from the analysis of the idle test signal.

## 5.2 - ANALYSIS OF THE ACCELEROMETERS

Starting from the data measured during the test, a very interesting aspect that can be analysed is the vibrational behaviour of the three mounts used to fix the powertrain of the vehicle to the chassis; since these three mounts are the medium through which all the vibrations coming from the powertrain are transmitted to the rest of the vehicle, is very useful to analyse the damping effect due to the presence of these components.

For this purpose, during the tests for each mount two accelerometers have been placed to make possible the comparison between the vibration present in the powertrain side and in the chassis side.

Also for this analysis, between all the tests performed on the vehicle, the more interesting is the Sweep one (Run Up or Coast Down cases), because with the data coming from this type of test is possible to quickly explore a wide range of frequency, corresponding to the wide range of engine's speed crossed during the test. The orientation of the axis and the position of each couple of accelerometers are depicted in **Figure 5.6**.

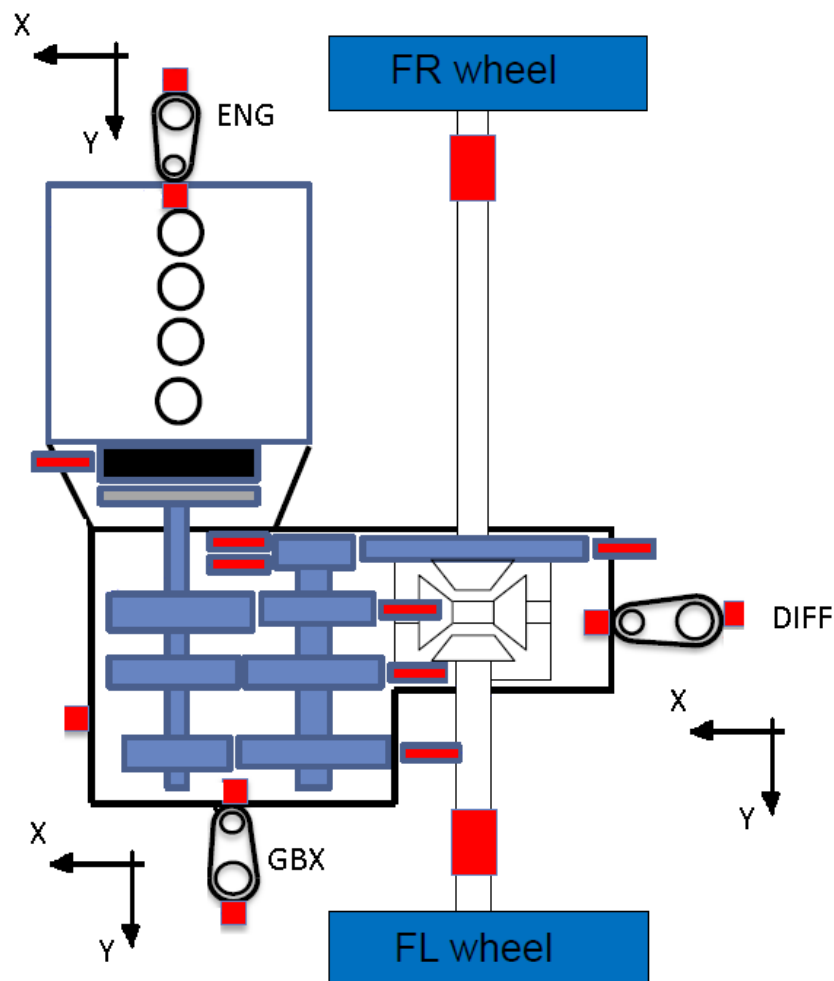


**Figure 5.6:** Position and orientation of the accelerometers installed in the vehicle's powertrain.

### 5.2.1 - ACCELEROMETERS OF THE ENGINE'S MOUNT

To qualitatively define the type of test, it is better to graphically show the velocity signal of the flywheel, which in this case is relative to a Run Up test performed in neutral gear. Starting from the engine's mount, the analysis on the same cartesian component of the acceleration between the chassis and the powertrain sides is carried on in parallel. Considering now the  $x$  component, the two measured signals are the ones depicted in **Figure 5.7**.

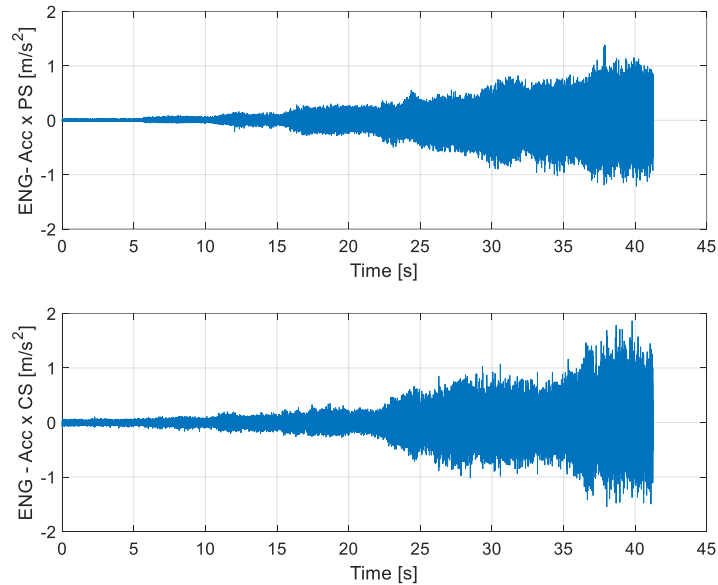


**Figure 5.7:** Signal of the  $x$  component measured by the engine's mount accelerometers

Since the graphical representation of this type of signals is not significant due to their high instantaneous variation, instead of the plot it is better to define them through some numerical values that characterize the two signals, such as the mean value, the Root Mean Square (RMS), the minimum and the maximum values. In **Table 5.1** are reported the values relative to all the signals of the engine's mount, while in **Figure 5.8** is shown the speed signal of the flywheel acquired during the test, to qualitatively describe it; finally, in **Table 5.2** are listed the main data relative to this test.

Signal	Maximum [ $m/s^2$ ]	Minimum [ $m/s^2$ ]	Mean value [ $m/s^2$ ]	RMS [ $m/s^2$ ]
ENG X PS	1.385	-1.210	0	0.195
ENG X CS	1.865	-1.543	0	0.231
ENG Y PS	1.312	-1.608	0	0.225
ENG Y CS	3.082	-2.678	0	0.418

ENG Z PS	1.499	-1.701	0	0.393
ENG Z CS	0.938	-1.036	0	0.150

**Table 5.1:** Characteristic values of the accelerations signals of the engine's mount

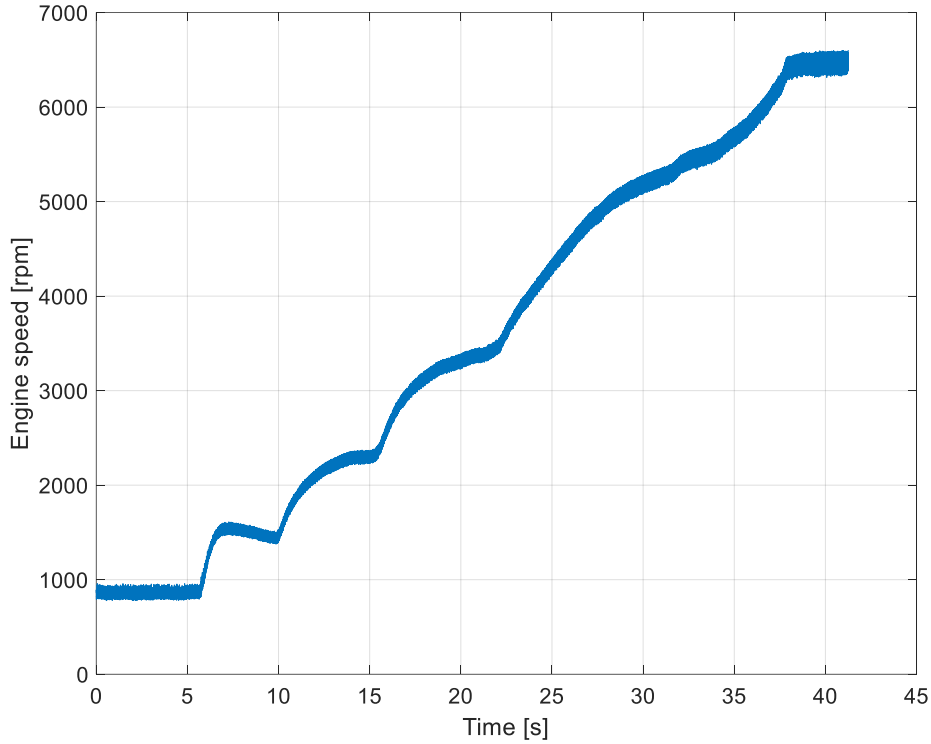


**Figure 5.8:** Flywheel's speed signal acquired during the test

Type of test	K1 clutch status	K2 clutch status	Gear engaged	Engine's speed interval [rpm]
Run Up	Engaged - speed tracking	Engaged - speed tracking	N	778-6'603

**Table 5.2:** Main parameters of the Run Up test with the gearbox in neutral position

As it has been already explained in the chapter of the signals processing, the analysis of each component of the accelerometer is performed comparing the two signals (chassis side and powertrain side) using their spectrograms and the estimation of the transfer function. For the  $x$  component of the engine's mount, these results are depicted in **Figure 5.9**.

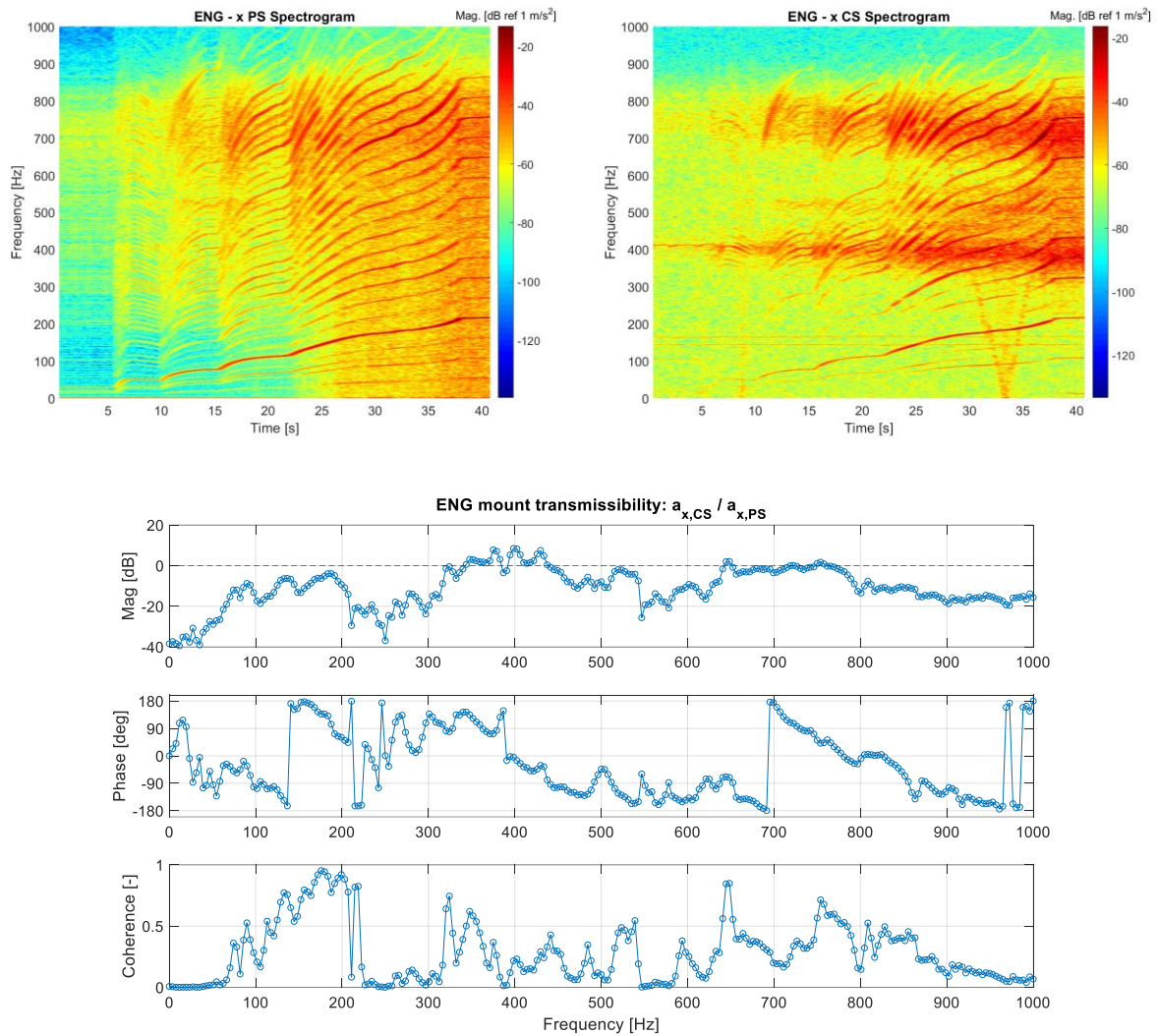


**Figure 5.9:** Spectrograms and transfer function estimation of the 2 signals along  $x$  of the engine mount

Looking at the results, it is possible to observe that on the spectrogram of the signal on the chassis side, in two frequency ranges around respectively 400 and 800 Hz, some resonance phenomena occurs, due to the structure of the chassis in the point in which the engine's mount is connected to it; in addition, these resonance phenomena are the reason why the coherence plot is characterized by a lot of oscillations, since in these frequencies the coherence's value tends to increase. From a damping point of view, along the  $x$  direction mount results effective below 320 Hz and in the range 550-650 Hz, while for other frequencies its damping effect is negligible.

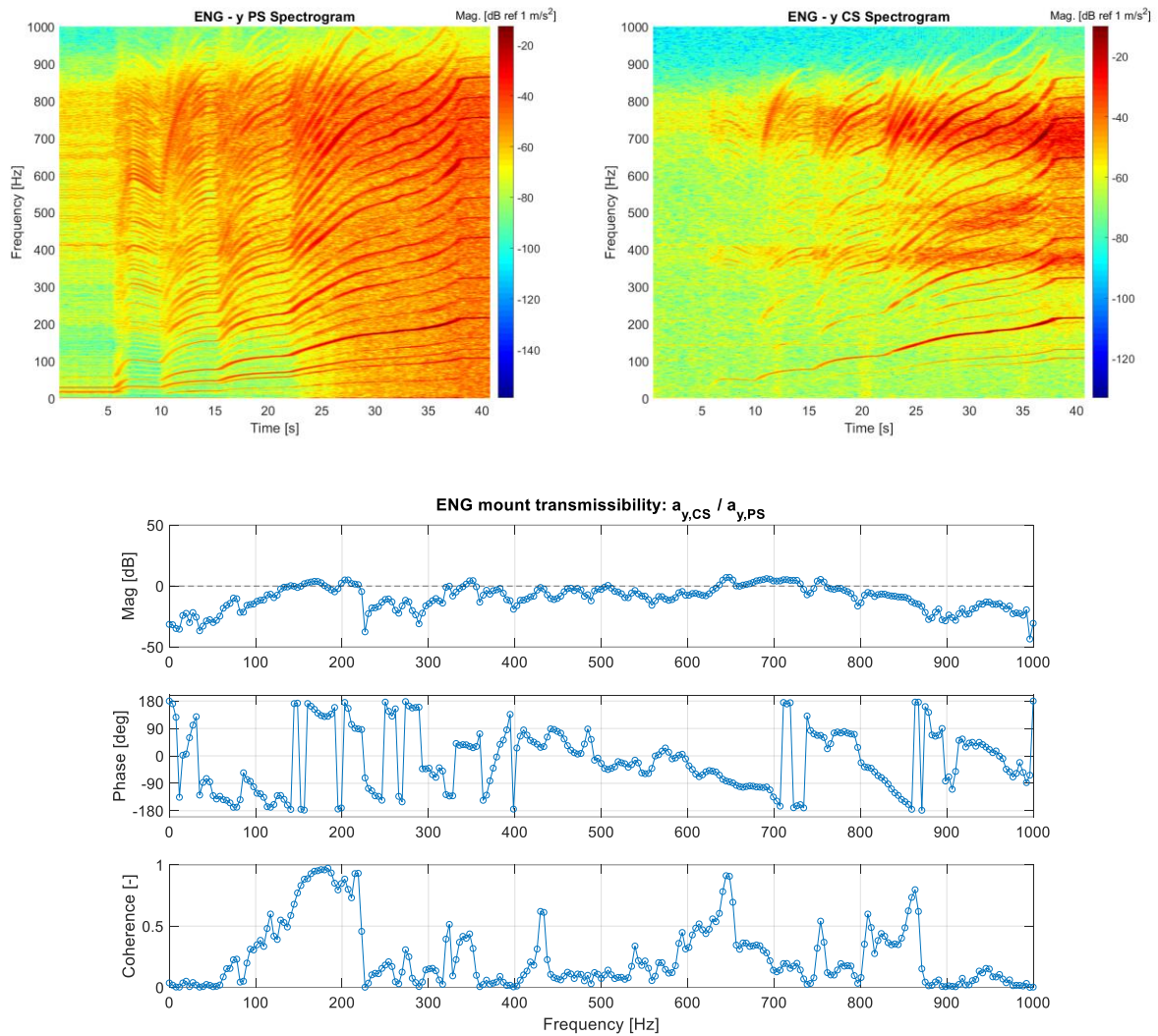


**Figure 5.10:** Spectrograms and transfer function of the accelerations signal of the engine's mount along  $y$

Considering now the results relative to the  $y$  direction, depicted in **Figure 5.10**, there is a similar behaviour of the chassis as in the previous case. Also this signal on the chassis side is characterized by higher values than the signal of the powertrain's side in certain frequency ranges, i.e. between 130 and 220 Hz and between 640-780 Hz. For this reason, along this direction the magnitude plot has a value close to 0 dB almost over all the frequency range between 0 and 1'000 Hz, and it means that practically no damping effect is given by the mount.

For what concerns the  $z$  component of the accelerations, this is the only direction for the engine's mount in which the vibrations are effectively damped by the presence of the mount itself. Observing these results, shown in **Figure 5.11**, is possible to see again the presence of the resonance on the chassis side; however, in this case the resulting amplitudes are reduced respect the other two directions, so the mount has an effective damping effect: this result is confirmed by the magnitude plot of the transfer function.

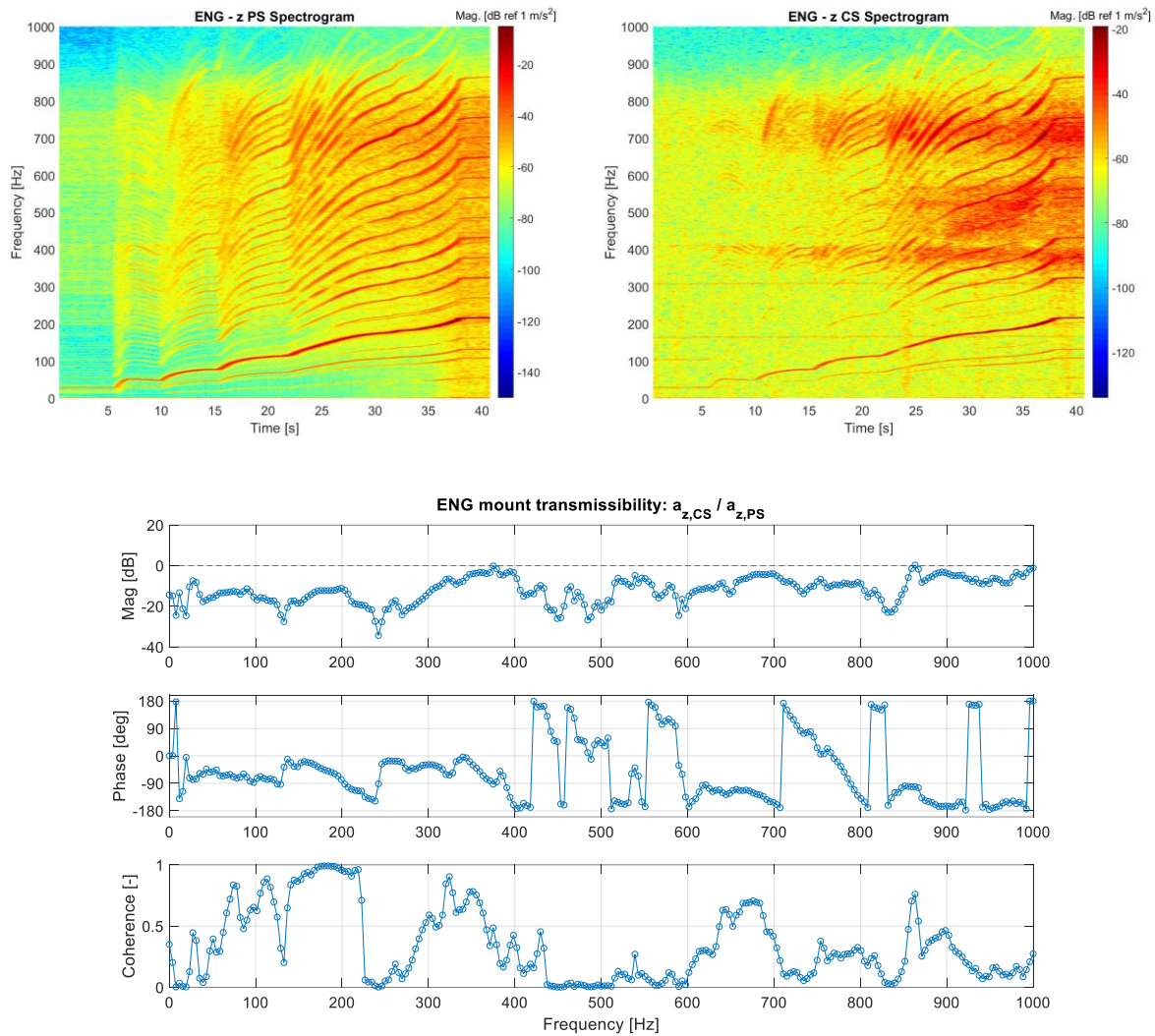


**Figure 5.11:** Spectrograms and transfer function of the accelerations signal of the engine's mount along z

Considering all these three transfer functions, is important to notice that they are characterized by a low magnitude around the frequency of 240 Hz, a typical value for the resonance frequency of the first powertrain bending mode. By choosing the nodes of this mode as position for the mounts an antiresonance can be obtained.

Applying the orders analysis to all the signals considered until this point, is possibly to graphically see the damping effect due to the engine's mount for each order. This type of analysis is performed re-sampling the accelerometers signal respect the angular position of the engine's crankshaft, so the considered orders are referred to the engine. The effect of the mount in terms of amplitudes is shown in **Figure 5.12**, while the corresponding results in terms of phase are in **Figure 5.13**.

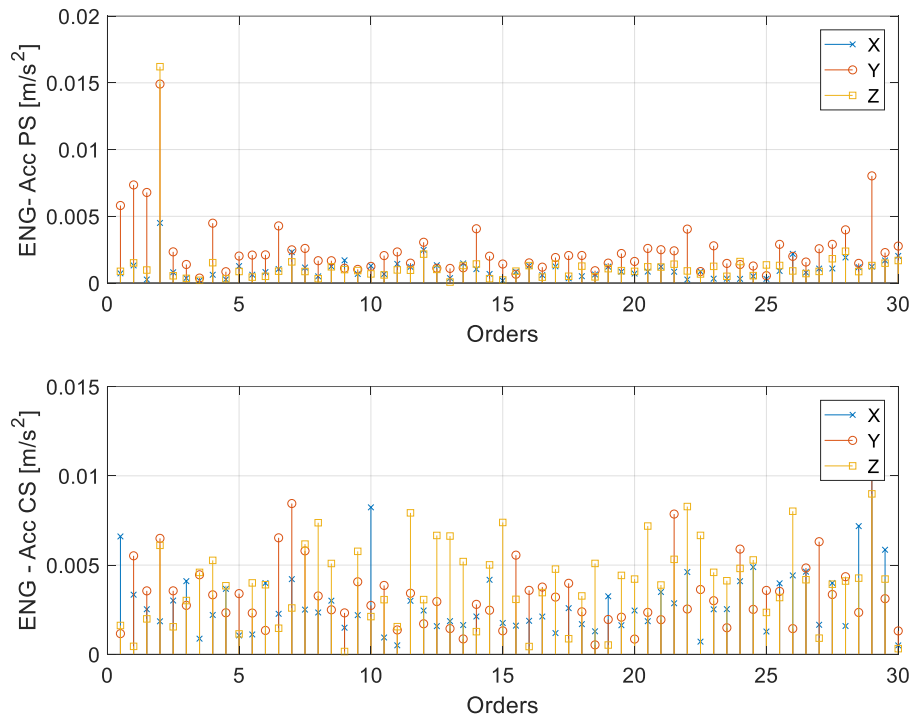


Figure 5.12: Amplitudes of the engine's mount accelerations signals in the order domain

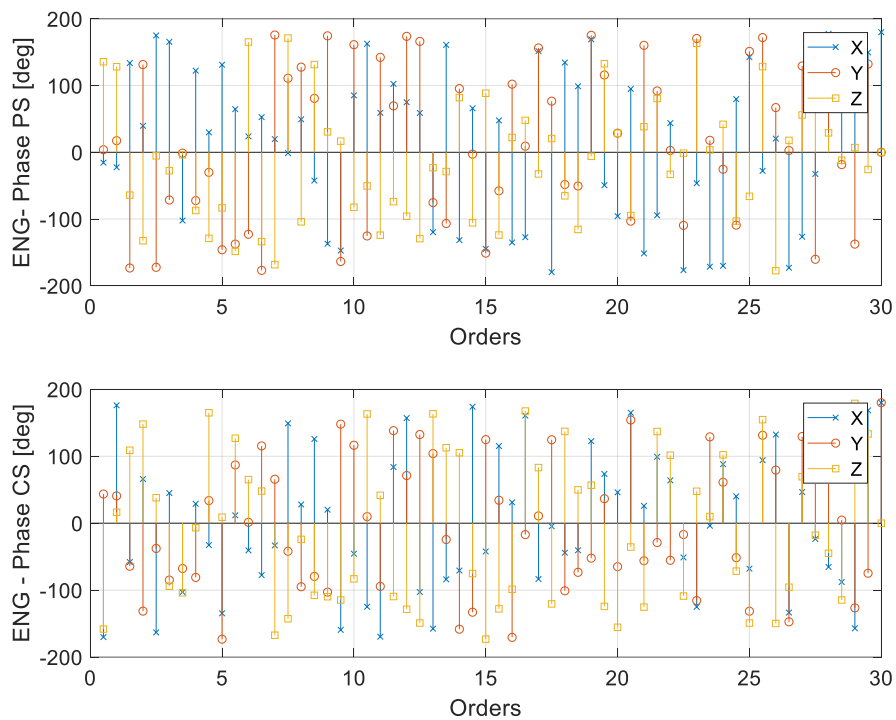


Figure 5.13: Phases of the engine's mount accelerations signals in the order domain

### 5.2.2 - ACCELEROMETERS OF THE DIFFERENTIAL'S MOUNT

The analysis of the accelerometers of the differential's mount is performed considering the signals acquired during a Run Up test in 5<sup>th</sup> gear. The main parameters of this test are described in **Table 5.3**, while the representative signal of the engine's speed during the test is depicted in **Figure 5.14**.

Type of test	K1 clutch status	K2 clutch status	Gear engaged	Engine's speed interval [rpm]
Run Up	Engaged - torque transmission	Engaged - speed tracking	5	1'360-2'982

**Table 5.3:** Main parameters of the Run Up test in 5<sup>th</sup> gear

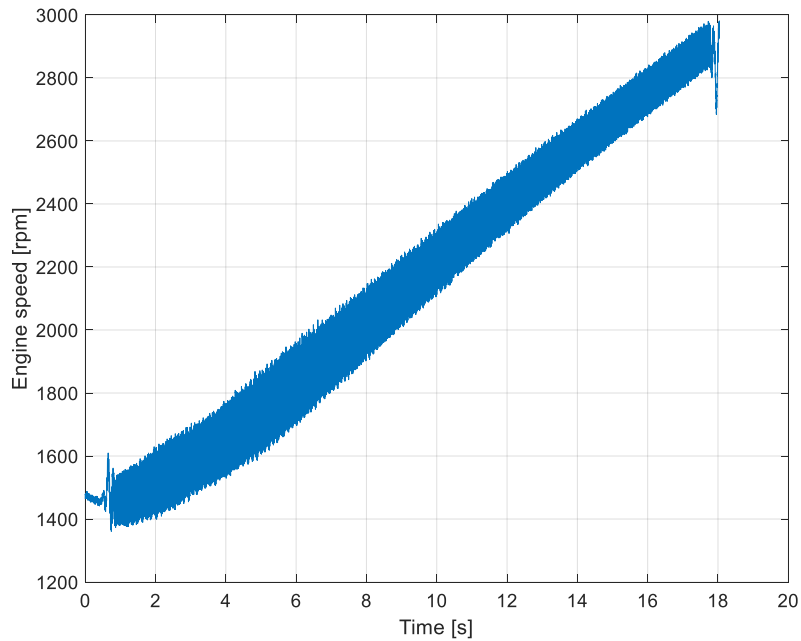


**Figure 5.14:** Flywheel speed signal measured during the Run Up test performed in 5<sup>th</sup> gear

As in the previous case, the six signals of the accelerometers are described by their characterizing parameters present in **Table 5.4**.

Signal	Maximum [m/s <sup>2</sup> ]	Minimum [m/s <sup>2</sup> ]	Mean value [m/s <sup>2</sup> ]	RMS [m/s <sup>2</sup> ]
DIFF X PS	0.098	-0.049	0	0.015
DIFF X CS	0.023	-0.097	0	0.009

DIFF Y PS	0.219	-0.120	0	0.034
DIFF Y CS	1.049	-0.482	0	0.046
DIFF Z PS	5.702	-5.526	0	1.218
DIFF Z CS	0.1422	-0.066	0	0.014

**Table 5.4:** Characterizing values of the differential's accelerometers signals

Considering now the  $x$  component of the accelerometers of the differential mount, the results of the analysis of these signals are shown in **Figure 5.15**.

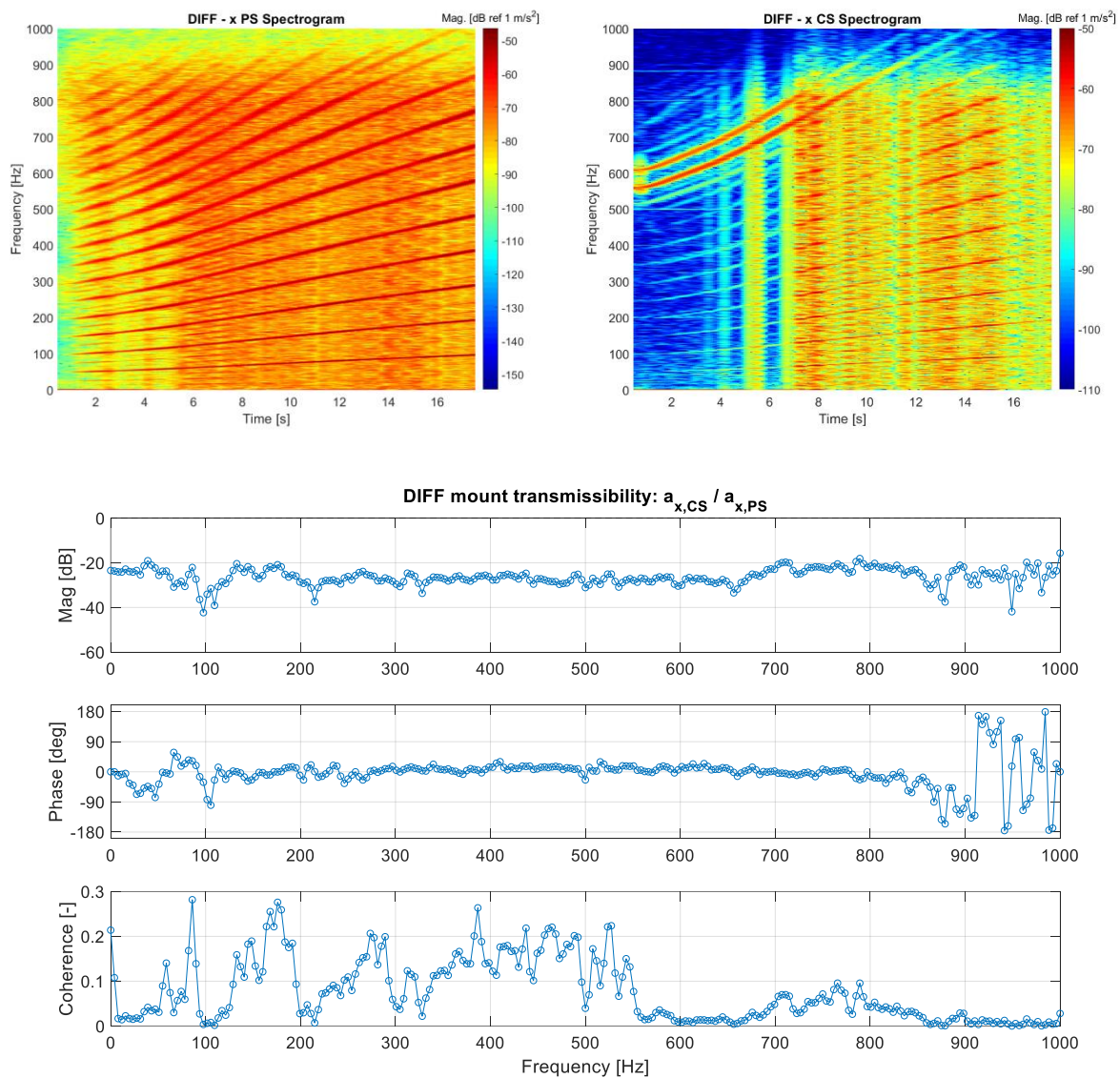


**Figure 5.15:** Spectrograms and transfer function of the accelerations signal of the differential's mount along  $x$

For this couple of accelerometers, the entity of the vibrations transferred from the powertrain is very small and the mount has a good filtering effect higher than 10 dB of attenuation over all the frequency range.

In **Figure 5.16** are shown the results for the  $y$  direction.

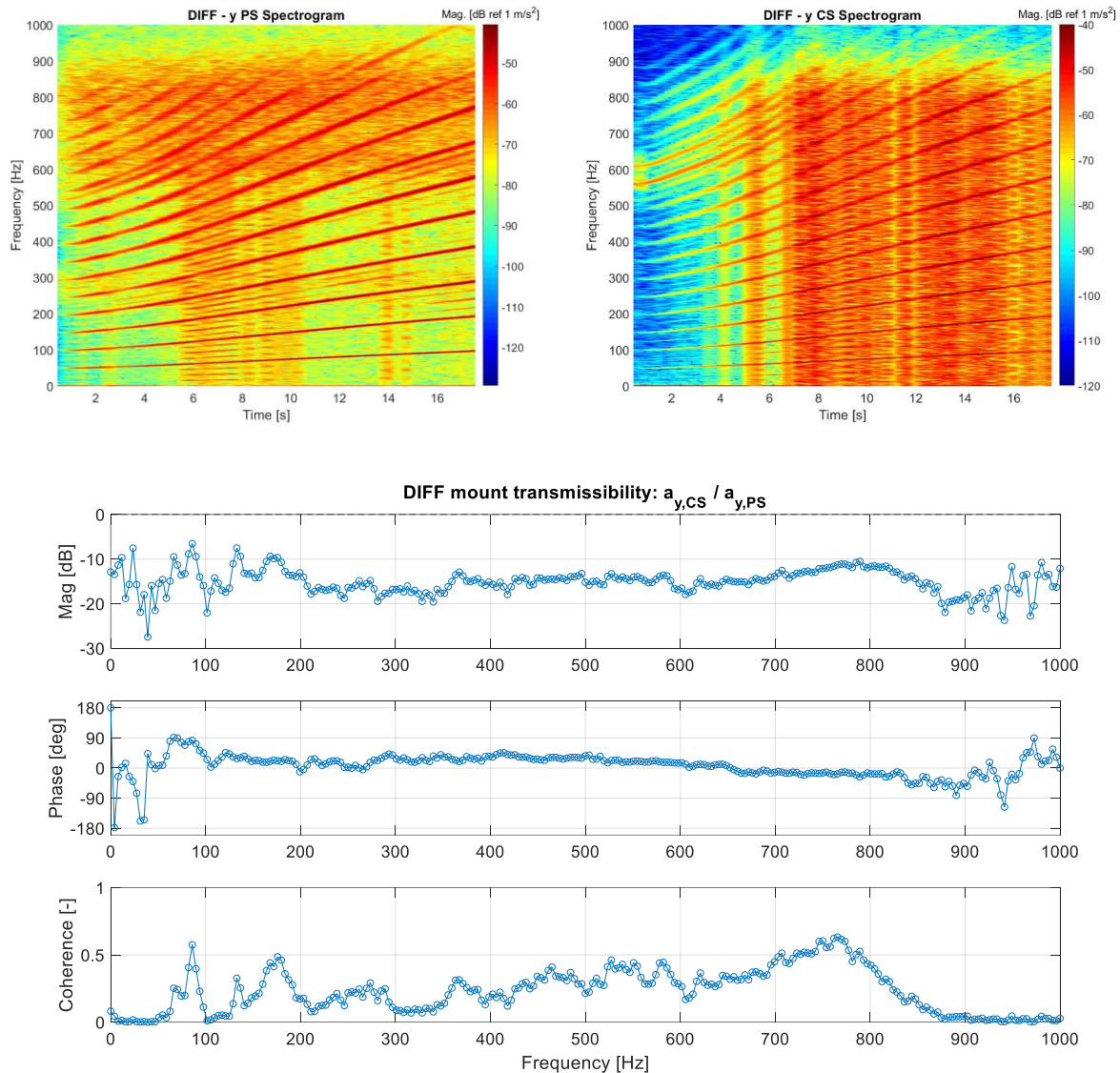


**Figure 5.16:** Spectrograms and transfer function of the accelerations signal of the differential's mount along  $y$

For the signals along this direction the behaviour is like the one of the previous case. Nevertheless, the effective damping effect due to the mount estimated by the function can be validated qualitatively comparing the results given by the two spectrograms.

Considering the  $z$  component of the accelerations, from their characteristic values is possible to observe that the signal measured on the powertrain side reaches very high values respect the corresponding signal on the chassis side; this is due to the differential's structure and its mechanical connection with the final drive gear, with a consequent wide frequency range (between 600 and 900

Hz) in which resonance occurs. Since the vibrations measured on the chassis side are consistently lower, the estimated damping effect of the mount is highly effective; in fact, all the values of the magnitude plot are below -40 dB, representative of a very good damping.

This is shown in **Figure 5.17**.

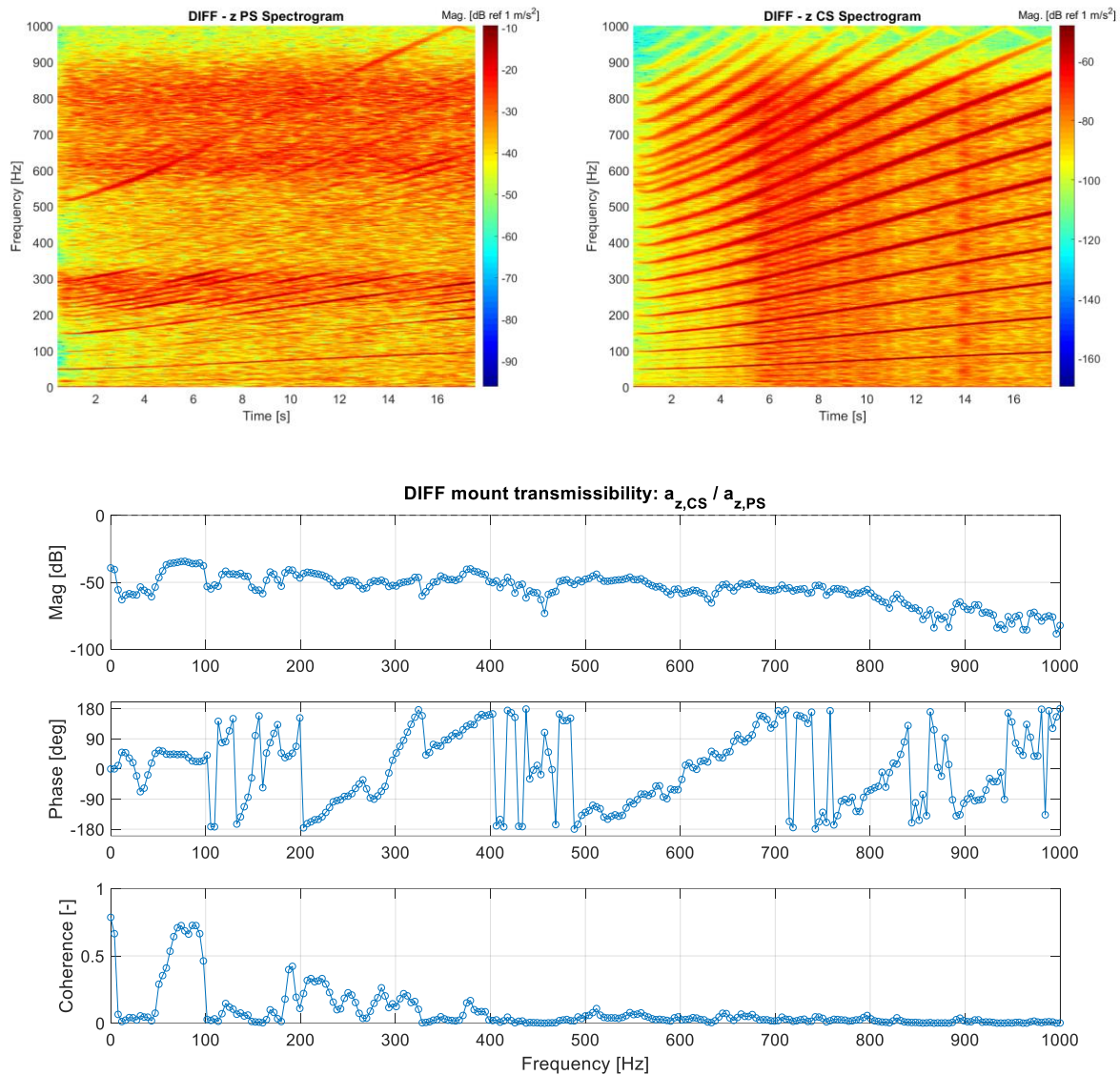


**Figure 5.17:** Spectrograms and transfer function of the accelerations signal of the differential's mount along z

Also in this case, the damping of the mount can be described by the comparison of the amplitudes of the orders between the powertrain and the chassis side; these results are shown in **Figure 5.18** for the x and y components; for scaling reason, the results for the z component are depicted in **Figure 5.19**.

The results of all the components for what concerns the phase are in **Figure 5.20**.

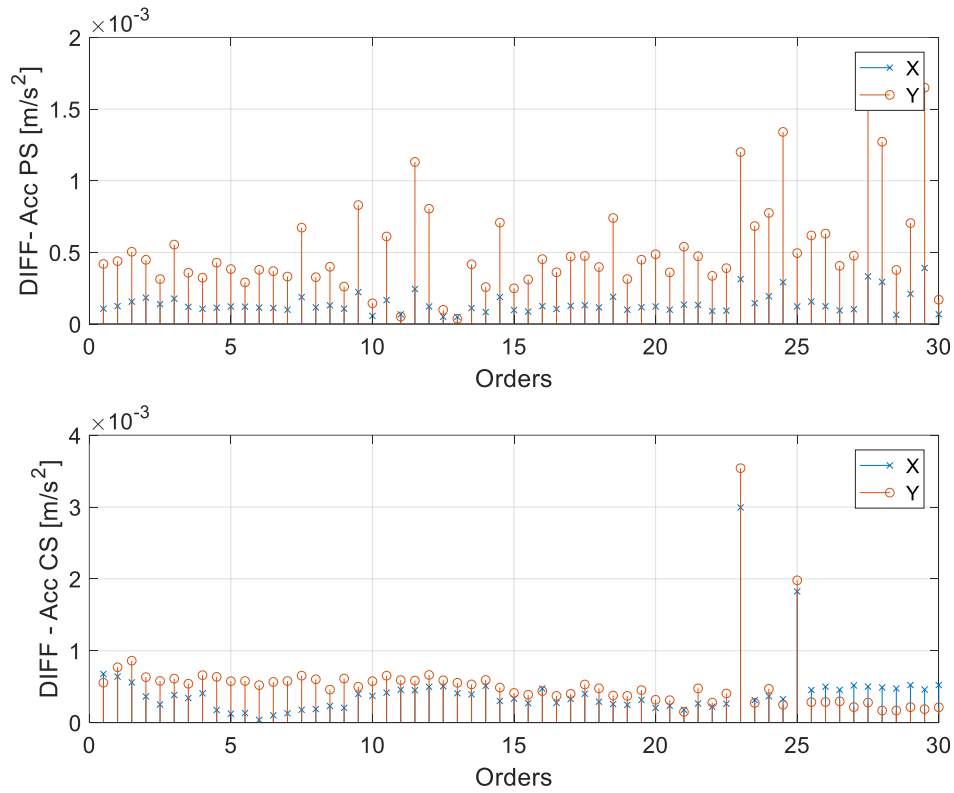


Figure 5.18: Amplitudes of the differential's mount accelerations signals in the order domain - x and y components

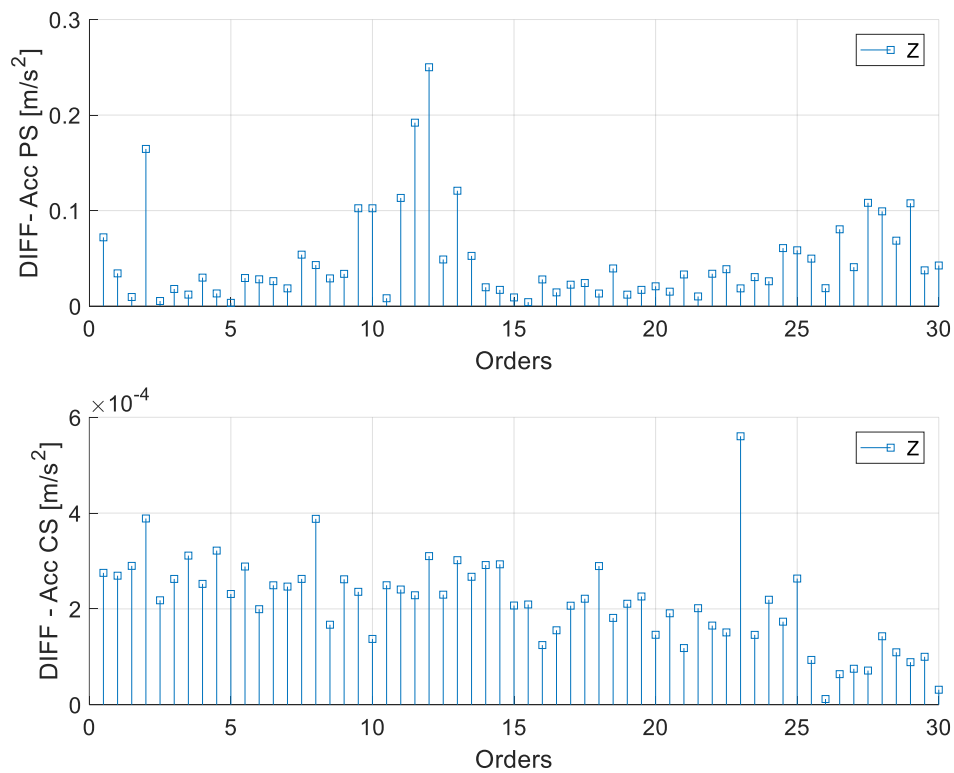


Figure 5.19: Amplitudes of the differential's mount accelerations signals in the order domain - z component

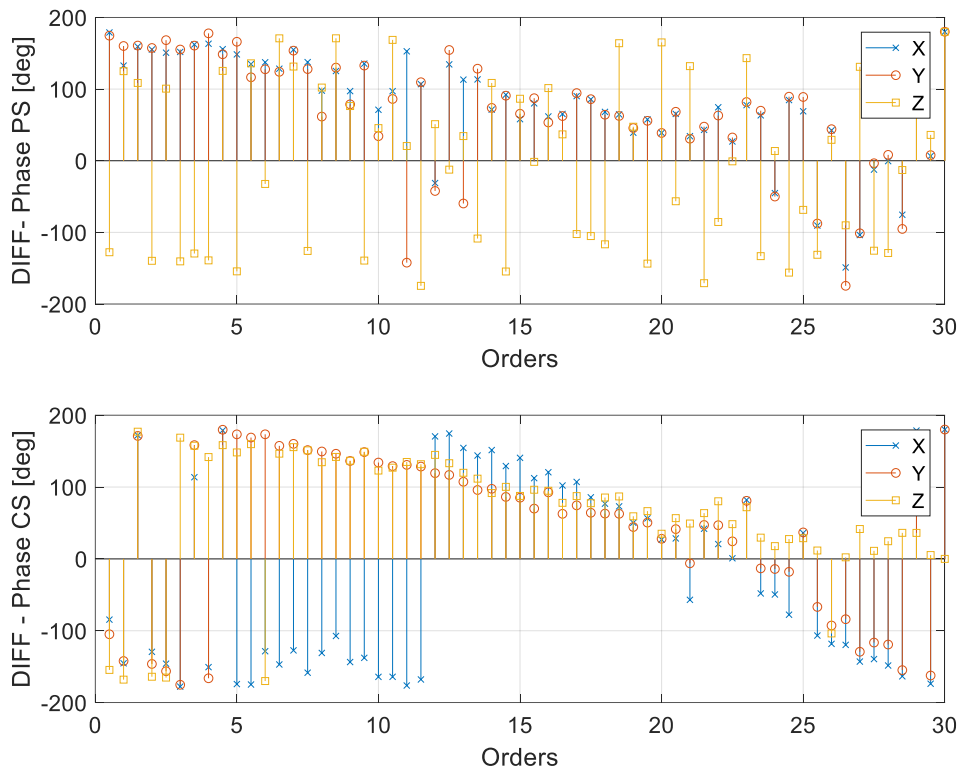


Figure 5.20: Phases of the differential's mount accelerations signals in the order domain

### 5.2.3 - ACCELEROMETER OF THE GEARBOX'S MOUNT

During the same test considered for the engine's mount accelerometers analysis, also the signal necessities for the analysis of the gearbox's mount have been acquired. The signals of the accelerometers, as in the other cases, are described by the parameters contained in **Table 5.5**.

Signal	Maximum [ $m/s^2$ ]	Minimum [ $m/s^2$ ]	Mean value [ $m/s^2$ ]	RMS [ $m/s^2$ ]
GBX X PS	13.358	-14.240	0	2.587
GBX X CS	0.297	-0.345	0	0.052
GBX Y PS	20.935	-21.599	0	3.105
GBX Y CS	0.859	-0.889	0	0.119
GBX Z PS	15.949	-14.447	0	2.777
GBX Z CS	0.607	-0.659	0	0.087

Table 5.5: Characterizing values of the gearbox's accelerometers signals

Looking at the values in the table, is easily predictable that the mount of the gearbox is characterized by a great damping effect. Starting from the accelerations signals along the  $x$  component, the two resulting spectrograms and the estimation of the transfer function are shown in **Figure 5.21**.

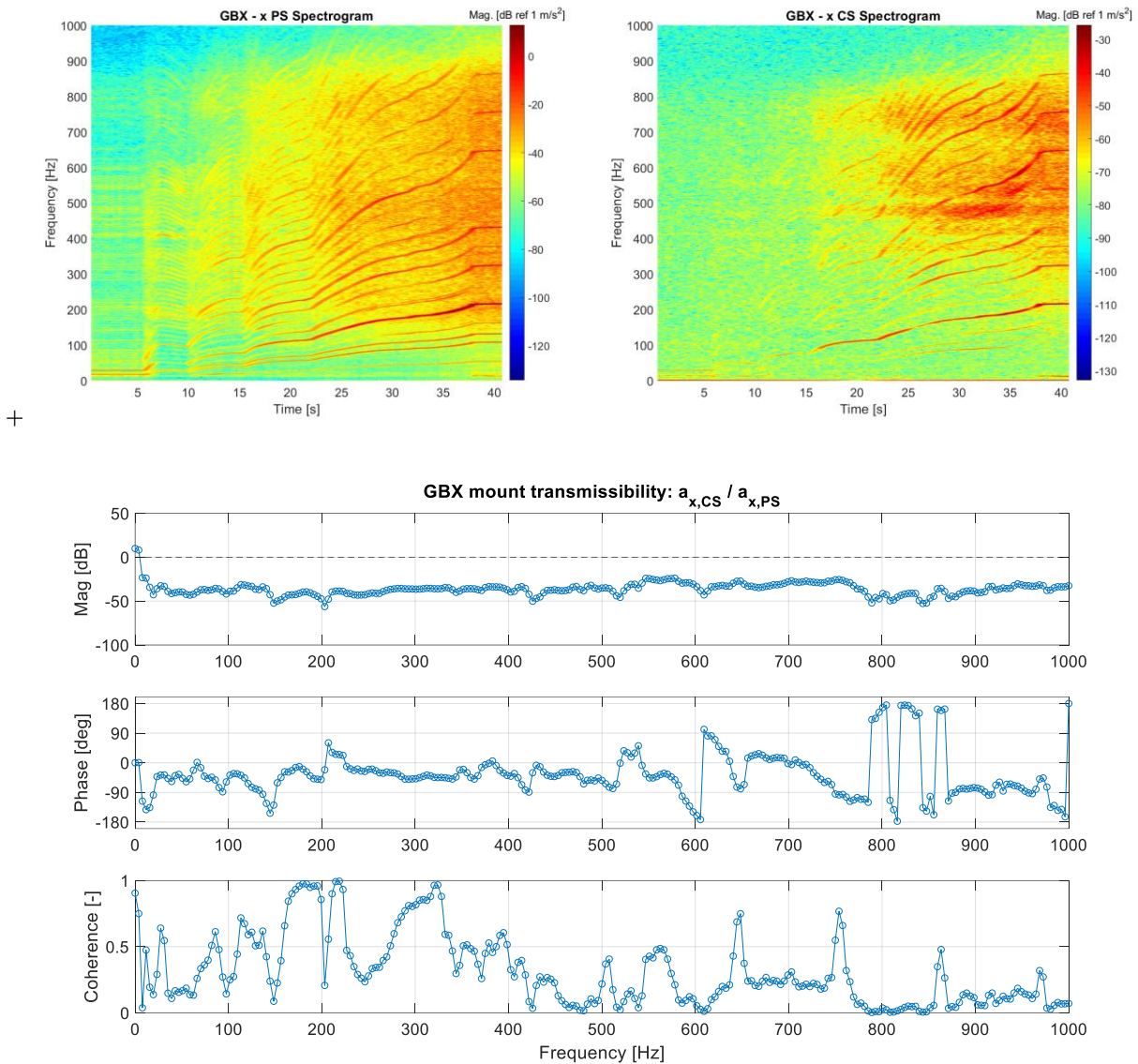


**Figure 5.21:** Spectrograms and transfer function of the accelerations signal of the gearbox's mount along  $x$

As in some of the previous cases, some vibrational phenomena are due to the connection of the mount to the vehicle's chassis and to the structure of the gearbox itself; however, the damping of the mount along this direction is very good for the entire considered range of frequencies, almost -23 dB. At low frequencies, in some small intervals of frequencies coherence of the estimation reaches values close to 1, meaning that the estimation has a good reliability and linearity between input and output.

Considering the  $y$  component of the accelerations of this mount, the graphical results are shown in the usual way in **Figure 5.22**.

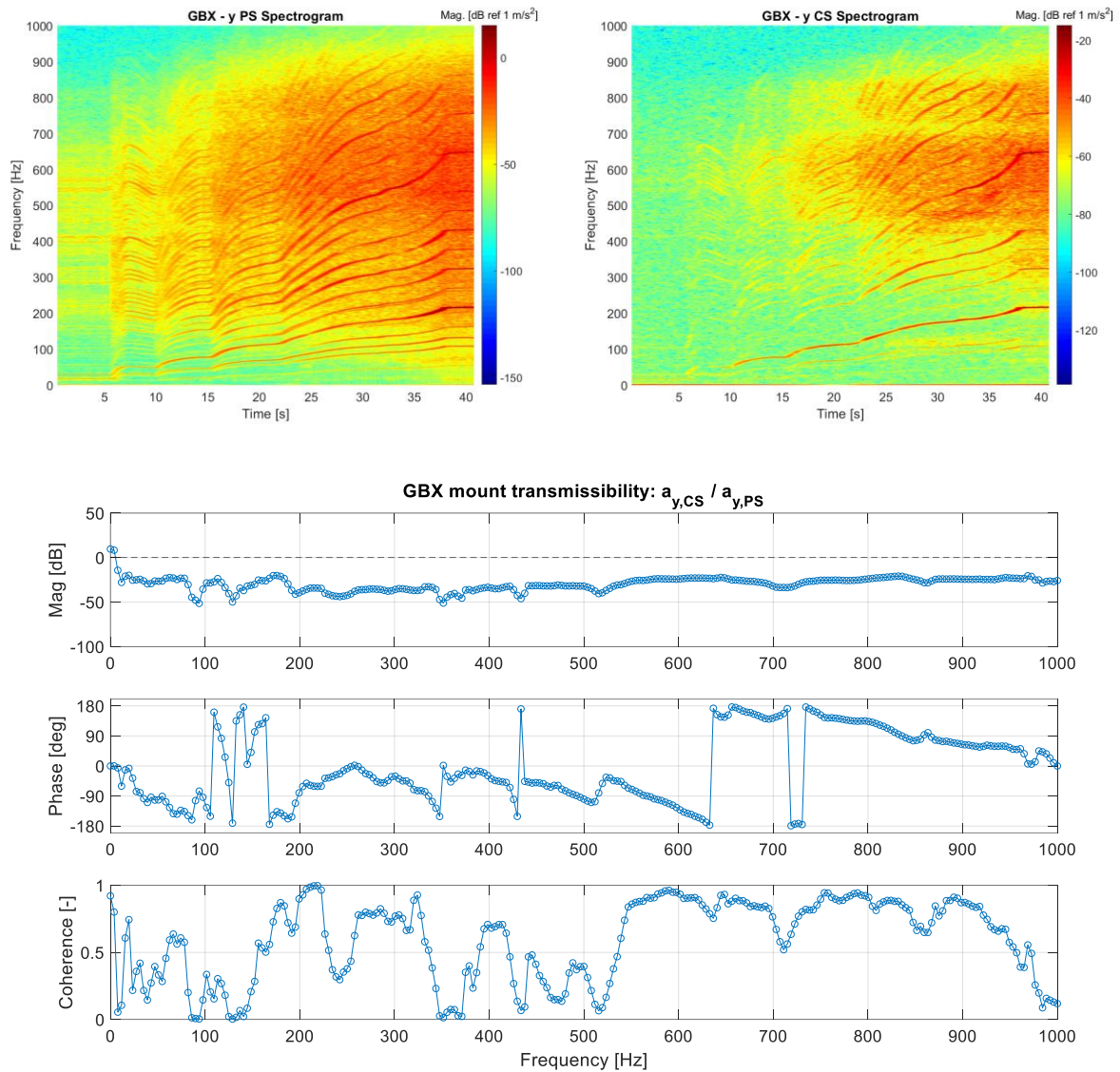


**Figure 5.22:** Spectrograms and transfer function of the accelerations signal of the gearbox's mount along  $y$

Along the  $y$  direction, the mount has practically the same effect observed along the  $x$  direction; in addition, in this case there is a wide range of frequencies between 550 and 950 Hz in which the coherence of the estimation is high (above 50%) and the characteristic of the magnitude plot is flat and with a very high level of damping. In the spectrogram plot of the signal measured on the chassis side, is clearly visible a wide range of frequencies in which the system's response is high.

The same behaviour of the  $x$  and  $y$  components describes the one of the  $z$  component for this mount; respect the vibrations of the  $y$  direction, in this case the entity of the resonances is lower, and there is only a small interval (130-230 Hz) in which the coherence of the transfer function's estimation is sufficiently high; nevertheless, the damping of the mount along this direction is very effective all over the range going from 0 to 1'000 Hz. These results are depicted in **Figure 5.23**.

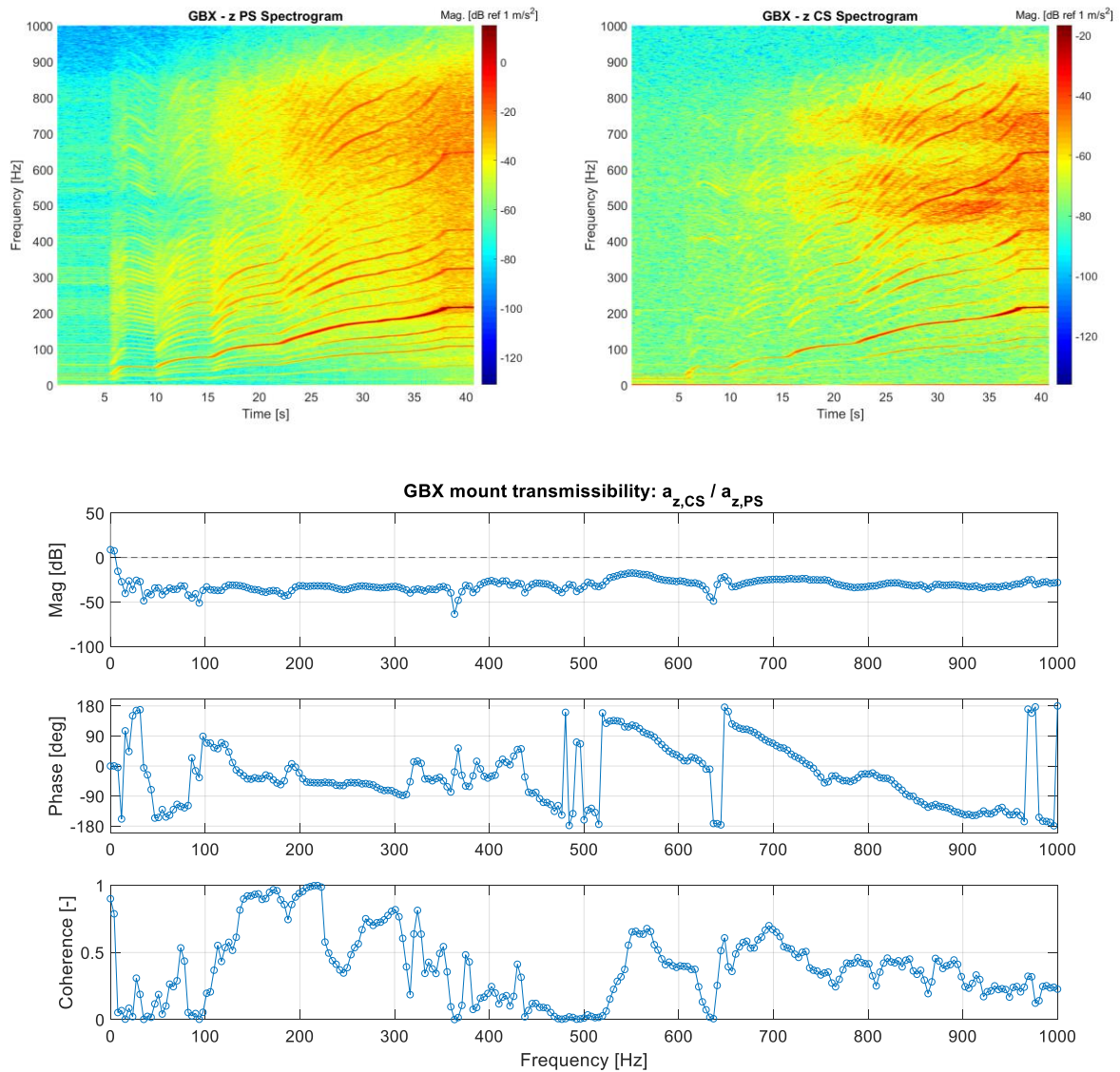


**Figure 5.23:** Spectrograms and transfer function of the accelerations signal of the gearbox's mount along z

Also in this case, a comparison between the vibration of the two sides of the mount is carried on in the orders domain; also with this analysis, the effect of vibration reduction due to the mount presence is clearly visible. These results are in **Figure 5.24** and **Figure 5.25**.

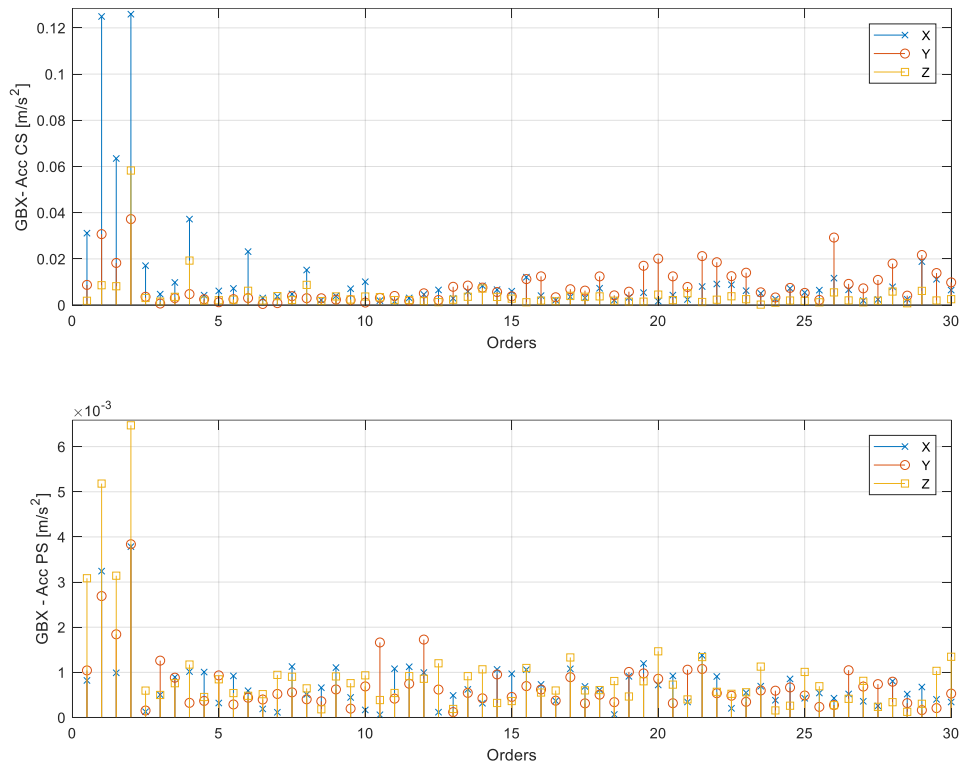


Figure 5.24: Amplitudes of the gearbox’s mount accelerations signals in the order domain

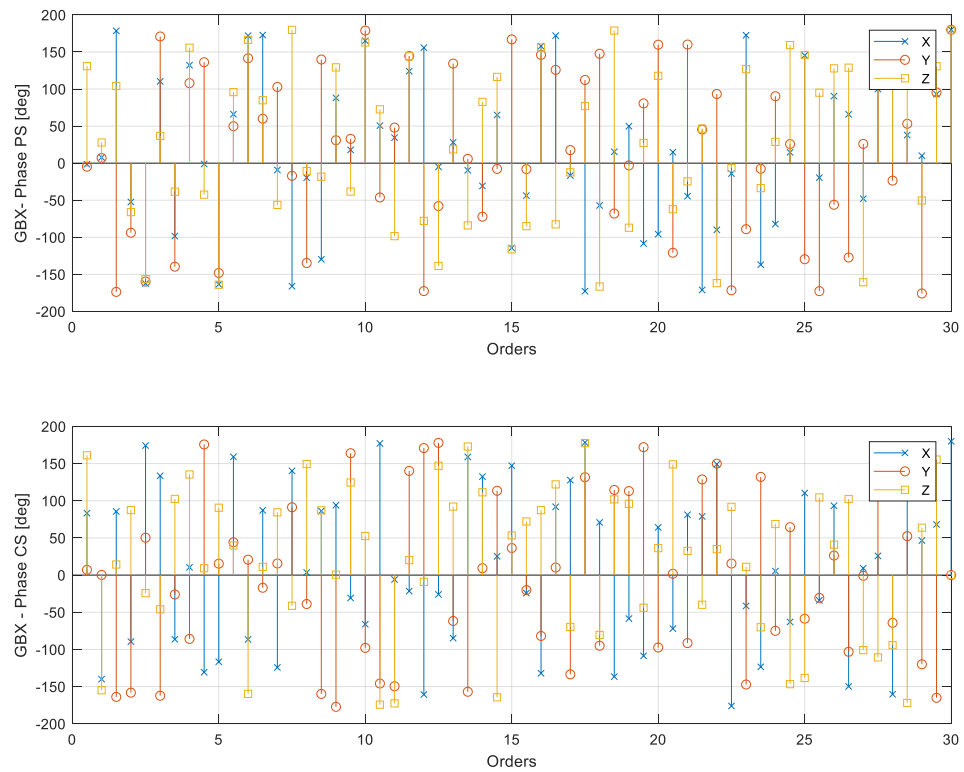


Figure 5.25: Amplitudes of the gearbox’s mount accelerations signals in the order domain

### 5.3 - ESTIMATION OF THE FRFs USING THE EXPERIMENTAL ALGORITHM

In this paragraph is performed the analysis relative to the speed signals measured by some of the different pick-ups installed on the vehicle, carried on in order to determine the FRFs of different gears of the vehicle's powertrain. Taking in consideration two different Sweep tests (composed by Run Up and Coast Down phases), performed respectively in second and sixth gear, for each test there are eight speed signal which are used in this analysis.

The signals are the measurement of the velocity of the following components:

- Engine flywheel;
- K1 clutch;
- K2 clutch;
- First idle gear;
- Second idle gear;
- Third idle gear;
- Lower secondary shaft;
- Differential.

The aim of this analysis is to compute the inertance of all the components (except the flywheel's auto-inertance, which value is imposed constant and equal to the reciprocal of the inertia) respect the torque's irregularities applied on the crankshaft. The torque is calculated, considering the error due to the approximation described in the previous chapter, as the product between the instantaneous acceleration of the flywheel and the moment of inertia of the crankshaft and the first mass of the Double Mass Flywheel (DMF). At this point, the estimation of the different FRFs is performed by the script implementation of the algorithm.

The results of the FRFs of each Sweep test will be divided between the Run Up and the Coast Down phases; this is due to the fact that the inertances during the two phases are different because of the non-linearities of the system and the variation of the parameters which are dependent from the load conditions of the engine.

Another important clarification is that, during this analysis, for the inertances calculation only the contributions of the 2<sup>nd</sup>, 4<sup>th</sup>, 6<sup>th</sup> and 8<sup>th</sup> orders are considered; this choice depends on the fact that the higher orders give a very small and consequently negligible contribution in terms of inertance.

In addition to this, before the calculation of the inertance as the ratio between the acceleration of the considered gear and the estimated torque, is better to plot the value of these accelerations as function of the engine's mean speed: in this way, an intermediate step between the orders spectrogram and the inertance plot is useful to control the correct procedure of the estimation algorithm.

The main parameters that characterizes the two tests are listed in **Table 5.6**; observing the limit values of the engine's speed range, it should be clear that a shorter speed range corresponds to a shorter frequency range over which the numerical estimation of the FRF is available.

Type of test	K1 clutch status	K2 clutch status	Gear engaged	Engine's speed interval [rpm]
Sweep	Engaged - speed tracking	Engaged - torque transmission	2 <sup>nd</sup>	1'000-5'200
Sweep	Engaged - speed tracking	Engaged - torque transmission	6 <sup>th</sup>	1'383-2'338

**Table 5.6:** Main parameters of the tests

Is interesting to observe that the number of points of the FRFs plots directly depends on the sampling frequency of the two original signals used as input for the experimental algorithm and on the time duration of the two phases of the Sweep test, i.e. the slope of the speed signals measured, of which the flywheel's one is the most representative of the test's characteristics.

The different FRFs computations are performed for one gear a time; however, depending on the gear engaged during the test (even or odd), some velocity signal is affected by the discontinuities due to the working principle of the DCT gearbox. For the 2<sup>nd</sup> gear test considered in this chapter, the signals of the K1 clutch, the first and the third idle gears are influenced by the pre-selection of the 3<sup>rd</sup> gear ratio: for this reason, the FRF estimation of this gears ins not performed because the results would not be significant.

The results relative to the first Sweep test performed in 2<sup>nd</sup> gear are shown from **Figure 5.26** to **Figure 5.34**.

# ENGINE FLYWHEEL

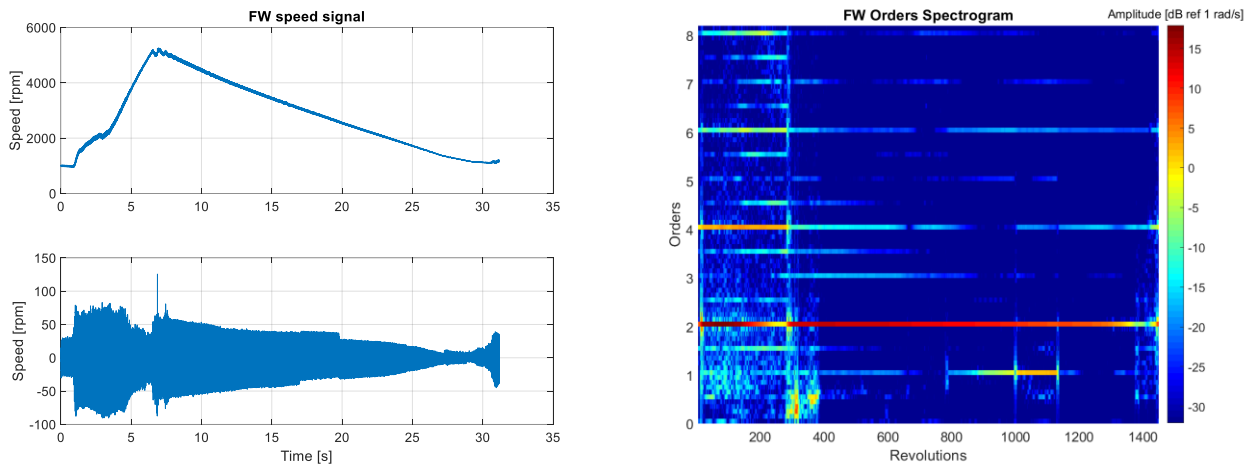


Figure 5.26: Engine flywheel's velocity signal and its orders spectrogram - 2<sup>nd</sup> gear Sweep test

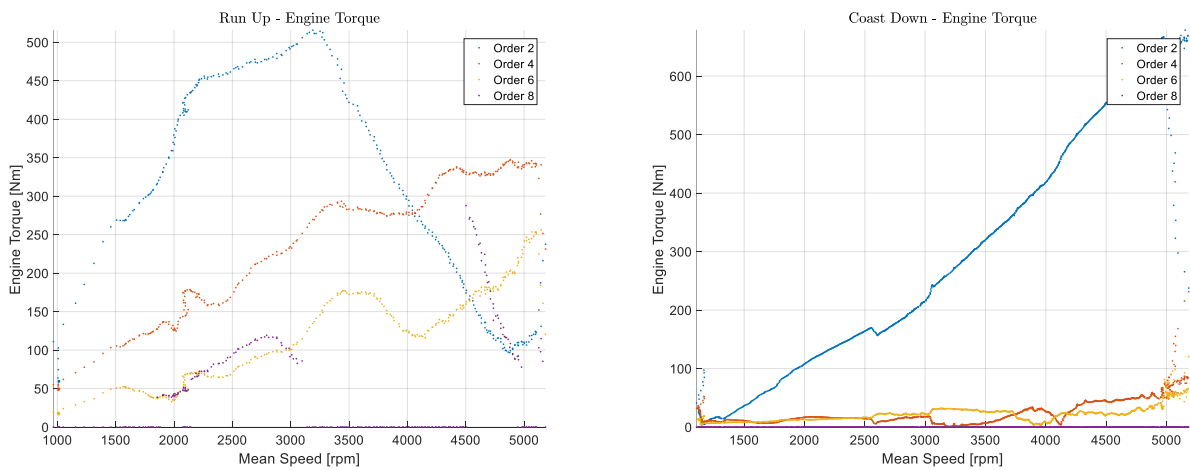


Figure 5.27: Engine flywheel's torque's harmonics - 2<sup>nd</sup> gear Sweep test

# K2 CLUTCH

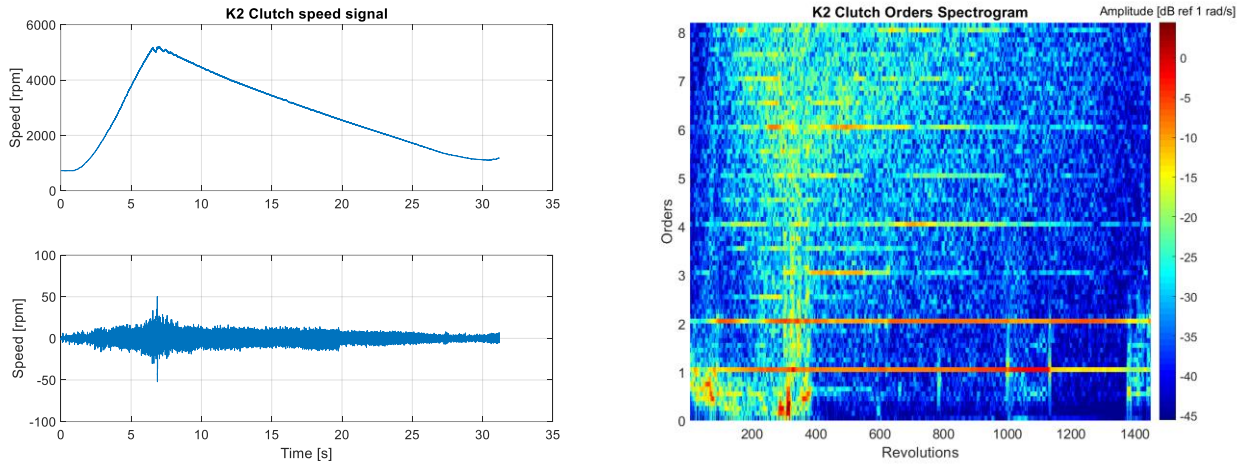


Figure 5.28: K2 clutch's velocity signal and its orders spectrogram - 2<sup>nd</sup> gear Sweep test

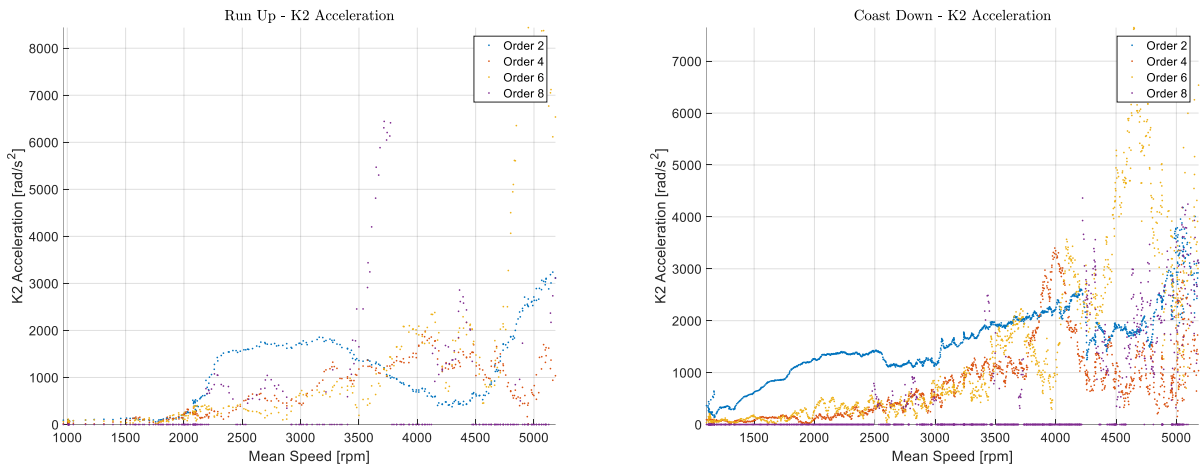


Figure 5.29: K2 clutch's accelerations - 2<sup>nd</sup> gear Sweep test

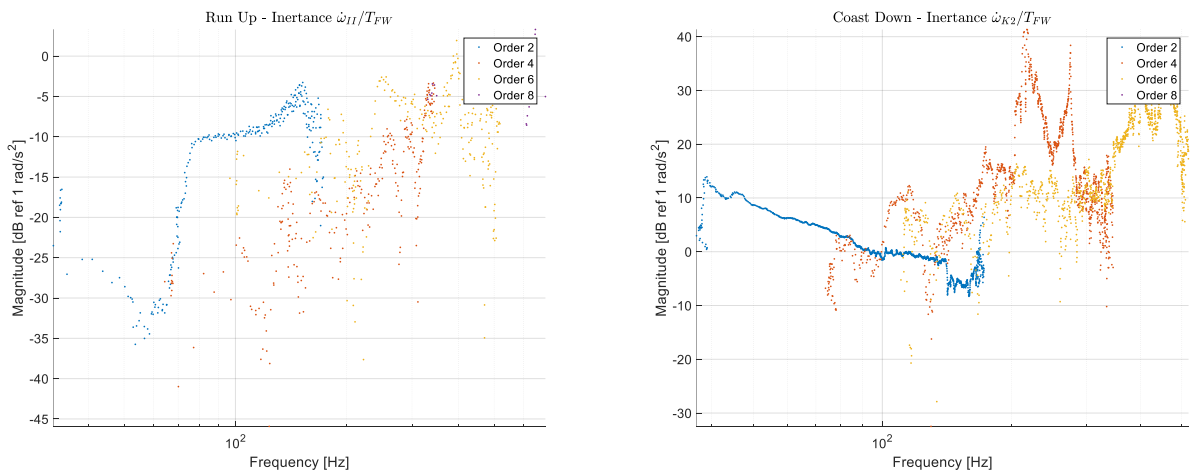


Figure 5.30: K2 clutch's inertance - 2<sup>nd</sup> gear Sweep test

## SECOND GEAR

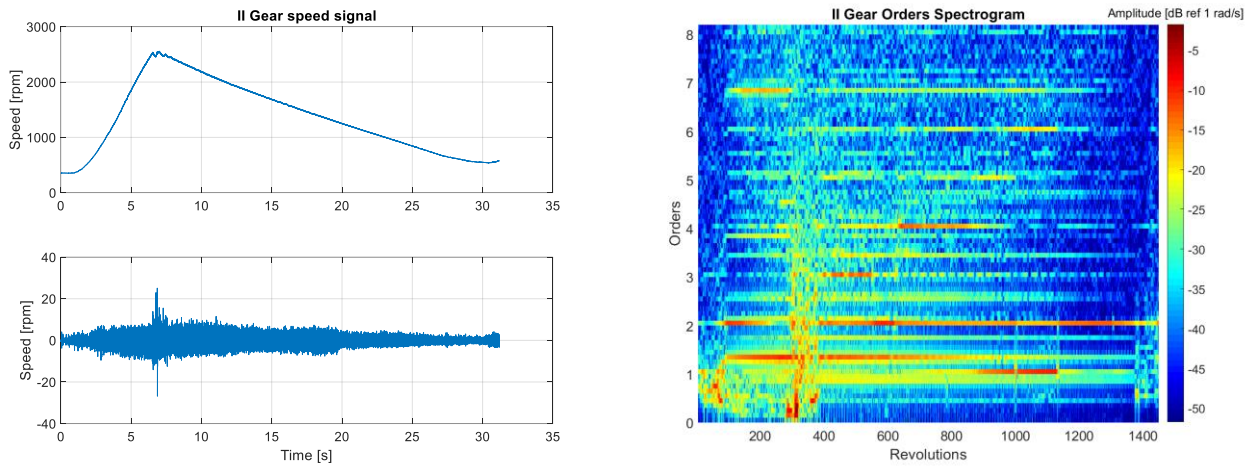


Figure 5.28: Second gear's velocity signal and its orders spectrogram - 2<sup>nd</sup> gear Sweep test

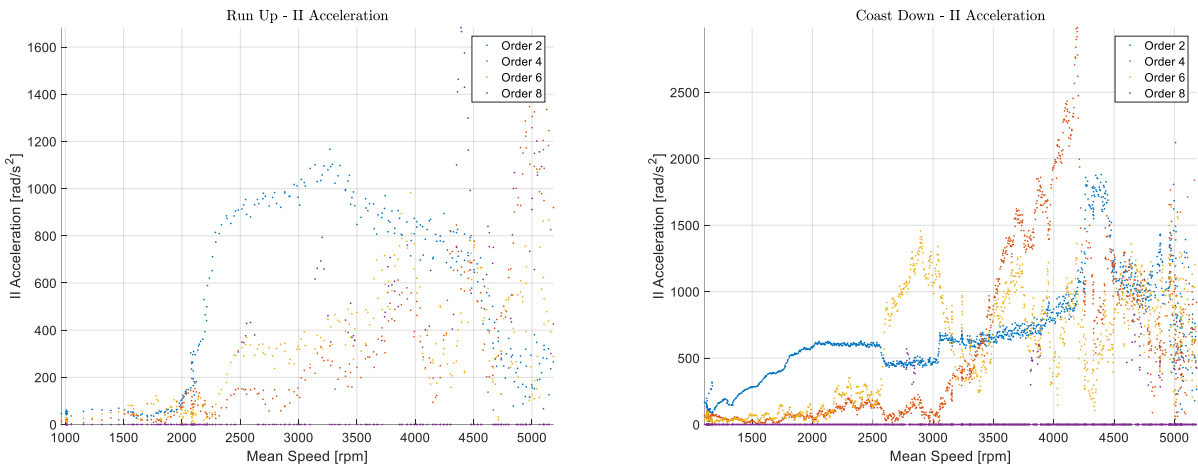


Figure 5.29: Second gear's accelerations - 2<sup>nd</sup> gear Sweep test

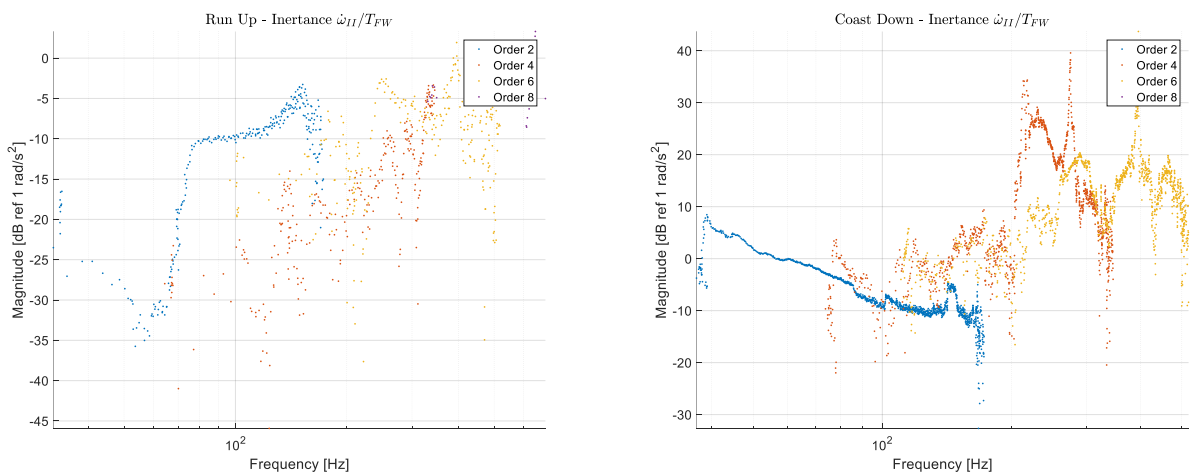


Figure 5.33: Second gear's inertance - 2<sup>nd</sup> gear Sweep test

## LOWER SECONDARY SHAFT

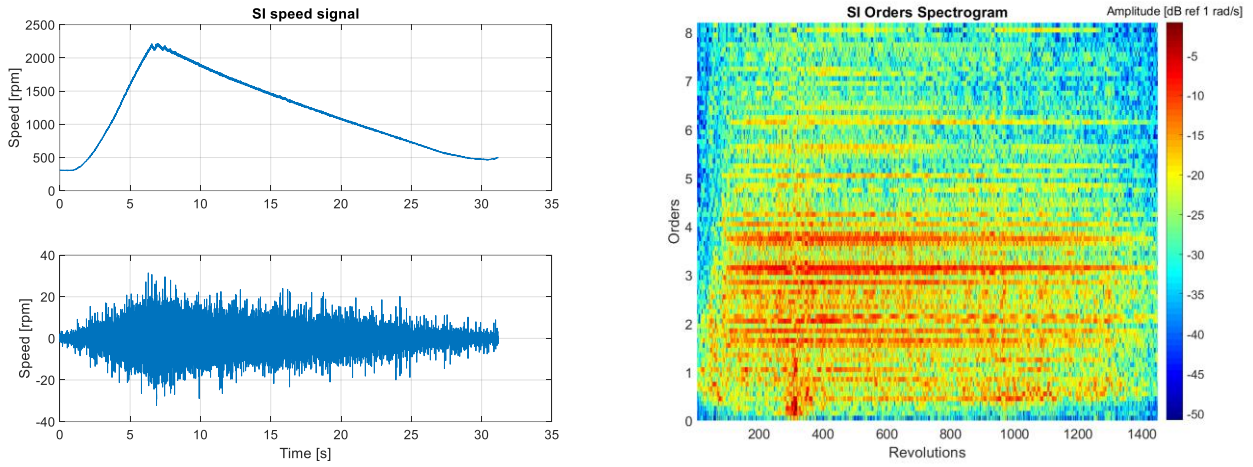


Figure 5.34: Lower secondary shaft's velocity signal and its orders spectrogram - 2<sup>nd</sup> gear Sweep test

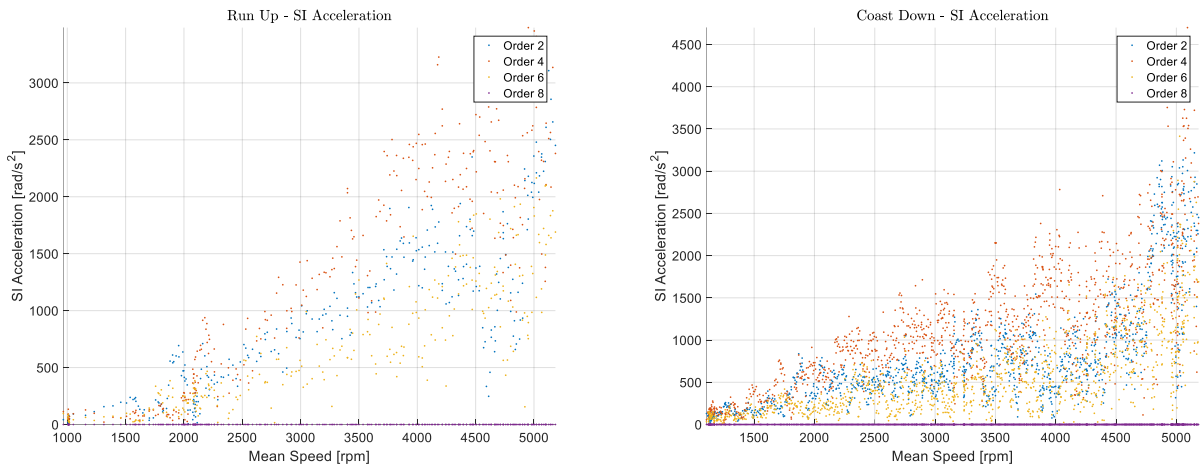


Figure 5.30: Lower secondary shaft's accelerations - 2<sup>nd</sup> gear Sweep test

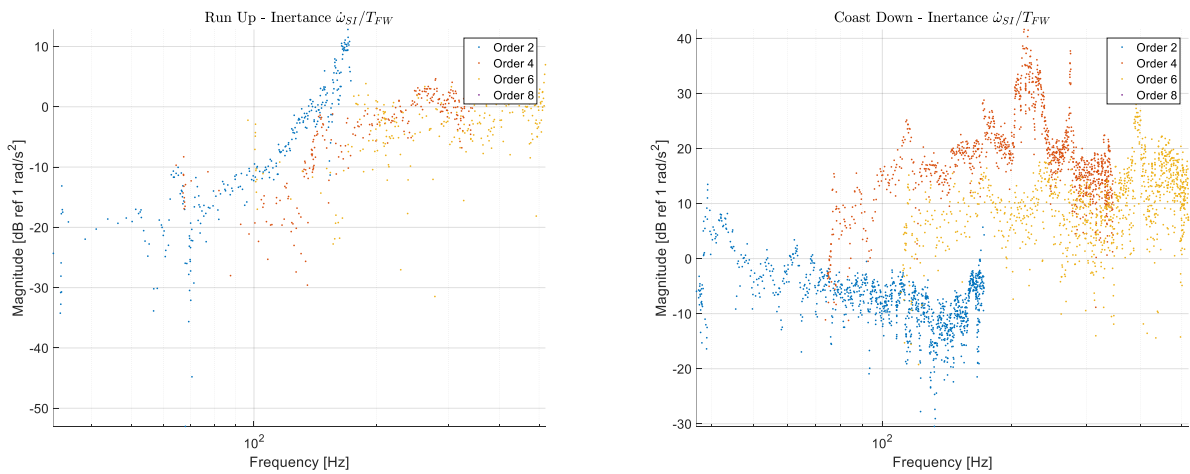


Figure 5.31: Lower secondary shaft's inertia - 2<sup>nd</sup> gear Sweep test

# DIFFERENTIAL

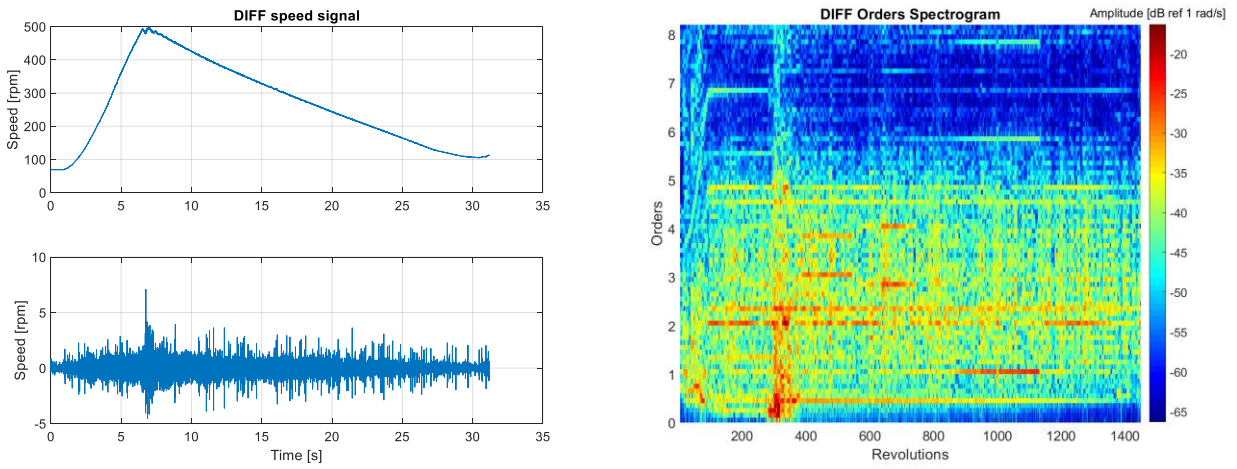


Figure 5.32: Differential's velocity signal and its orders spectrogram - 2<sup>nd</sup> gear Sweep test

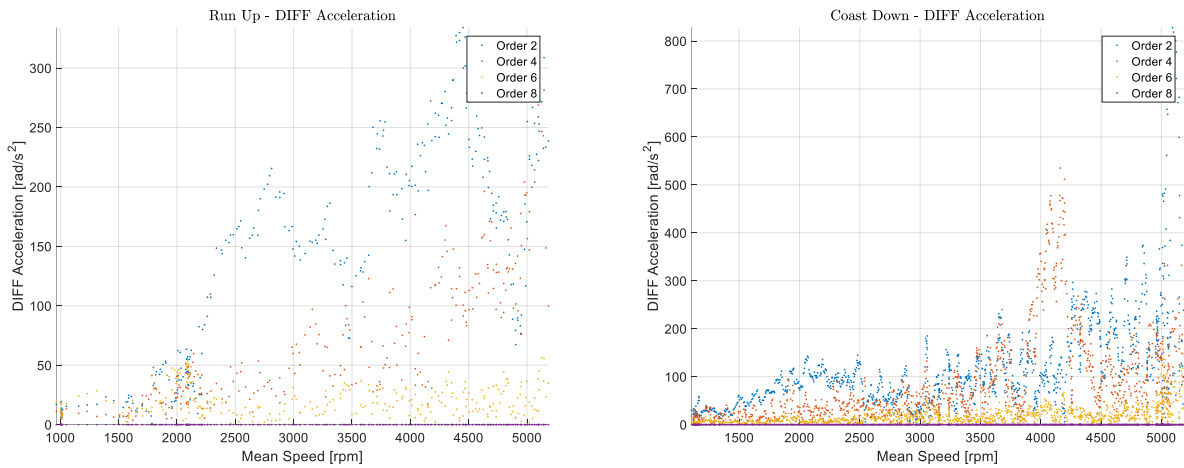


Figure 5.33: Differential's accelerations - 2<sup>nd</sup> gear Sweep test

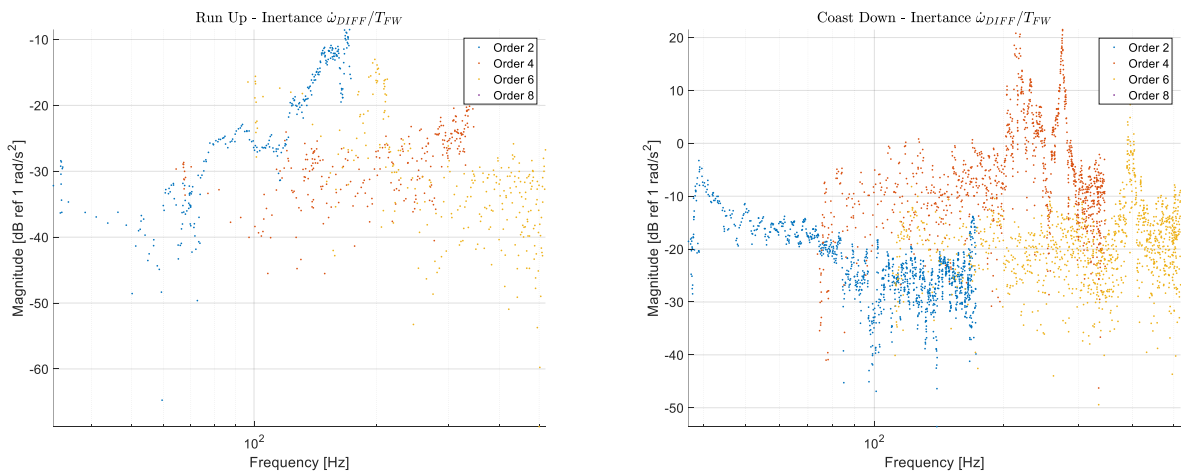


Figure 5.34: Differential's inertia - 2<sup>nd</sup> gear Sweep test

All the graphical results related to the 2<sup>nd</sup> gear Sweep test are characterized by a relative low number of point for the Run Up phase: as already said, this is due to the short time duration of this phase during the test. In a similar way, since the Coast Down phase of the test has a longer time duration, the higher number of point gives a higher precision in term of frequency for the estimation of the inertance. Another factor influencing the quality of the results is the presence of noise inside the original signal; in fact, the velocity signals characterized by strong instantaneous variation in their amplitude transfer this trend also to the respective FRF estimation. Also the fact that the value of the torque is not measured but calculated with a certain approximation can give raise to a certain error, also if all the plotted results are referred to values of frequency for which this error is lower than the maximum admissible.

At this point, the FRF algorithm is applied to a different Sweep test: this time, the test is performed in 6<sup>th</sup> gear and it means that the test is characterized by a lower acceleration of the vehicle, with a consequent higher time duration of the Run Up phase of the test. Is important to pay attention to the fact that these results are limited to the 6<sup>th</sup> order, because the contributions relative to the 8<sup>th</sup> are negligible. In addition, in this case the FRF estimation can be applied to all the available signals, since the 6<sup>th</sup> gear is the last one, and no pre-selection phases affect the input velocity signals.

Results are shown from **Figure 5.35** to **Figure 5.57**.

# ENGINE FLYWHEEL

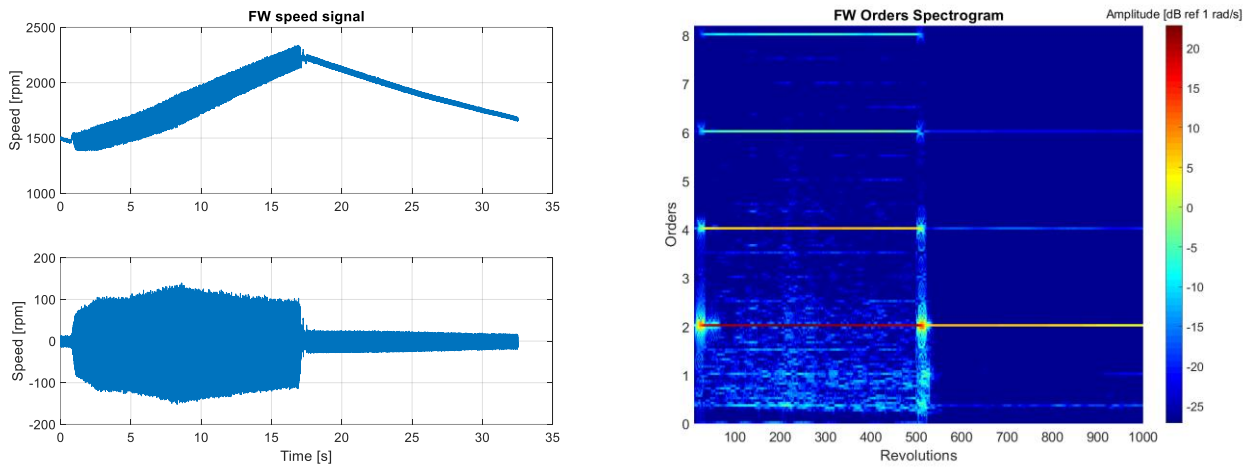


Figure 5.35: Engine flywheel's velocity signal and its orders spectrogram - 6<sup>th</sup> gear Sweep test

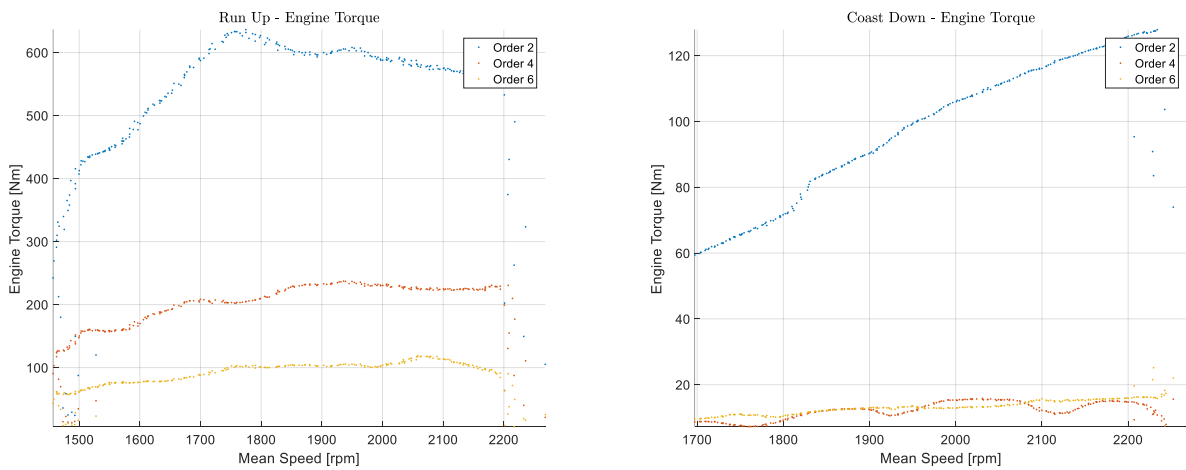


Figure 5.36: Engine flywheel's torque's harmonics - 6<sup>th</sup> gear Sweep test

# K1 CLUTCH

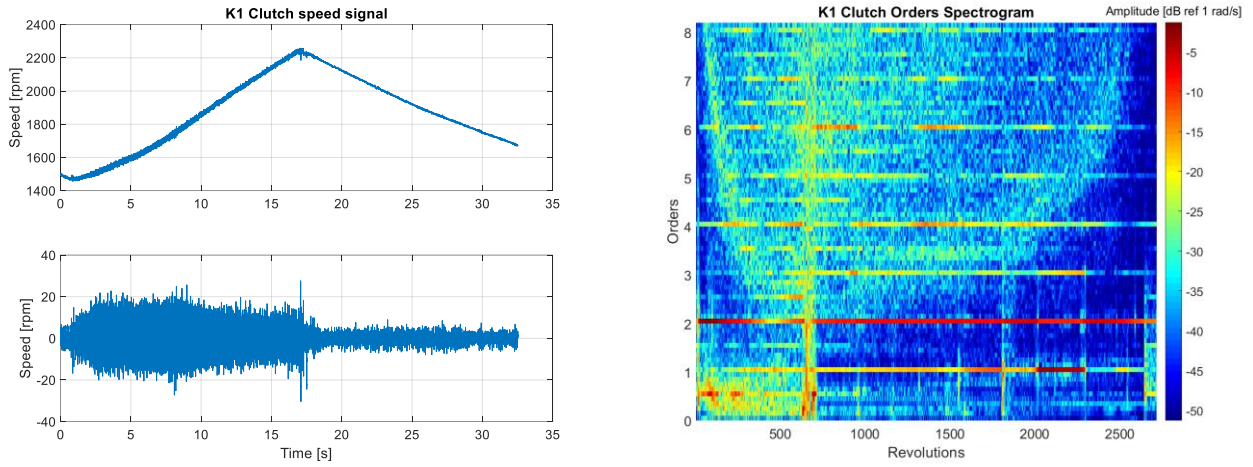


Figure 5.37: K1 clutch's velocity signal and its orders spectrogram - 6<sup>th</sup> gear Sweep test

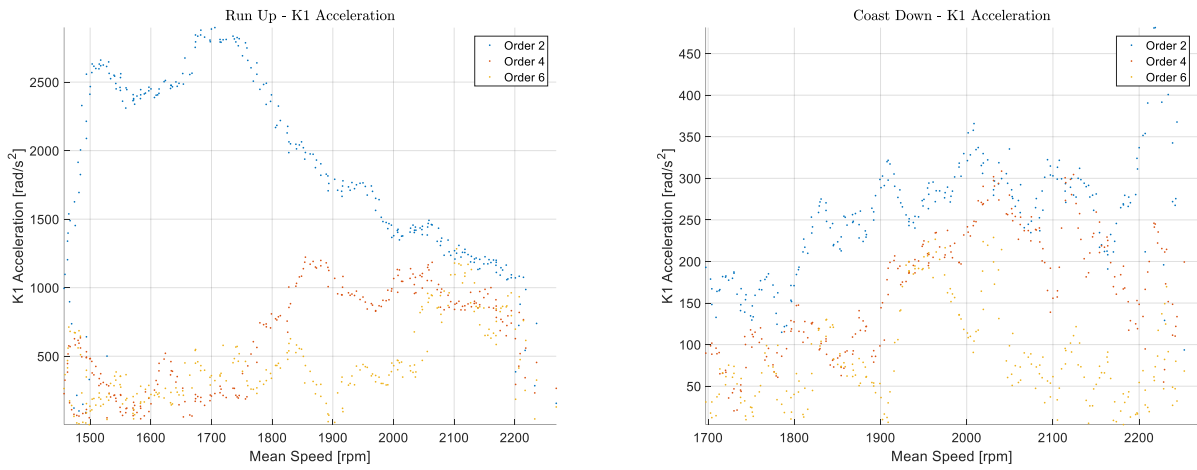


Figure 5.38: K1 clutch's accelerations - 6<sup>th</sup> gear Sweep test

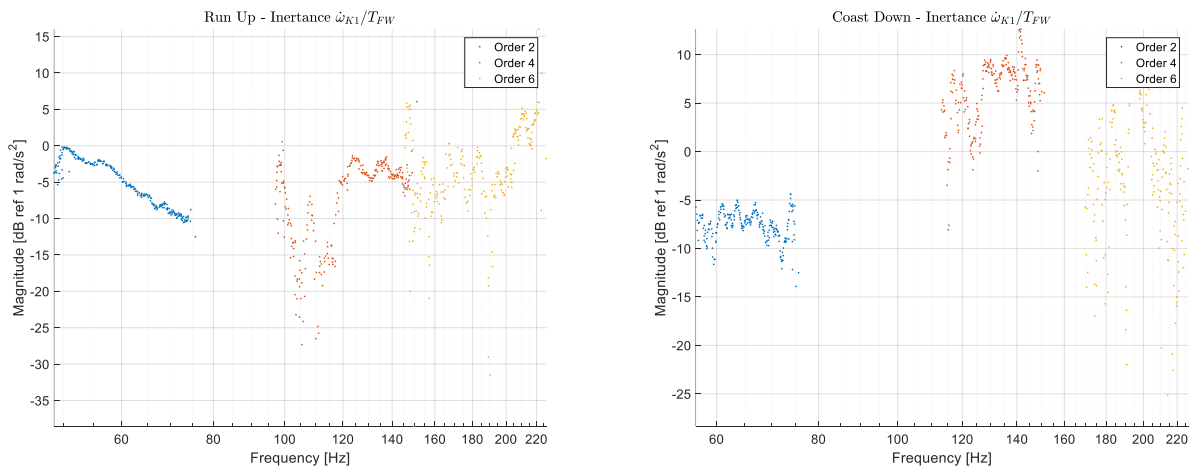


Figure 5.39: K1 clutch's inertance - 6<sup>th</sup> gear Sweep test

# K2 CLUTCH

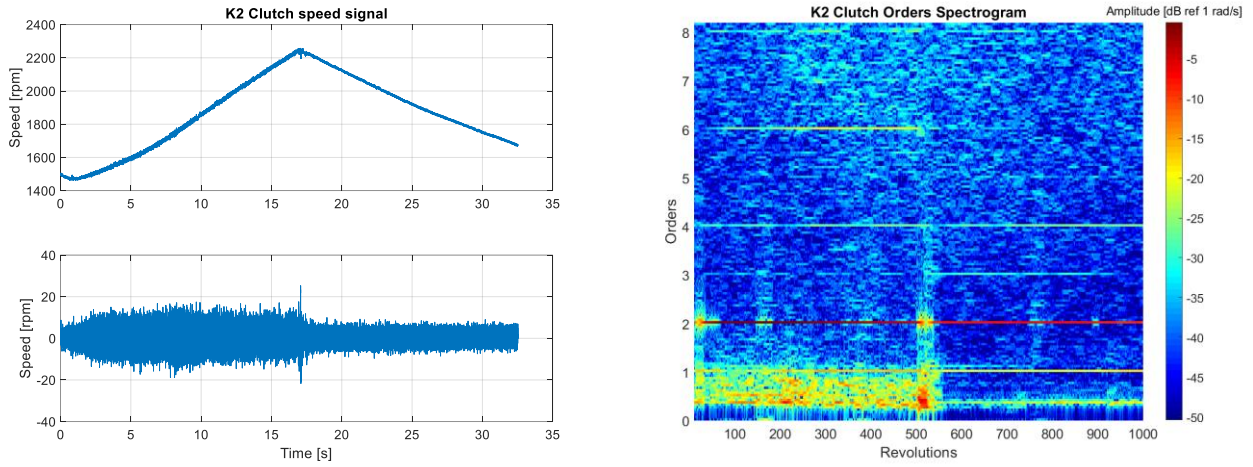


Figure 5.40: K2 clutch's velocity signal and its orders spectrogram - 6<sup>th</sup> gear Sweep test

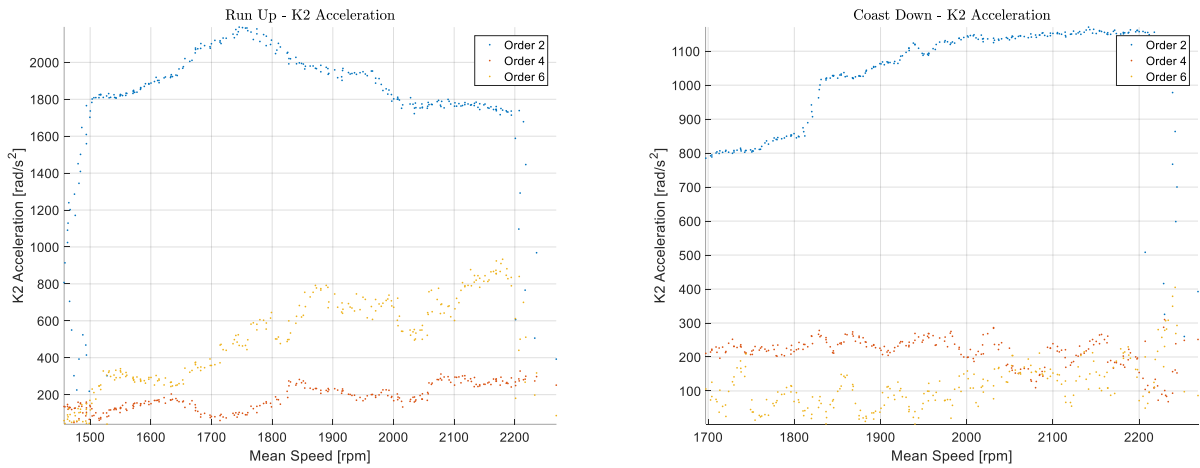


Figure 5.41: K2 clutch's accelerations - 6<sup>th</sup> gear Sweep test

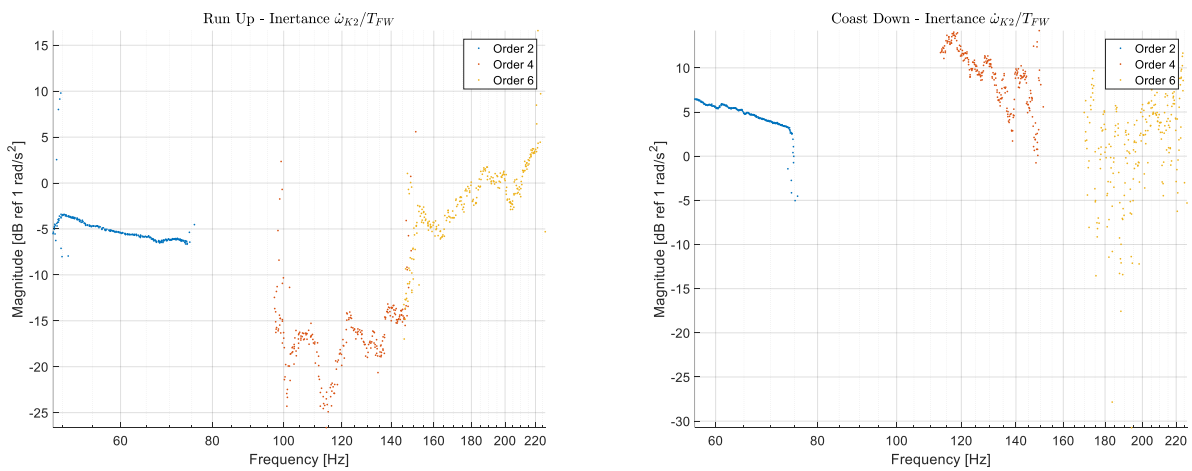


Figure 5.42: K2 clutch's inertance - 6<sup>th</sup> gear Sweep test

# FIRST GEAR

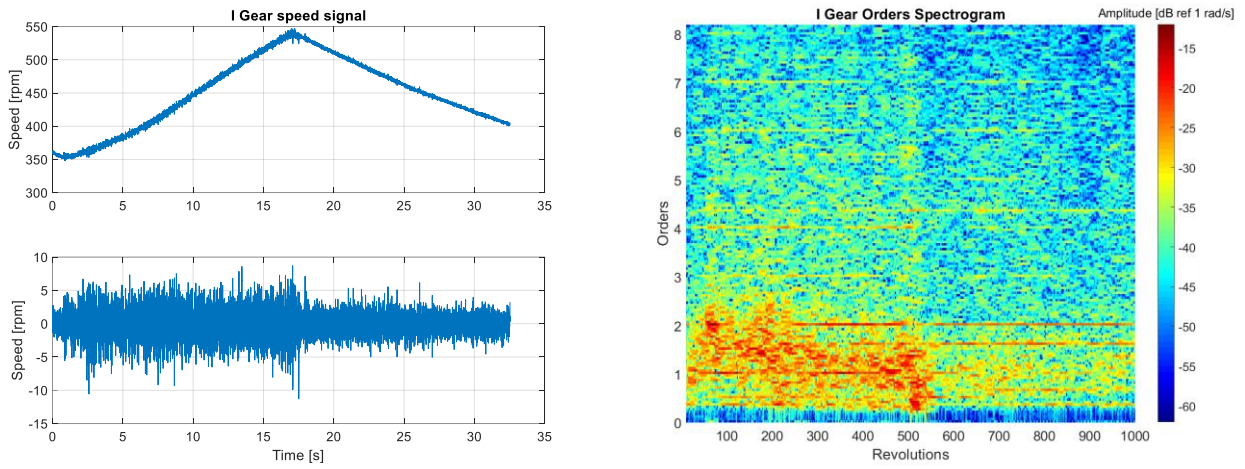


Figure 5.43: First gear's velocity signal and its orders spectrogram - 6<sup>th</sup> gear Sweep test

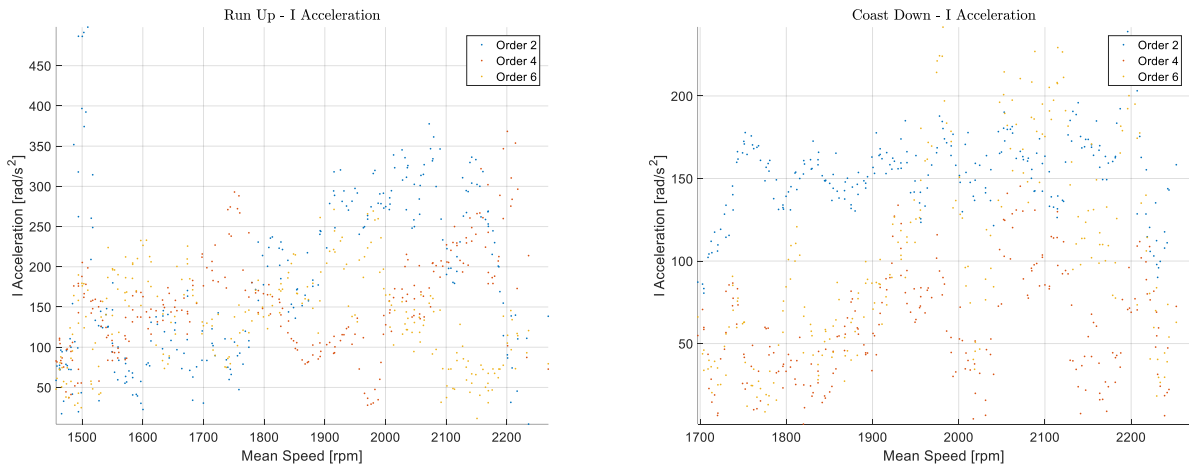


Figure 5.44: First gear's accelerations - 6<sup>th</sup> gear Sweep test

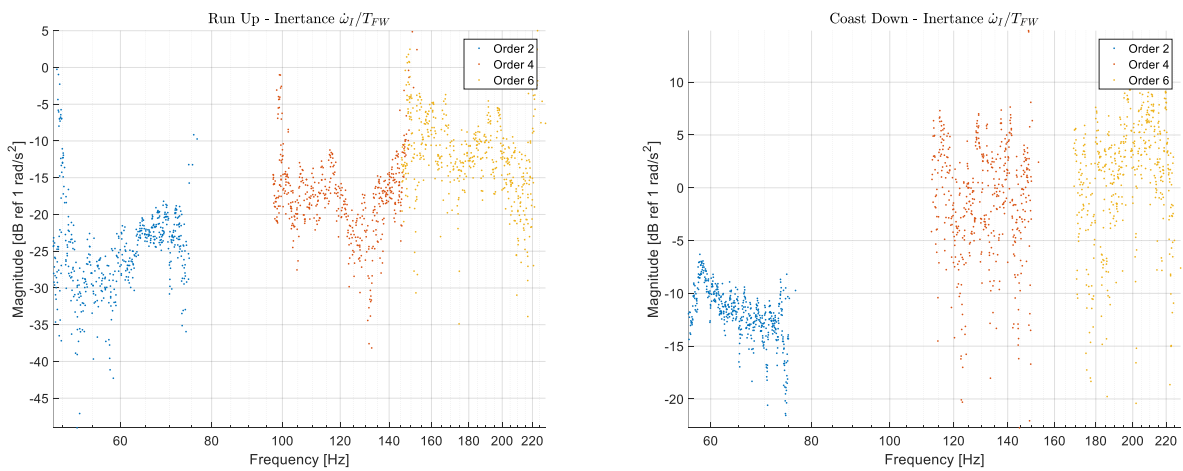


Figure 5.45: First gear's inertance - 6<sup>th</sup> gear Sweep test

## SECOND GEAR

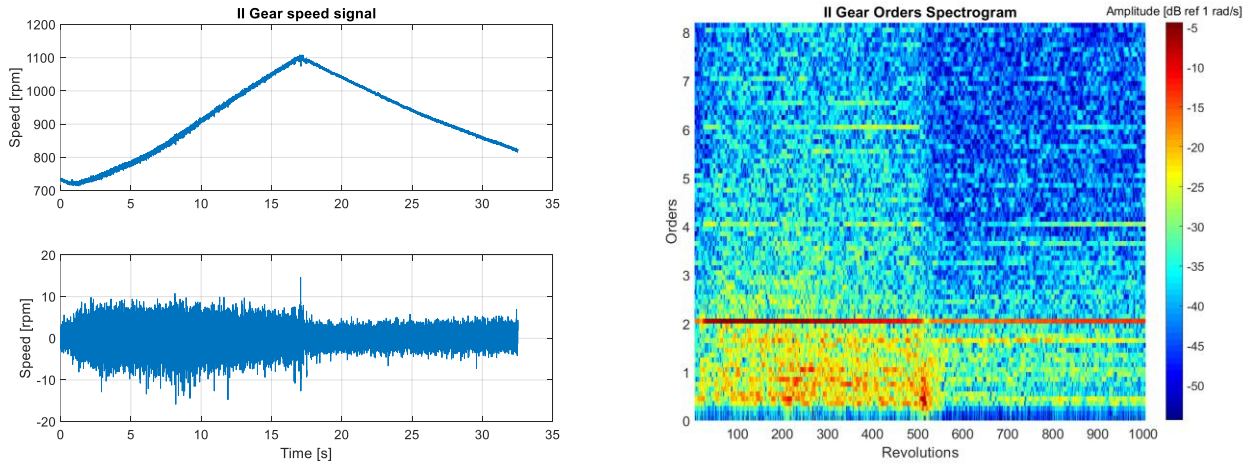


Figure 5.46: Second gear's velocity signal and its orders spectrogram - 6<sup>th</sup> gear Sweep test

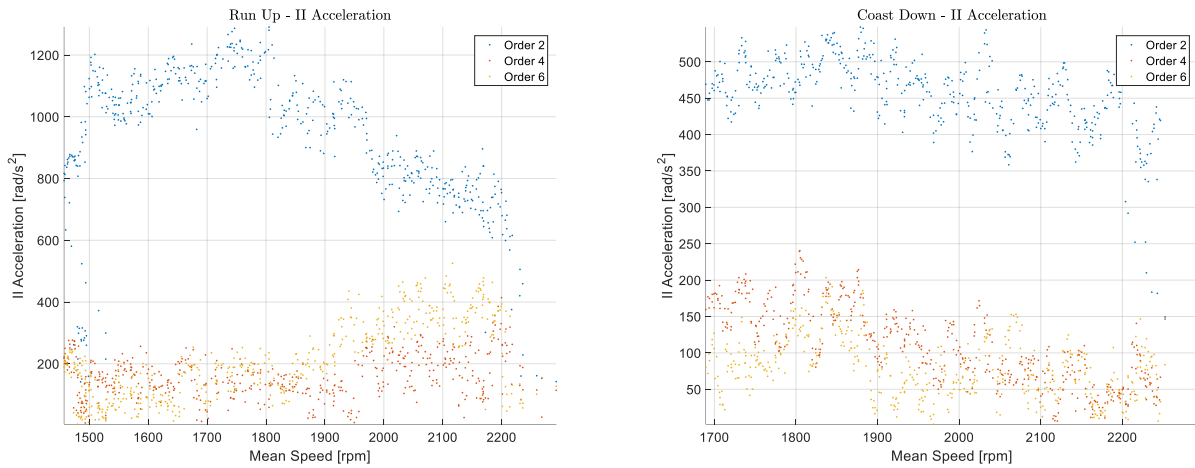


Figure 5.47: Second gear's accelerations - 6<sup>th</sup> gear Sweep test

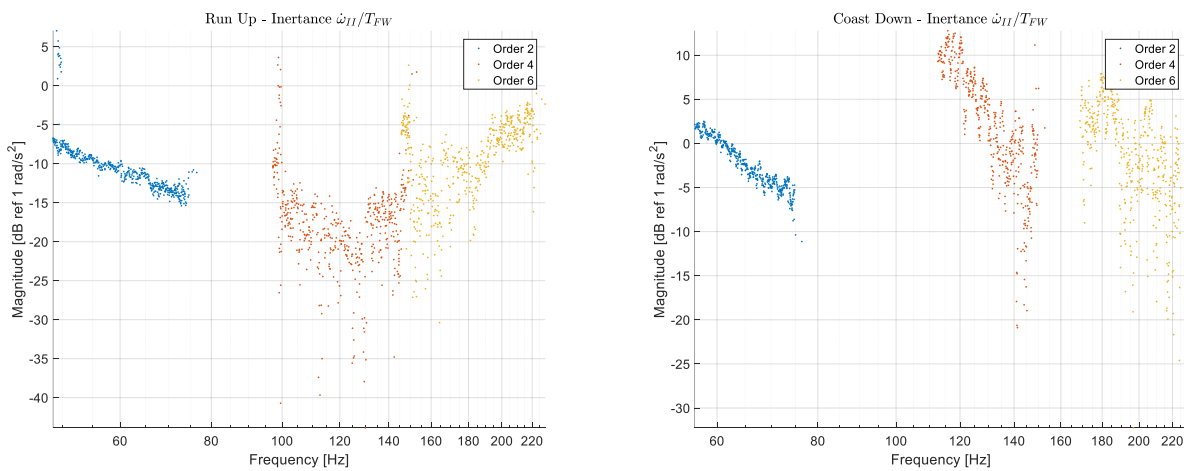


Figure 5.48: Second gear's inertance - 6<sup>th</sup> gear Sweep test

# THIRD GEAR

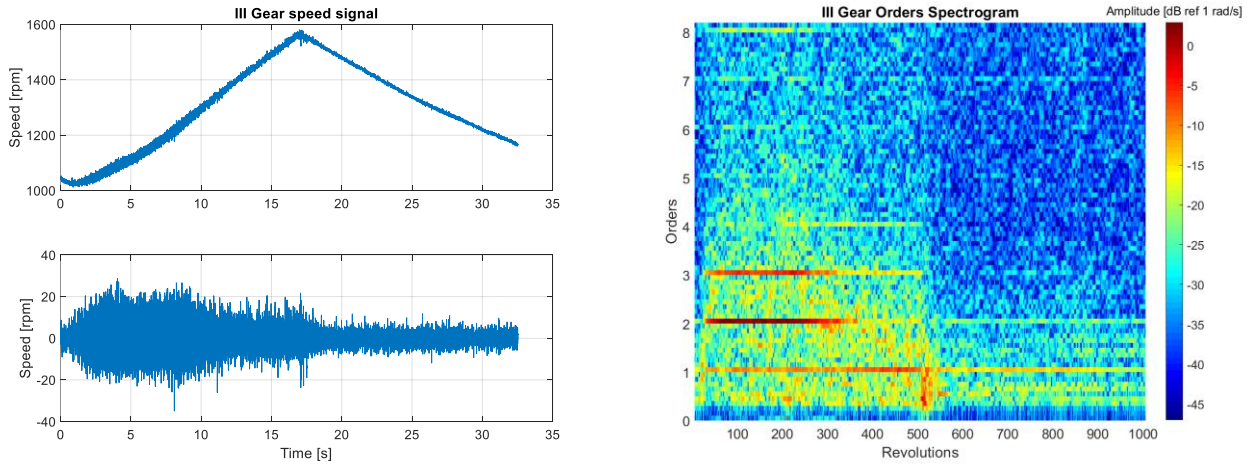


Figure 5.49: Third gear's velocity signal and its orders spectrogram - 6<sup>th</sup> gear Sweep test

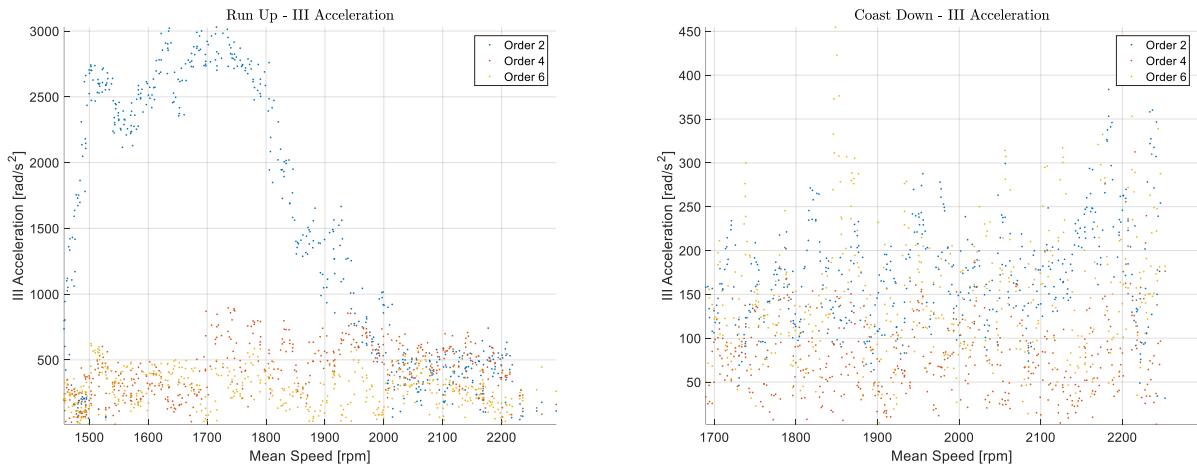


Figure 5.50: Third gear's accelerations - 6<sup>th</sup> gear Sweep test

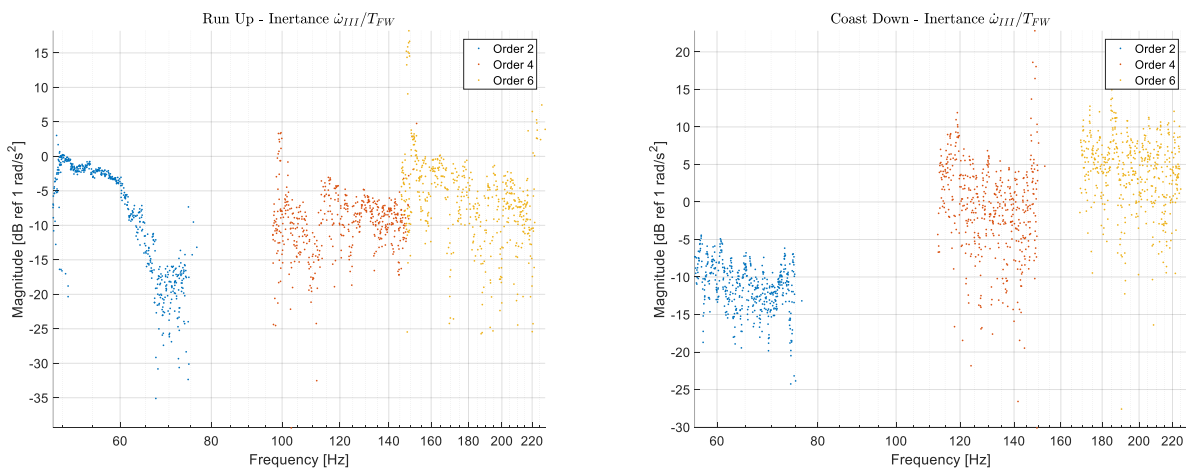


Figure 5.51: Third gear's inertia - 6<sup>th</sup> gear Sweep test

## LOWER SECONDARY SHAFT

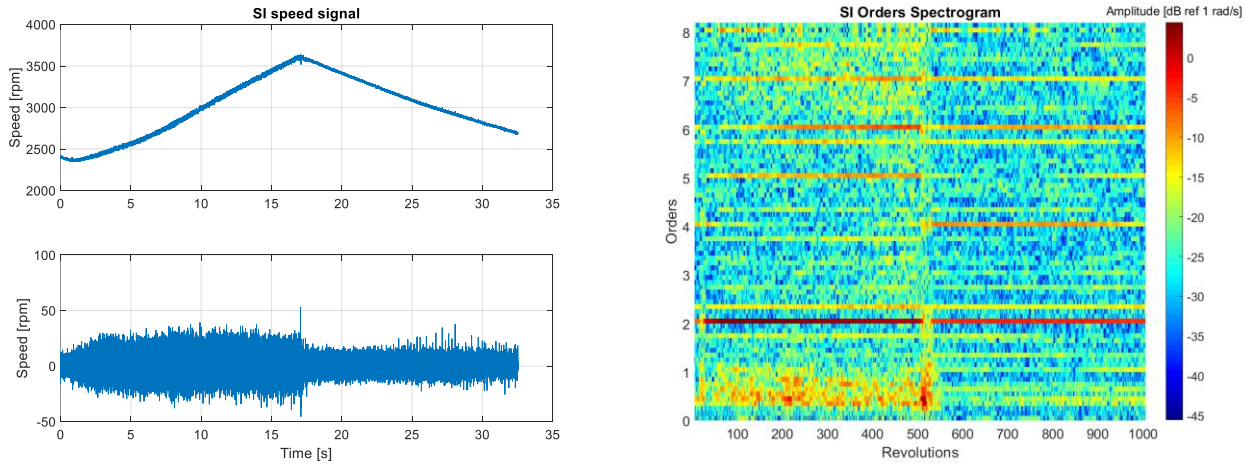


Figure 5.52: Lower secondary shaft's velocity signal and its orders spectrogram - 6<sup>th</sup> gear Sweep test

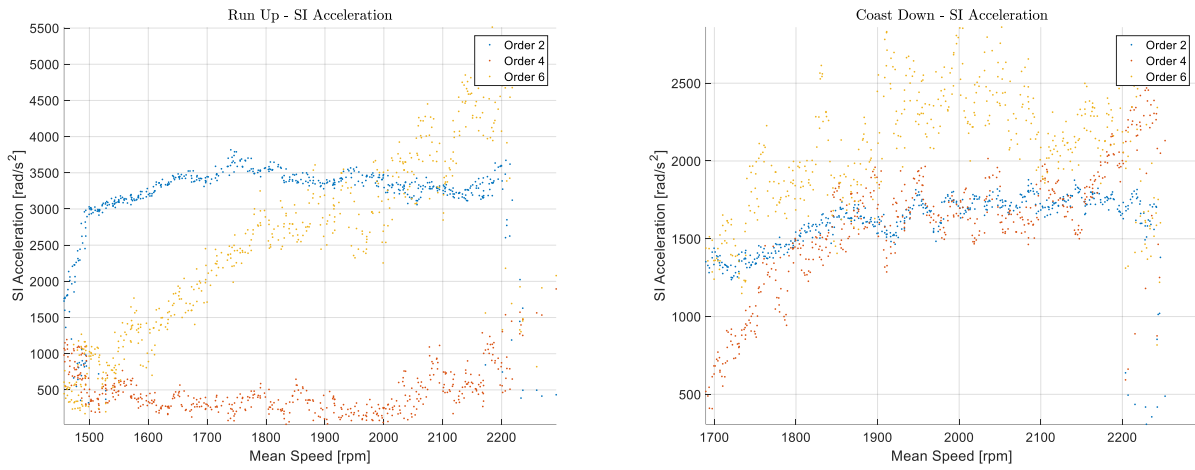


Figure 5.53: Lower secondary shaft's accelerations - 6<sup>th</sup> gear Sweep test

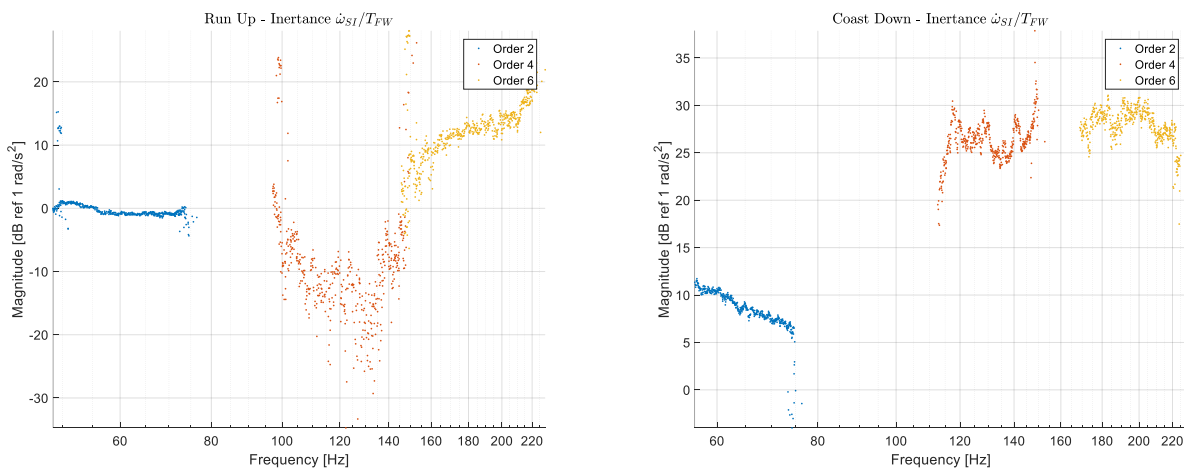


Figure 5.54: Lower secondary shaft's inertia - 6<sup>th</sup> gear Sweep test

# DIFFERENTIAL

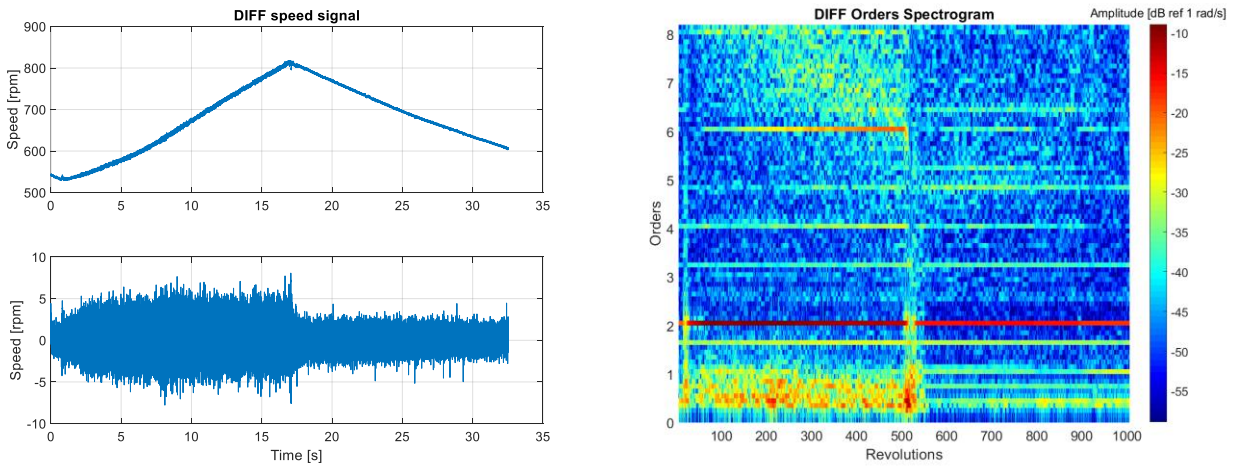


Figure 5.55: Differential's velocity signal and its orders spectrogram - 6<sup>th</sup> gear Sweep test

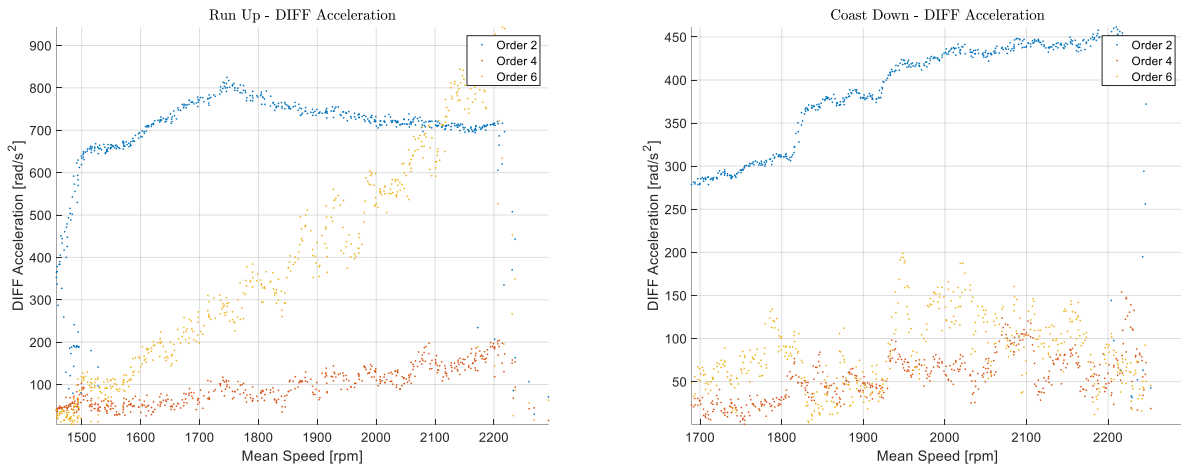


Figure 5.56: Differential's accelerations - 6<sup>th</sup> gear Sweep test

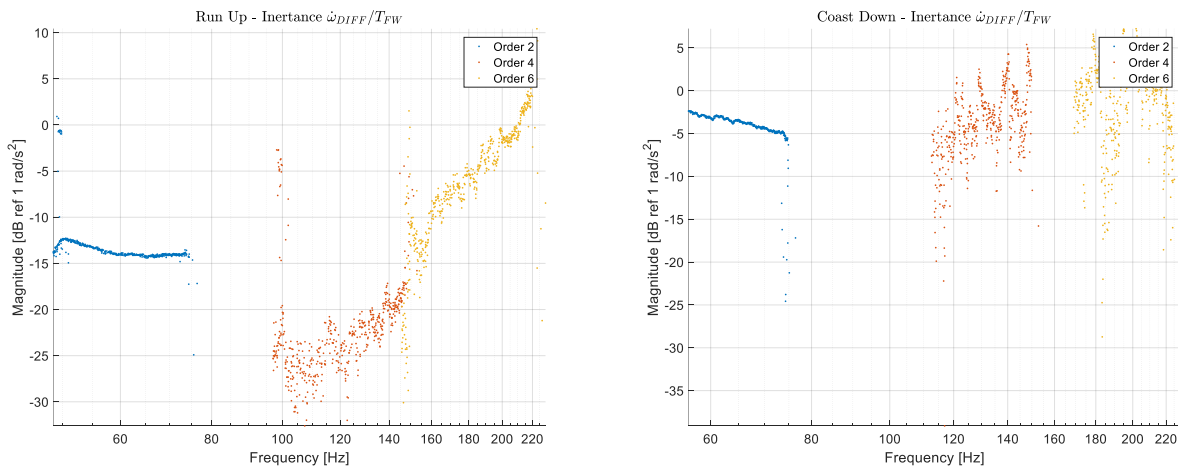


Figure 5.57: Differential's inertia - 6<sup>th</sup> gear Sweep test

Usually, a higher time duration of the test leads to a better resolution in terms of frequency of the results; however, in this case the effect is not very evident. The reason is that since the engine's maximum speed is relatively low, the revolutions performed by the crankshaft are lower than the case of the Sweep test in 2<sup>nd</sup> gear. Since all the signals are re-sampled respect the angular position of the flywheel, lots of samples of the signal are lost during the interpolation process necessary to build the synchronous signals. However, the resolution in term of inertance for the 2<sup>nd</sup> order is sufficiently good, and to this order corresponds the main contribution in terms of amplitude for almost all the signals considered.

## 5.4 - A DIFFERENT APPLICATION OF THE FRF ALGORITHM

The FRF experimental algorithm can be also applied in different cases from the calculation of the inertance described in the previous paragraph. Another possible application can be the estimation of the FRF that links the engine's torque to the acceleration measured by an accelerometer placed on one of the mounts. In this paragraph, an example of this application is described.

Let's consider the two signals depicted in **Figure 5.58**, representing the engine's flywheel speed signal and the acceleration signal along the z direction (chassis side) of the engine's mount, both measured during a Run Up test performed in neutral gear.

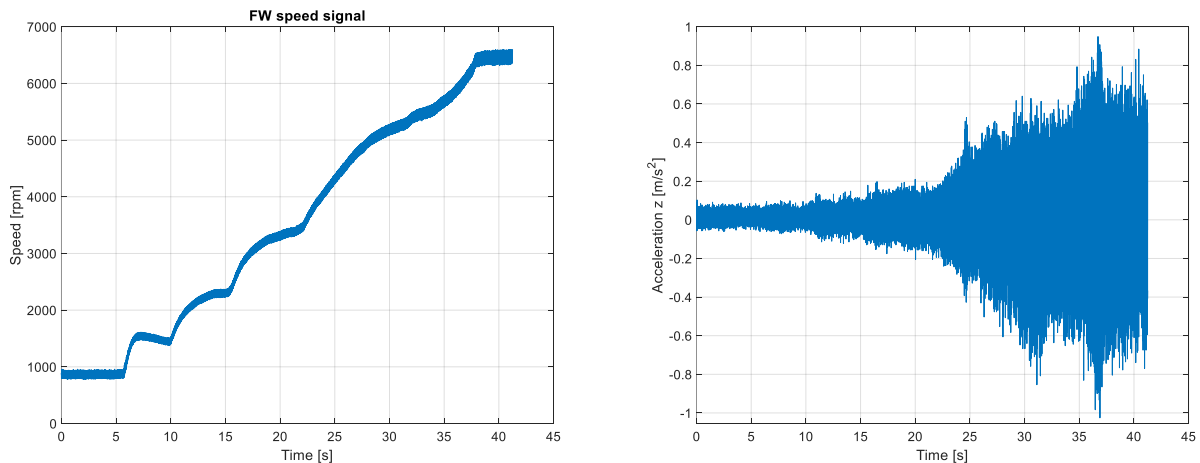


**Figure 5.58:** Input and output for the FRF's estimation

In order to compute this type of FRF, is necessary to estimate the torque with the same procedure described in the previous chapter. For what concerns the acceleration's signal, with a procedure similar to the one applied to the speed signal, after its re-sampling respect the flywheel's angular position, its spectrograms in order is computed. At this point, from the  $S$  matrix of the spectrogram,

the rows corresponding to the orders in interest are extracted and, through the point-by-point ratio with the estimated torque, finally the FRF is computed. This result is shown in **Figure 5.59**.

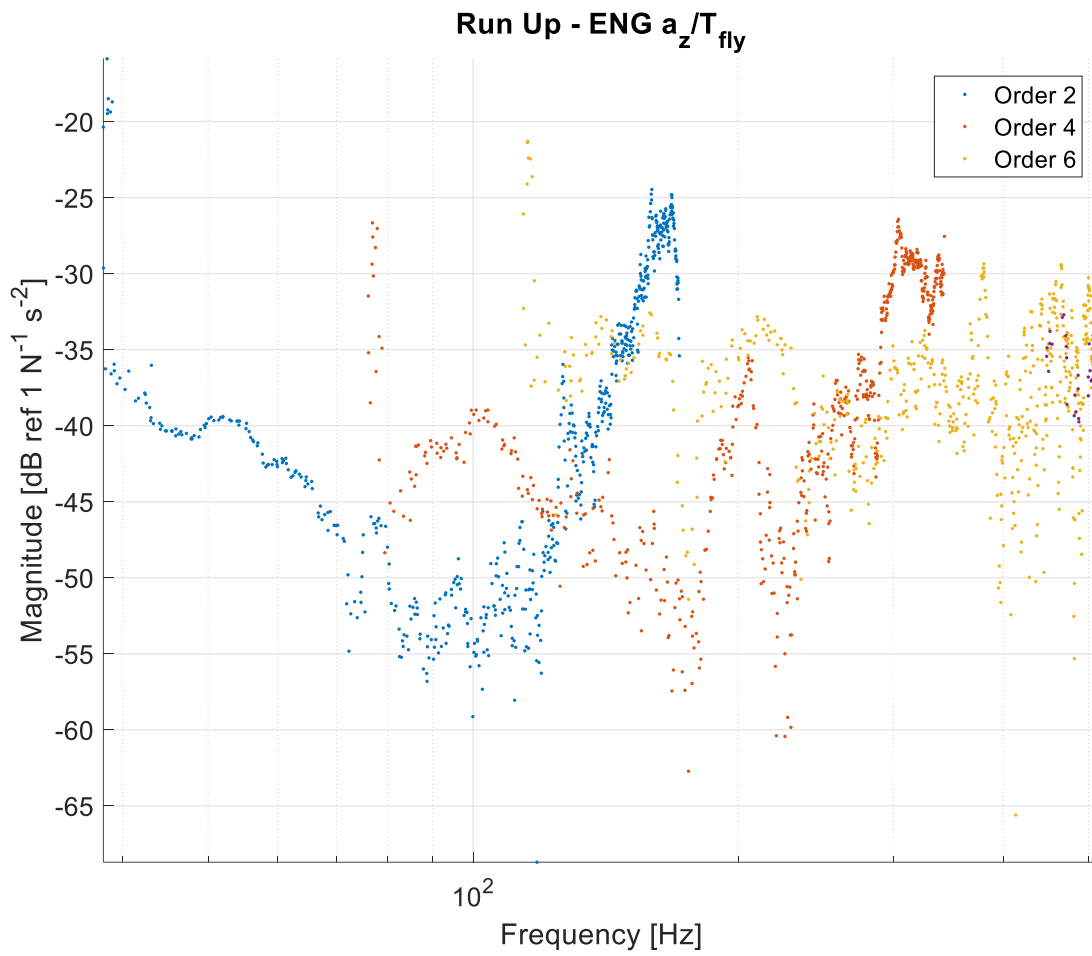


**Figure 5.59:** FRF estimation of the acceleration along z respect the engine's torque

## 6 - CONCLUSIONS

The main conclusion of this work is related to the application of the FRF estimation algorithm and to the most important issues that affects its results. In particular, the algorithm results very effective for the estimations derived from data obtained by the simulation of the model, even if some of its parameters are varied, but is not as effective as in the case of experimental data.

The main limitations of this type of application of the FRF algorithm are related to the non-linearities of the real system (the vehicle's powertrain). This non-linear behaviour is due to the dependence of the system's parameters on the frequency and amplitude of the external torque applied to it; in addition, also the presence of frictions and some micro-slipping phenomena between the plates of the clutches determine these non-linearities. Moreover, the conditions on the system between the Run Up and Coast Down phases are not symmetric, and some disturbance due to the road profile are transmitted through the vehicle's chassis to the sensors that measures the signals, further moving away the system from the linearity.

All these contributions make that for these experimental data a unique FRF does not exist: the system's characterization is better approximated by a band of FRFs than by a single FRF, that can give a qualitatively estimation of the system's response, anyway.

A further improvement of the FRF estimation algorithm could be the narrowing down of these FRFs band introducing, if possible, some operations aimed to consider the source of non-linearities that affect the experimental data measurement.

## APPENDIX A - COMPLETE MATLAB CODES

### A.1 - FRF ESTIMATION ALGORITHM

```
clear all
close all
clc
%% load data
[f_name,f_dir]=uigetfile(pwd,'Selezionare il file relativo alla prova: ');
F_mat=fullfile(f_dir,f_name);
load(F_mat)
%% elements length homogenization
zzzz=whos;
for(cont1=1:length(zzzz))
    dimvet(cont1)=zzzz(cont1).size(1);
end
dim=unique(dimvet);
for(cont2=1:length(dim)-1)
    if(dim(cont2)/dim(cont2+1)>0.995)
        for(cont1=1:length(zzzz))
            if zzzz(cont1).size(1)==dim(cont2+1)
                eval([zzzz(cont1).name, ' = ',zzzz(cont1).name,'(1:', ...
                    num2str(dim(cont2)),')'];]);
            end
        end
    end
end
clear zzzz dimvet dim cont1 cont2
%% transmission ratios data
Z_volano=135;
Z_condotte=[54 59 33 44];           % [I II III IV]
Z_ponte=[16 16];                   % [SS SI]
Z_diff=71;
Z_primario=[13 25 23 45];
J_tot=0.0392+0.085;                % [kg*m^2] inerzia albero + prima massa volano
tau_gbx=Z_condotte./Z_primario;
tau_finale=Z_diff/Z_ponte(1);
%% gears definition
comp=["FW";"K1";"K2";"I";"II";"III";"SI";"DIFF"];
type=["RunUp"; "CoastDown"];
```

```

Z_ord=[135 23 25 54 59 33 16 71];
%% function acceleration_computation
flag_plot=1; % 1=plot si
for cont1=1:length(comp)
    [RU_acc{cont1}, RU_vel{cont1}, CD_acc{cont1}, CD_vel{cont1}] ...
        =Acceleration_computation(n_FW, n_FW_time, eval(['n_' char(comp ...
            (cont1))]), eval(['n_' char(comp(cont1)) '_time'])), ...
            Z_ord(cont1),flag_plot,comp(cont1));
end
%% zeros removal
for cont3=1:length(comp)
    for cont2=1:length(RU_acc{cont3}(8,:))
        if RU_acc{cont3}(8,cont2)<280
            RU_acc{cont3}(8,cont2)=0+0i;
        end
    end
end
for cont3=1:length(comp)
    for cont2=1:length(CD_acc{cont3}(8,:))
        if CD_acc{cont3}(8,cont2)<280
            CD_acc{cont3}(8,cont2)=0+0i;
        end
    end
end
%% torque estimation
RU_Teng=J_tot.*RU_acc{1};
CD_Teng=J_tot.*CD_acc{1};
%% accelerations plots
% run up
% engine's torque
figure('units','normalized','outerposition',[0 0 1/2 3/4])
set(gca,'fontsize',14)
xlabel('Mean Speed [rpm]')
ylabel('Engine Torque [Nm]')
grid on
hold all
title('Run Up - Engine Torque','interpreter','latex')
set(gca,'fontsize',16)
axis tight

```

```

for cont3=2:2:length(RU_Teng(:,1))
    plot(RU_vel{1}/(pi).*30,abs(RU_Teng(cont3,:))/(2*pi), '.')
end
legend('Order 2','Order 4', 'Order 6', 'Order 8')
% gears accelerations
for cont4=2:length(comp)
    figure('units','normalized','outerposition',[0 0 1/2 3/4])
    set(gca,'fontsize',14)
    xlabel('Mean Speed [rpm]')
    ylabel([char(comp(cont4)) ' Acceleration [rad/s^2]'])
    grid on
    hold all
    title(['Run Up - ' char(comp(cont4)) ' Acceleration'],'interpreter','latex')
    set(gca,'fontsize',16)
    axis tight
    for cont3=2:2:length(RU_Teng(:,1))
        plot(RU_vel{cont4}/(pi).*30,abs(RU_acc{cont4}(cont3,:)), '.')
    end
    legend('Order 2','Order 4', 'Order 6', 'Order 8')
end
% coast down
% engine's torque
figure('units','normalized','outerposition',[0 0 1/2 3/4])
set(gca,'fontsize',14)
xlabel('Mean Speed [rpm]')
ylabel('Engine Torque [Nm]')
grid on
hold all
title('Coast Down - Engine Torque','interpreter','latex')
set(gca,'fontsize',16)
axis tight
for cont3=2:2:length(CD_Teng(:,1))
    plot(CD_vel{1}/(pi).*30,abs(CD_Teng(cont3,:))/(2*pi), '.')
end
legend('Order 2','Order 4', 'Order 6', 'Order 8')

```

```

% gears accelerations
for cont4=2:length(comp)
    figure('units','normalized','outerposition',[0 0 1/2 3/4])
    set(gca,'fontsize',14)
    xlabel('Mean Speed [rpm]')
    ylabel([char(comp(cont4)) ' Acceleration [rad/s^2]'])
    grid on
    hold all
    title(['Coast Down - ' char(comp(cont4)) 'Acceleration'],'interpreter', ...
          'latex')
    set(gca,'fontsize',16)
    axis tight
    for cont3=2:2:length(CD_Teng(:,1))
        plot(CD_vel{cont4}/(pi).*30,abs(CD_acc{cont4}(cont3,:)), '.')
    end
    legend('Order 2','Order 4','Order 6','Order 8')
end

%% inertances
for cont2=1:length(comp)
    Inertance=20*log10(abs(RU_acc{cont2}./RU_Teng));
    figure('units','normalized','outerposition',[0 0 1/2 3/4])
    xlabel('Frequency [Hz]')
    ylabel('Magnitude [dB ref 1 rad/s^2]')
    grid on
    hold all
    title(['Run Up - Inertance ', '$\dot{\omega}_{' char(comp(cont2)) '} / ...
          T_{FW}$'],'interpreter','latex')
    set(gca,'fontsize',16,'xscale','log')
    axis tight
    for cont3=2:2:length(RU_Teng(:,1))
        st=1;
        f_o=RU_vel{cont2}/(2*pi).*cont3;
        plot(f_o(st:end),Inertance(cont3,st:end), '.')
    end
    % ylim([-10 30])
    legend('Order 2','Order 4','Order 6','Order 8')
end

```

```

for cont2=1:length(comp)
    Inertance=20*log10(abs(CD_acc{cont2}./CD_Teng));
    figure('units','normalized','outerposition',[0 0 1/2 3/4])
    xlabel('Frequency [Hz]')
    ylabel('Magnitude [dB ref 1 rad/s^2]')
    grid on
    hold all
    title(['Coast Down - Inertance ', '$\dot{\omega}_{'} char(comp(cont2)) ' / ...
          T_{FW}$'], 'interpreter', 'latex')
    set(gca, 'fontsize', 16, 'xscale', 'log')
    axis tight
    for cont3=2:2:length(CD_Teng(:,1))
        st=1;
        f_o=CD_vel{cont2}/(2*pi).*cont3;
        plot(f_o(st:end), Inertance(cont3, st:end), '.')
    end
    % ylim([-10 30])
    legend('Order 2', 'Order 4', 'Order 6', 'Order 8')
end

```

## A.2 - ACCELERATION'S COMPUTATION FUNCTION

```

function [RU_acc, RU_vel, CD_acc, CD_vel]=Acceleration_computation(n_ref, ...
    t_ref_time, s, t, Z, flag_plot, disp)
%% preliminary operations
disp2=char(disp);
if disp2(1)=='I'
    disp2=[disp2 ' Gear'];
end
if disp2(1)=='K'
    disp2=[disp2 ' Clutch'];
end
%% mean value removal
Fs=round(mean(diff(t).^-1));
[b,a]=butter(2, 10*(2/Fs), 'low');
s_mean=filtfilt(b,a,s);
s_det=s-s_mean;

```

```

%% plot original signals
if flag_plot==1
    figure('units','normalized','outerposition',[0 0 1/2 3/4])
    subplot(2,1,1)
    plot(t,s)
    grid on
    ylabel('Speed [rpm]')
    set(gca,'fontsize',16)
    title([disp2 ' speed signal'])
    subplot(2,1,2)
    plot(t,s_det)
    grid on
    ylabel('Speed [rpm]')
    xlabel('Time [s]')
    set(gca,'fontsize',16)
end

%% unit conversion
s=s*2*pi/60;
s_det=s_det*2*pi/60;

%% synchronous re-sampling
n_vol_mean=filtfilt(b,a,n_ref);
max_ord=Z/2;
delta_ord=1;
theta=cumtrapz(t_ref_time,n_vol_mean*2*pi/60); % espresso in [rad]
delta_theta=[0:(2*pi)/(2*max_ord):theta(end)]'; % definizione asse theta
                                                    [rad]
delta_t=interp1(theta,t,delta_theta,'linear','extrap'); % vettore tempo a
                                                         passo angolare
                                                         costante [s]
s_theta=interp1(t,s_det,delta_t,'linear','extrap'); % segnale sincrono [rad/s]

%% spectrogram in orders
Fs_ord=2*max_ord;
ord_res=0.1;
F_v=0:ord_res:F_s_ord;
t_win=1/ord_res;
WIND=round(t_win*F_s_ord);
ol=round(0.9*WIND); % overlap delle finestre delle FFT
[S,O,G]=spectrogram(s_theta>window(@rectwin,WIND),ol,F_v,F_s_ord);
maxs=max(max(20*log10((2*abs(S)/WIND))));

```

```

%% spectrogram plot
if flag_plot==1
    figure('units','normalized','outerposition',[0 0 1/2 3/4])
    surf(G,0,20*log10((2*abs(S)/WIND)), 'EdgeColor','none')
    axis xy
    axis tight
    colormap(jet)
    view(0,90);
    xlabel('Revolutions');
    ylabel('Orders');
    ylim([0 8.2])
    caxis([maxs-50 maxs])
    hold on
    grid on
    hcb=colorbar;
    title(hcb,'Amplitude [dB ref 1 rad/s]')
    title([disp2 ' Orders Spectrogram'])
    set(gca,'fontsize',16)
end
%% extraction of the rows
speed=interp1(teta./(2*pi),n_ref*pi/30,G,'linear','extrap'); % [rad/s]
[maxv,maxp]=max(speed);
RU_vel=speed(1:maxp);
CD_vel=speed(maxp:end);
for(cont=1:8)
    RU_acc(cont,:)=2*S(cont/ord_res+1,1:maxp)/WIND*1i*2*pi.*RU_vel*cont;
    CD_acc(cont,:)=2*S(cont/ord_res+1,maxp:end)/WIND*1i*2*pi.*CD_vel*cont;
end
end

```

### A.3 - ANALYSIS OF THE 3 D.O.F. MODEL

```

clear all
close all
clc

```

```

%% parameters of the system
I1=0.2; I2=0.05; I3=2.7278;
K1=800; K2=25000;
c1=2; c2=5;
%% matrices
M=diag([I1,I2,I3]);
K=[K1,-K1,0
   -K1,K1+K2,-K2
   0,-K2,K2];
C=[c1,-c1,0
   -c1,c1+c2,-c2
   0,-c2,c2];
%% for cycle for inertance calculation
% frequency vector
f=logspace(-1,3,1000);
w_vet=2*pi*f;
for cont=1:length(w_vet)
    w=w_vet(cont);
    K_dyn=(K+i*w*C-M*w^2); % dynamic stiffness matrix
    Rec=K_dyn^-1; % receptance matrix
    Mob=j*w*Rec; % mobility matrix
    Iner=-w^2*Rec; % inertance matrix
    % extraction of the FRFs in interest
    Iner_31(cont)=Iner(3,1); % w3_dot/T1
    Iner_13(cont)=Iner(1,3); % w1_dot/T3
    Iner_11(cont)=Iner(1,1); % auto-inertance w1_dot/T1
end
%% plot FRF
% plot auto-inertance
figure;
subplot(2,1,1)
semilogx(f,20*log10(abs([Iner_11])), 'linewidth',2); grid on; ...
    ylabel('Mod [dB ref 1 rad/s^2/Nm]'); title('Inertance (1,1)');
subplot(2,1,2)
semilogx(f,180/pi*phase([Iner_11]), 'linewidth',2); grid on; ...
    ylabel('phase [deg]'); xlabel('Frequency [Hz]')
% plot Iner(3,1)
figure;
subplot(2,1,1)

```

```

semilogx(f,20*log10(abs([Iner_13])), 'linewidth',2); grid on; ...
    ylabel('Mod [dB ref 1 rad/s^2/Nm]'); title('Inertance (3,1)');
subplot(2,1,2)
semilogx(f,180/pi*phase([Iner_13]), 'linewidth',2); grid on; ...
    ylabel('phase [deg]'); xlabel('Frequency [Hz]')
%% tolerance
fin_v=20*log10(abs([Iner_11(end)]));
tbi=(fin_v-1)*ones(length(f),1);
tbs=(fin_v+1)*ones(length(f),1);
figure; % hold all
semilogx(f,20*log10(abs([Iner_11])), 'linewidth',2); grid on; ...
    ylabel('Mod [dB ref 1 rad/s^2/Nm]'); title('Inertance (1,1)');
hold all
plot(f(580:end),tbi(580:end), 'r')
plot(f(580:end),tbs(580:end), 'r')
xlabel('Frequency [Hz]')
title('Tolerance band')
%% calculation of the response due to a simulated external torque
% input signal
% run up + coast down
fs=2000; % sampling frequency
n0=800; n1=5000; Dt=50; % sweep parameters
t_n_eng=0:1/fs:Dt; % time vector
n_RunUp=n0+(n1-n0)/(Dt/2)*t_n_eng(1:round(end/2)); % run up speed
n_CoastDown=n1+(n0-n1)/(Dt/2)*(t_n_eng(round(end/2)+1:end)-t_n_eng ...
    (round(end/2))); % coast down speed
n_eng=[n_RunUp n_CoastDown];
figure; plot(t_n_eng,n_eng, 'linewidth',2); grid on; ...
    title('engine mean speed [rpm]'); xlabel('time[s]')
% angle calculation
theta_eng=1/fs*cumtrapz(n_eng*pi/30);
%% sum of irregularities
ord_exc=[2 4 6]; % harmonics orders
phi=[0 0 0]; % harmonics phases
Amp_ord=1*[29 15 6]; % harmonics amplitudes
Dn_eng=0;
figure; hold all

```

```

for cont1=1:length(phi)
    % signal build adding the harmonic contributions
    Dn_eng = Dn_eng + Amp_ord(cont1)*sin(ord_exc(cont1)*theta_eng+phi(cont1));
    plot(t_n_eng,Dn_eng)
    xlim([1 1.05]); grid on
end
n_eng=Dn_eng+n_eng;
legend('order 2','order 2+4','order 2+4+6'); xlabel('time [s]'); ...
    ylabel('n_1 [rpm]')
%% engine's torque estimation: T=I*w_dot
w_eng=n_eng*pi/30;
w_dot=diff(w_eng)./diff(t_n_eng);
T_eng=I1*w_dot;
figure; plot(t_n_eng(1:end-1),T_eng); ylabel('T_{eng}[Nm]'); ...
    xlabel('time [s]'); title('Input Torque estimation')
%% 3 DOF system response due to the estimated input torque knowing the FRF
% input definition
t=t_n_eng;
u=T_eng;
% FRF: w3_dot/T1
F=f;
AMP=abs([Iner_13]); % amplitude
PHA=180/pi*phase([Iner_13]); % phase
% frequency axis for IFFT requirements
N=length(t); % number of points of the time vector
T=t(end)-t(1); % input time duration
df=1/T; % required FRF's frequency
dt=t(2)-t(1);
freg=[0:(N-1)/2,(1-N)/2:-1]*(fs/(N-1)); % bidirectional frequency axis
wreg=[0:(N-1)/2,(1-N)/2:-1]*(fs*2*pi/(N-1));
[a,ind_in]=min(abs(freg-F(1)));
[b,ind_end]=min(abs(freg-F(end)));
[c,ind_in_neg]=min(abs(freg+F(1)));
[d,ind_end_neg]=min(abs(freg+F(end)));
% resample FRF AMP and PHA to meet IFFT requirements
AMP_res=interp1(F,AMP,[freg(ind_in):df:freg(ind_end)], 'linear','extrap');
PHA_res=interp1(F,unwrap(PHA,inf),[freg(ind_in):df:freg ...
    (ind_end)], 'linear','extrap');

```

```

% FRF amplitude vector for IFFT requirements
A_req=zeros(N,1);
A_req(1:ind_in-1)=AMP(1);      % modification to avoid 0 value at low frequencies
A_req(ind_in:ind_end)=AMP_res;
A_req(ind_end+1:ind_end_neg-1)=AMP(1);
A_req(ind_end_neg:ind_in_neg)=fliplr(AMP_res);
A_req(ind_in_neg:end)=AMP(1);
figure; plot(freq,20*log10(A_req),'-b');xlabel('Frequency [Hz]'); ...
        ylabel('|H(w)| (dB)'); grid on; title('Frequency response function')
% FRF phase vector for IFFT requirements
P_req=zeros(N,1);
P_req(1:ind_in-1)=PHA(1);
P_req(ind_in:ind_end)=PHA_res;
P_req(ind_end+1:ind_end_neg-1)=PHA(1);
P_req(ind_end_neg:ind_in_neg)=-fliplr(PHA_res);
P_req(ind_in_neg:end)=-PHA(1);
figure; plot(freq,P_req,'-b'); xlabel('Frequency [Hz]'); ...
        ylabel('phase(H(w)) [deg]'); grid on; title('Frequency response function')
% FRF vector that meets IFFT requirements
H_req=A_req.*exp(1i*P_req*pi/180);
%% impulse response
h_imp=ifft(H_req).*N/T;
figure; hold all; plot(t,h_imp,'-b'); legend('Impulse response'); ...
        xlabel('t [s]'); ylabel('h(t)'); grid on
%% convolution, time-domain
w_3_dot_=(conv(u,h_imp))*dt;
figure; hold all; plot(t,(w_3_dot_(1:length(t))*30/pi),'-b'); ...
        ylabel('${\dot{\omega}}_3(t)$','interpreter','latex'); xlabel('t [s]'); grid on
w_3_dot=w_3_dot_(1:length(t));
w_10=n0*pi/30;
w_30=w_10;
w_3=1/fs*cumtrapz(w_3_dot)+w_30;
%% velocity vector necessities for the validation of the FRF algorithm
w_eng=real(w_eng)*30/pi;
w_3=real(w_3)*30/pi;

```

# APPENDIX B - FIGURES AND TABLES INDEXES

## B.1 - FIGURES INDEX

FIGURE 2.1: SPEED SIGNAL OF THE ENGINE FLYWHEEL DURING THE IDLE TEST .....	2
FIGURE 2.2: AMPLITUDE AND PHASE OF THE FLYWHEEL SIGNAL IN THE FREQUENCY DOMAIN .....	4
FIGURE 2.3: GRAPHICAL REPRESENTATION OF THE SYNCHRONOUS RE-SAMPLING .....	6
FIGURE 2.4: AMPLITUDE AND PHASE OF THE FLYWHEEL SIGNAL IN THE ORDERS DOMAIN.....	7
FIGURE 2.5: FLYWHEEL SPEED SIGNAL ACQUIRED DURING THE RUN UP TEST .....	9
FIGURE 2.6: SPECTROGRAMS OF THE RUN UP SPEED SIGNAL - 4 CASES .....	10
FIGURE 2.7: HANNING'S WINDOW AND RECTANGULAR WINDOW .....	11
FIGURE 2.8: ORDERS SPECTROGRAM OF THE RUN UP SPEED SIGNAL.....	12
FIGURE 2.9: SIGNAL OF THE 2 ACCELEROMETERS OF THE ENGINE'S MOUNT DURING THE RUN UP TEST .....	13
FIGURE 2.10: SPECTROGRAMS OF THE 2 SIGNALS USED AS INPUT FOR TFESTIMATE .....	15
FIGURE 2.11: RESULT OF THE ESTIMATION OF THE TRANSFER FUNCTION (MAGNITUDE AND PHASE) AND ITS COHERENCE .....	15
FIGURE 3.1: SYSTEM WITH 1 TORSIONAL D.O.F. ....	16
FIGURE 3.2: SYSTEM WITH 1 D.O.F. WITH DIFFERENT REPRESENTATION .....	16
FIGURE 3.3: SIMULINK MODEL USED TO BUILD THE FICTITIOUS FLYWHEEL SIGNAL .....	18
FIGURE 3.4: FICTITIOUS SPEED SIGNALS OF THE FLYWHEEL AND OF THE DIFFERENTIAL .....	19
FIGURE 3.5: ORDERS SPECTROGRAMS OF THE 2 SIGNALS .....	20
FIGURE 3.6: INERTANCE OF THE DIFFERENTIAL'S ACCELERATION RESPECT THE ENGINE'S TORQUE - RUN UP PHASE .....	22
FIGURE 3.7: INERTANCE OF THE DIFFERENTIAL'S ACCELERATION RESPECT THE ENGINE'S TORQUE - PHASE.....	22
FIGURE 3.8: BLOCK DIAGRAM OF THE OPERATIONS REQUIRED TO COMPUTE THE INERTANCE .....	23
FIGURE 3.9: MODEL WITH 3 D.O.F. ....	24
FIGURE 3.10: INERTANCE $In3,1$ - AMPLITUDE AND PHASE .....	28
FIGURE 3.11: INERTANCE $In1,1$ - AMPLITUDE AND PHASE .....	29
FIGURE 3.12: APPLICATION OF THE TOLERANCE BAND FOR THE DEFINITION OF THE RELIABLE FREQUENCIES RANGE .....	30
FIGURE 3.13: FRF OF THE MODEL MIRRORED FOR NEGATIVE FREQUENCIES .....	31
FIGURE 3.14: IMPULSE RESPONSE OF THE 3 D.O.F. MODEL'S SYSTEM .....	33
FIGURE 3.15: RESPONSE OF THE SYSTEM TO THE DEFINED INPUT .....	33
FIGURE 3.16: SPEED SIGNALS OF THE MODEL: SPEED OF THE FIRST INERTIA (ON THE LEFT) AND OF THE THIRD INERTIA (ON THE RIGHT)....	34
FIGURE 3.17: ORDERS SPECTROGRAMS OF THE 2 SIGNALS.....	35
FIGURE 3.18: COMPARISON BETWEEN THE EXPERIMENTAL INERTANCE AND THE ONE OF THE MODEL - AMPLITUDE.....	36
FIGURE 3.19: COMPARISON BETWEEN THE EXPERIMENTAL INERTANCE AND THE ONE OF THE MODEL - PHASE.....	36
FIGURE 3.20: FRF'S AMPLITUDES COMPARISON - SHORTENED FREQUENCY RANGE .....	37
FIGURE 3.21: FRF'S PHASES COMPARISON - SHORTENED FREQUENCY RANGE .....	38
FIGURE 3.22: FRF'S AMPLITUDES COMPARISON - VARIATION OF ORDERS AMPLITUDE.....	39
FIGURE 3.23: FRF'S PHASES COMPARISON - VARIATION OF ORDERS AMPLITUDE.....	40
FIGURE 3.24: FRF'S AMPLITUDE COMPARISON - VARIATION OF SWEEP PHASES DURATIONS.....	40
FIGURE 3.25: FRF'S PHASES COMPARISON - VARIATION OF SWEEP'S PHASES DURATION .....	41
FIGURE 4.1: SCHEMATIC REPRESENTATION OF GEARS AND BEARING IN THE GEARBOX .....	43
FIGURE 4.2: 3D CAD MODEL OF THE GEARBOX .....	44
FIGURE 4.3: SCHEMATISATION OF THE LAYOUT OF THE SENSORS.....	48
FIGURE 5.1: VELOCITY SIGNAL OF THE FLYWHEEL MEASURED DURING THE IDLE TEST .....	51
FIGURE 5.2: AMPLITUDES AND PHASES OF THE IDLE VELOCITY SIGNAL IN THE FREQUENCY DOMAIN .....	52
FIGURE 5.3: VELOCITY SIGNAL OF THE FLYWHEEL MEASURED DURING THE RUN UP TEST .....	53
FIGURE 5.4: AMPLITUDES AND PHASES OF THE RUN UP SIGNAL IN THE ORDER DOMAIN .....	53
FIGURE 5.5: SPECTROGRAM OF THE SIGNAL OF THE RUN UP TEST .....	54
FIGURE 5.6: POSITION AND ORIENTATION OF THE ACCELEROMETERS INSTALLED IN THE VEHICLE'S POWERTRAIN. ....	55
FIGURE 5.7: SIGNAL OF THE $x$ COMPONENT MEASURED BY THE ENGINE'S MOUNT ACCELEROMETERS .....	56
FIGURE 5.8: FLYWHEEL'S SPEED SIGNAL ACQUIRED DURING THE TEST .....	57
FIGURE 5.9: SPECTROGRAMS AND TRANSFER FUNCTION ESTIMATION OF THE 2 SIGNALS ALONG $x$ OF THE ENGINE MOUNT .....	58
FIGURE 5.10: SPECTROGRAMS AND TRANSFER FUNCTION OF THE ACCELERATIONS SIGNAL OF THE ENGINE'S MOUNT ALONG $y$ .....	59
FIGURE 5.11: SPECTROGRAMS AND TRANSFER FUNCTION OF THE ACCELERATIONS SIGNAL OF THE ENGINE'S MOUNT ALONG $z$ .....	60
FIGURE 5.12: AMPLITUDES OF THE ENGINE'S MOUNT ACCELERATIONS SIGNALS IN THE ORDER DOMAIN .....	61
FIGURE 5.13: PHASES OF THE ENGINE'S MOUNT ACCELERATIONS SIGNALS IN THE ORDER DOMAIN .....	61
FIGURE 5.14: FLYWHEEL SPEED SIGNAL MEASURED DURING THE RUN UP TEST PERFORMED IN 5 <sup>TH</sup> GEAR .....	62
FIGURE 5.15: SPECTROGRAMS AND TRANSFER FUNCTION OF THE ACCELERATIONS SIGNAL OF THE DIFFERENTIAL'S MOUNT ALONG $x$ .....	63
FIGURE 5.16: SPECTROGRAMS AND TRANSFER FUNCTION OF THE ACCELERATIONS SIGNAL OF THE DIFFERENTIAL'S MOUNT ALONG $y$ .....	64
FIGURE 5.17: SPECTROGRAMS AND TRANSFER FUNCTION OF THE ACCELERATIONS SIGNAL OF THE DIFFERENTIAL'S MOUNT ALONG $z$ .....	65
FIGURE 5.18: AMPLITUDES OF THE DIFFERENTIAL'S MOUNT ACCELERATIONS SIGNALS IN THE ORDER DOMAIN - $x$ AND $y$ COMPONENTS ....	66
FIGURE 5.19: AMPLITUDES OF THE DIFFERENTIAL'S MOUNT ACCELERATIONS SIGNALS IN THE ORDER DOMAIN - $z$ COMPONENT .....	66

FIGURE 5.20: PHASES OF THE DIFFERENTIAL'S MOUNT ACCELERATIONS SIGNALS IN THE ORDER DOMAIN.....	67
FIGURE 5.21: SPECTROGRAMS AND TRANSFER FUNCTION OF THE ACCELERATIONS SIGNAL OF THE GEARBOX'S MOUNT ALONG $x$ .....	68
FIGURE 5.22: SPECTROGRAMS AND TRANSFER FUNCTION OF THE ACCELERATIONS SIGNAL OF THE GEARBOX'S MOUNT ALONG $y$ .....	69
FIGURE 5.23: SPECTROGRAMS AND TRANSFER FUNCTION OF THE ACCELERATIONS SIGNAL OF THE GEARBOX'S MOUNT ALONG $z$ .....	70
FIGURE 5.24: AMPLITUDES OF THE GEARBOX'S MOUNT ACCELERATIONS SIGNALS IN THE ORDER DOMAIN .....	71
FIGURE 5.25: AMPLITUDES OF THE GEARBOX'S MOUNT ACCELERATIONS SIGNALS IN THE ORDER DOMAIN .....	71
FIGURE 5.26: ENGINE FLYWHEEL'S VELOCITY SIGNAL AND ITS ORDERS SPECTROGRAM - 2 <sup>ND</sup> GEAR SWEEP TEST .....	74
FIGURE 5.27: ENGINE FLYWHEEL'S TORQUE'S HARMONICS - 2 <sup>ND</sup> GEAR SWEEP TEST .....	74
FIGURE 5.28: SECOND GEAR'S VELOCITY SIGNAL AND ITS ORDERS SPECTROGRAM - 2 <sup>ND</sup> GEAR SWEEP TEST.....	76
FIGURE 5.29: SECOND GEAR'S ACCELERATIONS - 2 <sup>ND</sup> GEAR SWEEP TEST .....	76
FIGURE 5.30: LOWER SECONDARY SHAFT'S ACCELERATIONS - 2 <sup>ND</sup> GEAR SWEEP TEST.....	77
FIGURE 5.31: LOWER SECONDARY SHAFT'S INERTANCE - 2 <sup>ND</sup> GEAR SWEEP TEST .....	77
FIGURE 5.32: DIFFERENTIAL'S VELOCITY SIGNAL AND ITS ORDERS SPECTROGRAM - 2 <sup>ND</sup> GEAR SWEEP TEST .....	78
FIGURE 5.33: DIFFERENTIAL'S ACCELERATIONS - 2 <sup>ND</sup> GEAR SWEEP TEST.....	78
FIGURE 5.34: DIFFERENTIAL'S INERTANCE - 2 <sup>ND</sup> GEAR SWEEP TEST.....	78
FIGURE 5.35: ENGINE FLYWHEEL'S VELOCITY SIGNAL AND ITS ORDERS SPECTROGRAM - 6 <sup>TH</sup> GEAR SWEEP TEST.....	80
FIGURE 5.36: ENGINE FLYWHEEL'S TORQUE'S HARMONICS - 6 <sup>TH</sup> GEAR SWEEP TEST.....	80
FIGURE 5.37: K1 CLUTCH'S VELOCITY SIGNAL AND ITS ORDERS SPECTROGRAM - 6 <sup>TH</sup> GEAR SWEEP TEST .....	81
FIGURE 5.38: K1 CLUTCH'S ACCELERATIONS - 6 <sup>TH</sup> GEAR SWEEP TEST .....	81
FIGURE 5.39: K1 CLUTCH'S INERTANCE - 6 <sup>TH</sup> GEAR SWEEP TEST .....	81
FIGURE 5.40: K2 CLUTCH'S VELOCITY SIGNAL AND ITS ORDERS SPECTROGRAM - 6 <sup>TH</sup> GEAR SWEEP TEST .....	82
FIGURE 5.41: K2 CLUTCH'S ACCELERATIONS - 6 <sup>TH</sup> GEAR SWEEP TEST .....	82
FIGURE 5.42: K2 CLUTCH'S INERTANCE - 6 <sup>TH</sup> GEAR SWEEP TEST .....	82
FIGURE 5.43: FIRST GEAR'S VELOCITY SIGNAL AND ITS ORDERS SPECTROGRAM - 6 <sup>TH</sup> GEAR SWEEP TEST .....	83
FIGURE 5.44: FIRST GEAR'S ACCELERATIONS - 6 <sup>TH</sup> GEAR SWEEP TEST .....	83
FIGURE 5.45: FIRST GEAR'S INERTANCE - 6 <sup>TH</sup> GEAR SWEEP TEST .....	83
FIGURE 5.46: SECOND GEAR'S VELOCITY SIGNAL AND ITS ORDERS SPECTROGRAM - 6 <sup>TH</sup> GEAR SWEEP TEST .....	84
FIGURE 5.47: SECOND GEAR'S ACCELERATIONS - 6 <sup>TH</sup> GEAR SWEEP TEST .....	84
FIGURE 5.48: SECOND GEAR'S INERTANCE - 6 <sup>TH</sup> GEAR SWEEP TEST .....	84
FIGURE 5.49: THIRD GEAR'S VELOCITY SIGNAL AND ITS ORDERS SPECTROGRAM - 6 <sup>TH</sup> GEAR SWEEP TEST .....	85
FIGURE 5.50: THIRD GEAR'S ACCELERATIONS - 6 <sup>TH</sup> GEAR SWEEP TEST .....	85
FIGURE 5.51: THIRD GEAR'S INERTANCE - 6 <sup>TH</sup> GEAR SWEEP TEST .....	85
FIGURE 5.52: LOWER SECONDARY SHAFT'S VELOCITY SIGNAL AND ITS ORDERS SPECTROGRAM - 6 <sup>TH</sup> GEAR SWEEP TEST.....	86
FIGURE 5.53: LOWER SECONDARY SHAFT'S ACCELERATIONS - 6 <sup>TH</sup> GEAR SWEEP TEST.....	86
FIGURE 5.54: LOWER SECONDARY SHAFT'S INERTANCE - 6 <sup>TH</sup> GEAR SWEEP TEST.....	86
FIGURE 5.55: DIFFERENTIAL'S VELOCITY SIGNAL AND ITS ORDERS SPECTROGRAM - 6 <sup>TH</sup> GEAR SWEEP TEST.....	87
FIGURE 5.56: DIFFERENTIAL'S ACCELERATIONS - 6 <sup>TH</sup> GEAR SWEEP TEST .....	87
FIGURE 5.57: DIFFERENTIAL'S INERTANCE - 6 <sup>TH</sup> GEAR SWEEP TEST.....	87
FIGURE 5.58: INPUT AND OUTPUT FOR THE FRF'S ESTIMATION .....	88
FIGURE 5.59: FRF ESTIMATION OF THE ACCELERATION ALONG $z$ RESPECT THE ENGINE'S TORQUE.....	89

## B.2 - TABLES INDEX

TABLE 2.1: PARAMETERS OF THE TWO DIFFERENT SPECTROGRAMS .....	9
TABLE 3.1: VALUES USED FOR THE INERTANCE CALCULATION OF THE 1 D.O.F. MODEL .....	21
TABLE 3.2: NUMERICAL VALUES ASSIGNED TO THE 3 D.O.F. MODEL'S PARAMETERS .....	27
TABLE 3.3: PARAMETERS OF THE 3 D.O.F. MODEL SIGNALS FOR THE PREVIOUS RESULTS .....	39
TABLE 3.4: PARAMETERS OF THE 3 D.O.F. MODEL'S SIGNALS VARIED FOR THE FINAL VALIDATION .....	39
TABLE 4.1: TECHNICAL DATA OF THE VEHICLE .....	42
TABLE 4.2: POSITIONS OF THE PICK-UPS INSTALLED ON THE VEHICLE'S POWERTRAIN .....	45
TABLE 4.3: LIST OF THE ACCELEROMETERS USED DURING THE TESTS .....	46
TABLE 4.4: LIST OF THE POSITION TRANSDUCERS.....	47
TABLE 4.5: MAIN PARAMETERS OF THE EXTENSOMETERS .....	47
TABLE 4.6: MICROPHONE CHARACTERISTIC.....	48
TABLE 4.7: MAIN SIGNALS ACQUIRED BY THE CAN NETWORK OF THE VEHICLE .....	49
TABLE 5.1: CHARACTERISTIC VALUES OF THE ACCELERATIONS SIGNALS OF THE ENGINE'S MOUNT .....	57
TABLE 5.2: MAIN PARAMETERS OF THE RUN UP TEST WITH THE GEARBOX IN NEUTRAL POSITION .....	57
TABLE 5.3: MAIN PARAMETERS OF THE RUN UP TEST IN 5 <sup>TH</sup> GEAR .....	62
TABLE 5.4: CHARACTERIZING VALUES OF THE DIFFERENTIAL'S ACCELEROMETERS SIGNALS.....	63
TABLE 5.5: CHARACTERIZING VALUES OF THE GEARBOX'S ACCELEROMETERS SIGNALS .....	67
TABLE 5.6: MAIN PARAMETERS OF THE TESTS .....	73

## **SPECIAL THANKS**

This thesis work is the end of a college course of study made by arguments that always make me feel curious and interested. Of course, that substantially contributed to its profitable end, but special thanks to who walked with me through this path are at least due.

Therefore, I wish to thank my thesis advisor, Prof. Alessandro Vigliani, and my co-advisors: Prof. Mauro Velardocchia and especially Prof. Enrico Galvagno, who more than everyone sustained me during this thesis work and always was available to clarify me any of my many doubts.

I duly wish to thank my mother Vilma and my father Aldo for the moral and economic help that gave me during my entire life and especially through these college years.

Finally, a special mention is due to my dear friend Enrico, whom I shared these college years with and who actively supported me in the drawing up of this thesis work.

## BIBLIOGRAPHIC NOTES

In this writing, references to these literary works were made:

- Galvagno E., Guercioni G.R., Vigliani A., *An alternative method for order tracking using autopower spectrum*, in “*Advances in Mechanical Engineering*”, Vol 7(11), 2015, 1-14.
- Martinengo M., *Banco prova cambi a doppia frizione: sviluppo software per prove HiL e caratterizzazione sperimentale di componenti. Tesi di Laurea Magistrale*, Politecnico di Torino, 2017.

For the mentioned scripts development, the following software were used:

- MATLAB (Version R2017b), © 1994-2018 The MathWorks, Inc.
- Simulink (Version 9.0), © 1994-2018 The MathWorks, Inc.

For the drawing up of this document, the following software was used:

- Microsoft Word 2016 MSO (Version 16.0.8431.2270), © 1983-2018 Microsoft, Corp.

**LORENZO MAGGIO**

© JULY 19, 2018